Functionalization of Nanocarbons and Application for Catalysis

September 2020

Muhammad Sohail Ahmad

The Graduate School of Natural Science and Technology

(Doctor Course)

Okayama University (Japan)

Summary

Catalysts are widely used in organic synthesis, environmental protection, and energy-related systems. The conventional catalysts are composed of noble transition metals or their oxides. The activity and selectivity of the metal catalysts can be tuned by modification of their ligands, and support materials, and numerous metal-based catalysts have been developed and used in diverse reactions. However, the transition metal-catalyzed reactions still have limitations due to the inherent drawbacks of the systems. Firstly, metal-based catalysts are generally expensive because of the high cost of transition metals, ligands, and support materials. Secondly, these metals are toxic and difficult to remove the trace amounts of residues from the products, which is problematic in the field of pharmaceuticals and electronic devices. Thirdly, some of the transition metal catalysts are very sensitive to moisture and oxygen; thus, special environment and techniques are needed. Finally, sometimes co-catalysts/additives are required to initiate the reactions and enhance the selectivity of the products. To address these problems, recently, nanocarbons have been widely explored to replace conventional metal-based catalysts.

In chapter 1, an introductory section, presents the background of this research and general consideration of state of the art in the field of carbocatalysis, focusing on active sites and applications for organic reactions. Initially, the carbon-based catalysts were applied for the functional group transformations, such as oxidation and esterification reactions. Recently, they have been used for the construction of C–C bonds, which are fundamental reactions in the synthesis of fine chemicals, medicinal and pharmaceutical agents, agrochemicals, and organic electronics materials; however, these reactions are performed under metal-based catalytic systems. Therefore, catalysts from sustainable materials, such as carbon, could replace the transition metal-based catalytic systems. Graphene-based materials have large surface area and a 2D morphology making accessible most of the atoms that make these materials suitable as a catalyst, and the structure of graphene is tunable by chemical treatment. This is one of the reasons why there is growing interest in exploring the potential of graphene-based materials as heterogeneous catalysts. Carbon materials as a catalyst have been developed since over 100 year ago, but it has not been mainstream materials due to the low activity. On the other hand, recent advantages of reliable and well-established production of graphene have motivated researchers to study carbocatalysts.

In chapter 2, the catalytic activity of the graphene-based carbon materials for the C−H functionalization reaction was investigated, and found that the carbocatalyst can facilitate the C−H functionalization of unactivated arenes to obtain biaryl products. In order to elucidate the nature of the intrinsic catalytic active site of carbons for the C−H functionalization reaction, in-situ electron spin resonance spectroscopy of the catalyst was performed before and after the reaction. It has been proposed that radical species and stable pyrrolic groups play an important role in this transformation, further, the mechanism was confirmed by density functional theory calculations. Regarding the recyclability of the carbocatalyst, it could be recycled up to several times without loss of significant activity. The chemical composition of the catalyst was not changed after several runs, as confirmed by Fourier transform infrared and X-ray photoelectron spectroscopy. The present methodology offers a diverse substrate scope without any dry or inert conditions and avoiding any expensive or toxic transition metals. Thus, this method opens the door for the development of an alternative to the metal-based coupling reactions.

In chapter 3, the efficiency and reactivity of the carbon nanomaterials were studied for the selective hydrogenation of nitroaromatic compounds. Usually, the selective hydrogenation of nitro moiety is a difficult task in the presence of other reducible functional groups such as alkene and alkyne with molecular hydrogen as a reducing agent. Recently, a similar reaction has been reported using Co, and N co-catalyst supported on carbon materials. In my study, the carbon-based catalyst without any metal can catalyze the selective reduction of the substituted nitro-groups using H_2 as a reducing agent. The analytical and experimental data suggested that the hydrogenation reaction proceeds via a radical mechanism in which the localized radicals of the carbocatalyst activate the molecular hydrogen and work as a reducing agent. Finally, the unusual activity of the carbocatalyst and high potentials for the selective hydrogenation of multi functionalized nitro compounds provide a great perspective to replace noble metal catalysts and contribute to simple and greener strategies for organic synthesis.

Chapter 4, comprasis the radical properties of the graphene based materials which may catalyse the alkylation reaction of ketones woth benzylic alcohols. The reaction mechanism of the alkylation of ketone with alcohol is still a matter of debate, is it a Meerwein-Ponndorf-Verley like process, or are hydrogen borrowing process by transition metals? Here, the alkylation reaction of ketones with benzylic alcohols via a radical pathway has been developed, where base treated

graphene works as an initiator of radical reaction. Mechanistic study support that the radical anion of the benzylic alcohol is proposed to be the key intermediate, which further undergoes coupling with ketones via aldol condensation to form a new C−C bond with water the only byproduct.

In chapter 5, the conclusion of the research results obtained in the duration of this doctoral thesis has led to the following points.

- The graphene-based carbocatalyst was utilized as a metal-free catalyst for the C−C coupling reactions.
- The chemoselective hydrogenation reaction of nitro-moieties was achieved using the carbocatalyst.
- Several experimental and analytical studies about the active sites of the carbocatalysts revealed that non-metal species (free radicals and pyrrolic groups) are involved in these transformations

List of Contents

Chapter 1

Chapter 2

Chapter 3

Chapter 4

Chapter 5

Chapter 1: General Introduction

1 Introduction

1.1 Introduction to catalysis

In the early 19th century, the scientific study of chemistry began with great interest. It was feasible, at this time, for a scientist to provide an annual report that demonstrated the progress of the achievements across the chemistry over the recent year. Approximately 200 years ago, the importance of undertaking this assignment for the Stockholm Academy of Sciences lay with the eminent chemist J.J. Berzelius (1779-1848), indeed, it had been done for many years.[1] In his work, Berzelius systematically reviewed various experimental observations in catalytic systems, both homogeneous and heterogeneous, which reported on the occurrence of chemical reactions happening only if within the presence of a small quantity of substances that weren't participating within the reaction by themselves.[2] He suggested that these observations may be rationally linked to the existence of an inherent new force, which he named it the *catalytic force,* with '*catalysis*' being the label used to depict the decomposition of bodies by this force.

Many bodies have the property of exerting on other bodies, which is even different from chemical affinity. Employing this action, they build decomposition in bodies and generate new compounds into the composition they do not enter. To this unknown new power, called it catalytic control, and also catalysis the decomposition of bodies by this force. [3] In the years of Berzelius's discovery, some other examples of catalytic action have also been reported; as science gets advanced, theoretical and experimental methodologies were proposed that might enable to precisely explore the rates of the chemical reactions.[2] After these discoveries, Ostwald define a catalyst as:

A reagent that increases the rate at which a chemical reaction system come up equilibrium, without being utilized in the process.[2]

Sustainable chemical processes are fundamental to enable the current and future worldwide production and use of energy and chemicals while avoiding adverse environmental consequences. Catalysis is crucial in developing sustainable strategies,[4] as clearly designated by one of the twelve principles of green chemistry.[5] In this context, the real catalyst should enable a reaction to proceed at mild conditions, engrossing minimum energy, low waste, a cost-effective process, and easy separation from the reaction mixture. Currently, up to 90% of all commercially available chemical

products involve using catalysts at a particular production stage,[6] which obscures the important role of catalysis in various industries and the world economy. Most of the catalytic reactions on industrial scales are accomplished via transition metal-based catalysis. Most of the chemical reactions utilize expensive metals, suffer from the limited natural abundance sources, and produce waste materials, presenting enormous sustainability and environmental challenges.

1.1.1 Issues for metal-catalyzed systems

Most of the catalysis is currently ruled by the use of transition metals (TMs), either as coordination complexes, free ions, clusters, or nanoparticles, that act as active sites.[7–12] TM catalysts have become the utmost studied homogeneous catalysts. By taking leverage of the metals d orbitals, these catalysts may activate the reagents and speed up the reactions via coordinations, ligand exchange, elimination, and insertion, etc., leading to the cleavage formation of H−H, C−C, and C−H bonds. The activity and selectivity of TM catalysts can be tuned on purpose, for example, by modification of their ligands, in this context, various TM catalysts have been developed and used in the diverse areas of the catalysis. Examples, i) asymmetric hydrogenation reactions catalyzed by Ru, Ir, and Rh, with ligands containing P or N, ii) asymmetric epoxidation, and dihydroxylation reactions catalyzed by Os or Ti complexes with cinchona alkaloid derivatives or tartaric acid, iii) metathesis reactions of olefin with Mo, or Ru catalysts, and lastly iv) Pd based system catalyzed coupling reactions between electrophiles and nucleophiles. Tons of chemicals and materials are produced every year via TM catalyzed reactions (oxidation and hydrogenation reaction, hydrosilation, hydroformylation, and the Wacker oxidation of ethylene, and many others). Surprisingly, the TM catalysts have been reported for organic transformations showing high activity (with turnover numbers 1×106 and turnover frequencies greater than $1\times105\ h^{-1}$) and enantioselectivity or even greater than those of enzyme systems.

However, the TM catalyzed reactions still have limitations due to the immanent drawbacks of the systems. Firstly, TM catalysts are generally expensive because of the high cost of the metals, support materials, and ligands. Secondly, TM is toxic and difficult to remove the trace amounts of debris from the products, which is problematic in the field of pharmaceuticals and electronic devices.[13–15] Thirdly, some of the TM catalysts are very sensitive to moisture and air; thus, a unique environment and techniques are required. Fourthly, in some cases, cocatalysts/additives are needed

to initiate the reactions and enhance the selectivity of the products.[16–22] lastly, the massive utilization of TM on the industrial scale does not meet the terms of sustainable developments.[23,24] Therefore, the need to develop highly active and alternative related method under TM free conditions are quite attractive.[25]

1.1.2 Metal-free catalysis: organocatalysis and carbocatalysis

Most of the organocatalysts are consist of small molecules; mostly, they are utilized in the homogeneous catalytic systems. Organocatalysts are more direct, easily accessible, and often less toxic compared with enzymes and inorganic catalysts. Organocatalysts may be advised as minimal biocatalysts because they are closer to the amino acid residues and co-factors that make up an enzyme. Because of the molecular characters of organocatalysts, stability, and recyclability are issues to be solved. For the sake of sustainability, switching the homogenous catalytic system into a heterogeneous catalytic system is desirable; thus, carbocatalyst is the green option for catalytic transformations. Accordingly, we will talk about carbon and its family briefly here.

1.1.3 In the early stage: how carbocatalysis started

The definition of carbocatalyst is *the catalytic system that uses carbon materials as a catalyst for organic transformations.* It should be famed that carbocatalysis are known for decades since the first discovery of catalytic activities of carbon materials.[26] In 1925, Rideal utilized active charcoal as a catalyst for the oxalic acid oxidation reaction.[27] In the absence of carbon materials, no conversion was observed.[28] The reaction is evident to start from the aerobic oxidization of carbon to generate geminal diols. In the presence of ambient oxygen, the diols further generate peroxide intermediates, which then reacts with the substrate to produce carbon dioxide and water (Scheme 1.1). Charcoal also shows other types of dehydration and oxidation ability.[29]

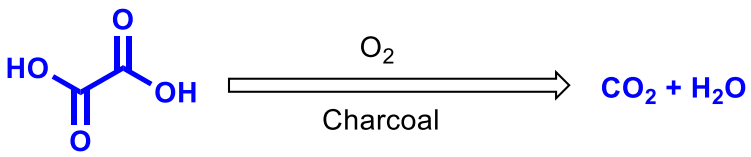

Scheme 1.1: *Charcoal as a catalyst for the aerobic oxidation of oxalic acid.*

Active carbon was used as a catalyst for the oxidative dehydrogenation (ODH) reaction of ethylbenzene to styrene in 1980.[30] Ritter used graphite for the degradation 4-chlorophenol, which yielded CO_2, HCl, and H_2O.[31] The reactivity of the graphite catalyst was found similar to that of Fenton's reagent.[32] Howbeit, carbon-based catalyst materials did not attract much attention at that time. Carbon-based catalysts can catalyze a series of reactions, but most of them show lower activity than metal-based catalysts. To crack the problem, researcher focused on large surface area materials. In 2010, Bielawski reported that graphene oxide (GO) could catalyze the aerobic oxidation of benzylic hydrocarbons.[33] After 2010, graphene-based materials have been progressively utilized as a carbocatalyst for various organic transformations such as oxidation,[34–36] reduction reaction,[37–39] and many others.[40–42] In this thesis, we have focused on the nature of the active site encountered in graphene-based materials in organic transformations. The active site is always associated with defect int eh structure of ideal graphene materials. Scheme 1.2 shows a pictorial illustration of some of the active sites that have been proposed to be active in catalysis.

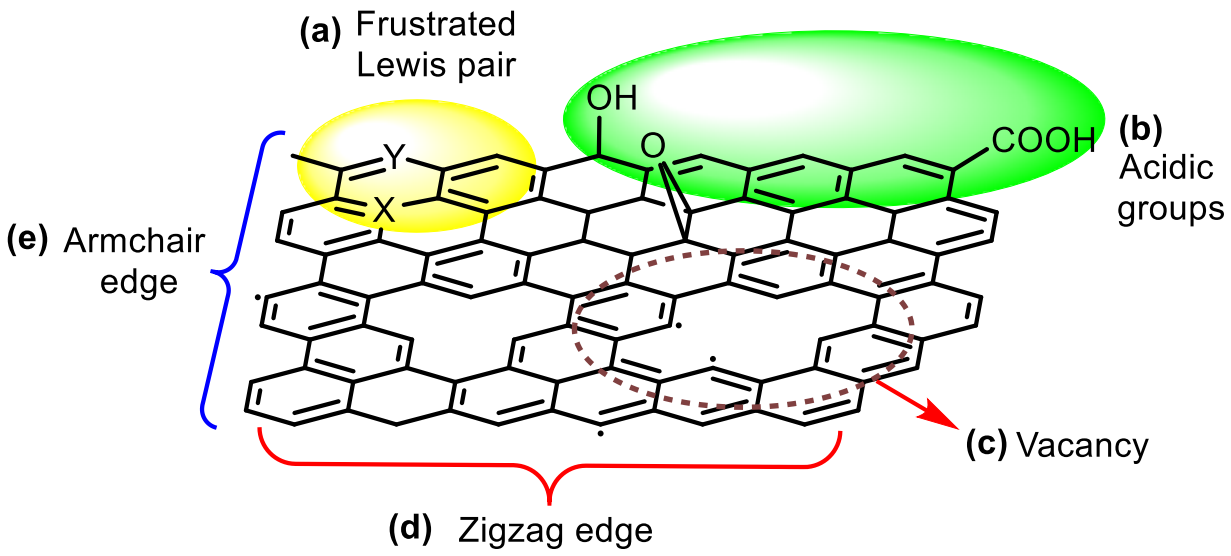

Scheme 1.2: *Possible active sites on the surface of graphene-based materials.*

1.2 Carbon and it's family (a brief discussion)

Carbon is one of the most abundantly available element in the earth's crust and can form strong covalent bonds with various elements yielding versatile carbonaceous compounds that constitute organic chemistry. Withal, what sets carbon apart from other elements is its tendency to generate strong covalent bonds with itself, resulting in an array of kinetically stable allotropes having different dimensions. The extensive structural diversity found for carbon materials can result in different properties, such as fullerenes, carbon nanotubes, graphite (sp^2 hybridization), and diamond (sp^3 hybridization).[43,44] With interest, graphite is characterized being dull, soft, and opaque. In contrast, the diamond stands out for being brilliant, transparent hard (Figure 1.1).

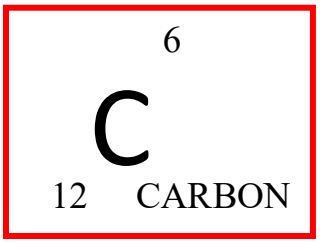

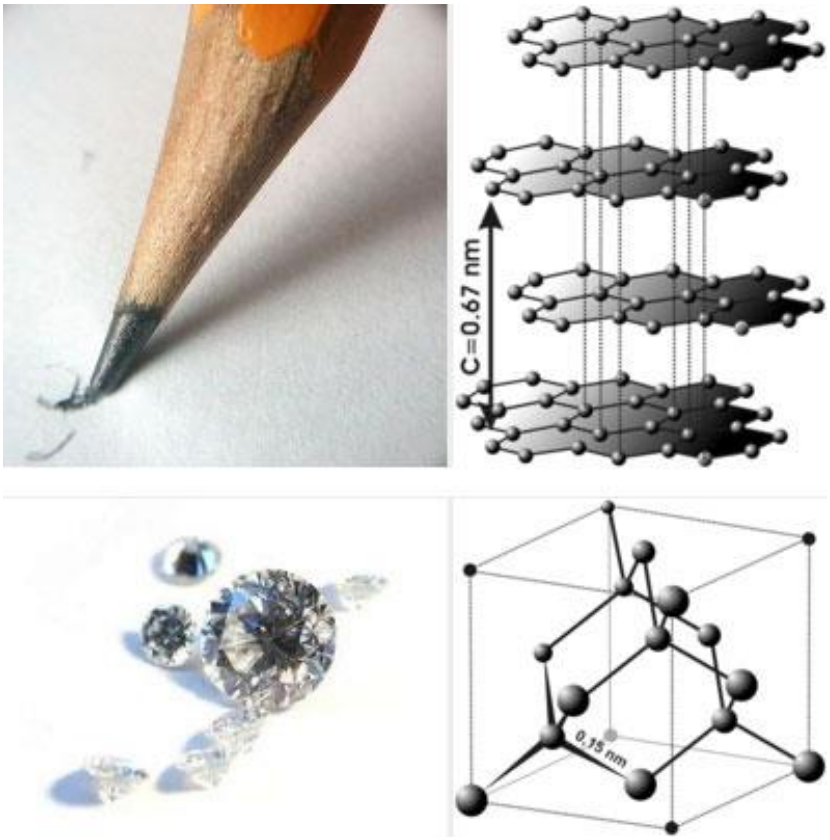

Figure 1.1: *Diamond (bottom) vs. graphene structure (top). Source: German Wikipedia, original upload 7. Feb 2004.*

Carbon nanomaterials are specifically attractive because of their mechanical and physicochemical properties, e.g., large surface area, electronic properties, corrosion resistance, and thermal stability. Due to these characteristics, carbon materials have been widely utilized as excellent catalytic supports for metal-based catalysts.[45,46] Nevertheless, amorphous carbon materials have different drawbacks, such as low stability and low oxidation resistance. Recently, many nanocarbon materials have been developed, e.g., fullerenes,[47] activated carbon,[48] carbon nanotubes,[49] carbon nanofibers,[50] and graphene-based materials[51] (Figure 1.2).

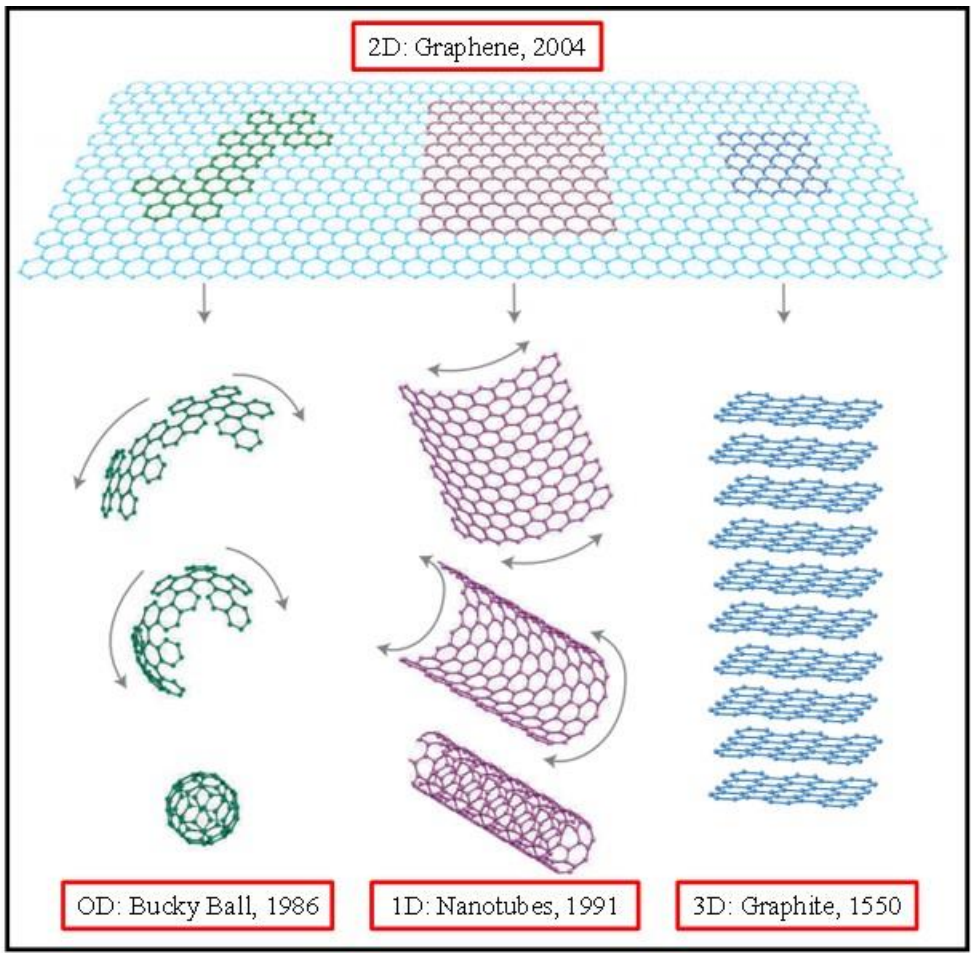

Figure 1.2: *Carbonaceous materials. Reprinted with permission from ref.*[52]*. Copyright 2007 springer Nature.*

The peculiar structure and the exceptional electrical, mechanical, and optical properties[53,54] of these materials have extensive development in various areas, for example, composite materials or optoelectronic sensors and many more. These carbon-based materials have also emerged as efficient support for the TM and metal nanoparticles in heterogeneous catalysis.[55] Comparing with the rest of the carbon family, graphene and its derivatives have recently attracted much attention of the researchers because of its outstanding properties.

Graphene, two-dimensional materials formed by a monolayer hexagonal arrangement of sp^2 hybridized carbon atoms, is two hundred times stronger than steel, very featherlight, and flexible. Besides, graphene materials offer the highest intrinsic carrier mobility at mild conditions

with a perfect atomic lattice and magnificent thermal, electrical, optical, and mechanical properties. Graphene was discovered and characterized by Andre Geim and Konstantin Novoselov in 2004 at the university of manchester, while both professors were awarded the Nobel Prize in 2010 *For their groundbreaking experiments regarding the 2-dimensional material (graphene).*

As commented previously, graphene materials have the largest surface area (2630 m^2/g) as compare to the rest of the nanostructures carbon materials (100 to 1000 m^2/g). Besides, in graphene oxide, the high degree of oxygenated groups present on the surface allows easy covalent, non-covalent, as well as ionic functionalization of the materials. The feature makes graphene materials ideal candidates ina new sustainable heterogeneous catalytic system.

1.3 Preparation methods of graphene-based carbocatalysts

Preparation of graphene and its derivatives have already been reported.[57–63] Therefore, this thesis only focuses on the preparation methods of graphene materials suitable for catalyst applications. GO and reduced graphene oxide (rGO), which contain a certain degree of defect sits, are by far the most common graphene-based carbocatalysts. The oxidation of graphite in the presence of potassium chlorate ($KClO_3$) and fuming nitric acid (HNO_3) was developed by B.C. Brodie, in 1859. He was the first to treat graphitic powder with $KClO_3$ in concentrated fuming HNO_3,[64] and got new materials, which was later determined to consist of carbon, oxygen, and hydrogen results, increasing the overall mass the flake graphite. Brodie method was further improved by Staudenmaier [65] in 1898, by adding concentrated sulfuric acid as an extra additive, which led to a highly oxidized graphite oxide in a single reaction vessel. In 1937 Hoffman[66] utilized concentrated sulfuric acid in combination with concentrated nitric acid and $KClO_3$ for the graphite oxide synthesis. In 1958 Hummer's and Offeman shows an alternative method[67] with the aid of strong acid (nitric and/or sulfuric acid) and oxidant (permanganate) (Scheme 1.3); however, the real structure of GO is still under argument (Figure 1.3).

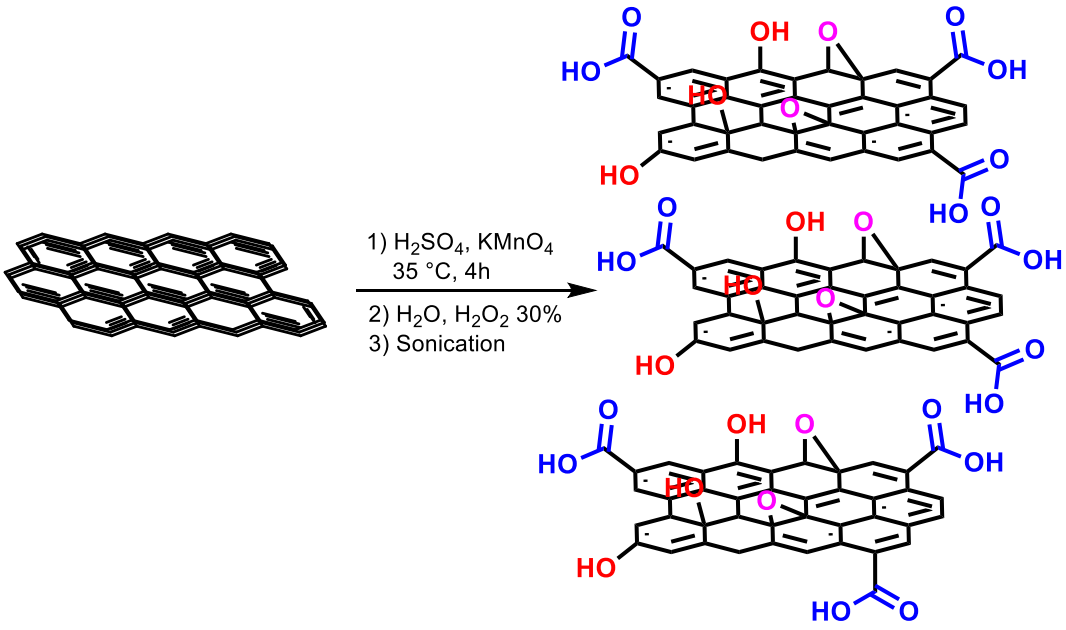

Scheme 1.3: *Modified Hummers-Offeman's method for the synthesis of GO.*

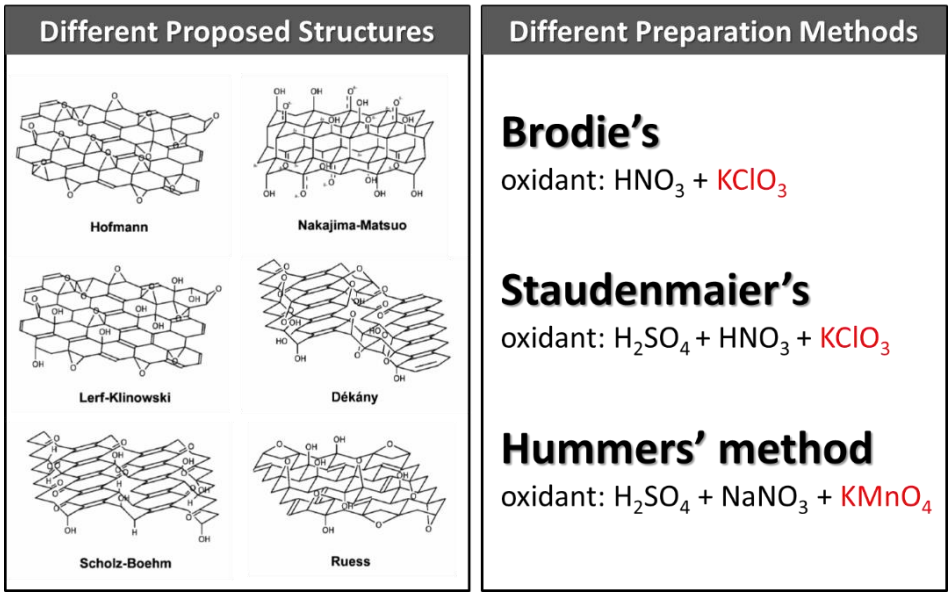

Figure 1.3: *Proposed structures of GO materials and reported methods for the synthesis of GO.*

The most popular method is Hummer's method, which has been further improved and modified.[68] For example, $NaNO_3$ converts to various harmful and environmentally unfriendly gases; thus, analogous ways that do not utilize this salt are desired. For instance, Kovtyukhova demonstrated that the pre-treatment of graphite with P_2O_5 and $K_2S_2O_8$ in H_2SO_4 enabled the $NaNO_3$-free synthesis of GO.[69] Likewise, pre-treating graphite with MnO_2[70] or irradiation of microwave[71] also promotes the efficient formation of GO (Figure 1.4, step 1). Tour utilized H_3PO_4 instead of $NaNO_3$,[72] and Shi noted that water enhances the oxidation of graphite (Figure 1.4, step 2).[73] Besides, treatment methods after oxidation water and H_2O_2 are reported to accelerate the oxidation degree of GO.[74,75] Despite many improved methods for GO production, as mentioned above, we have shown that the pre-oxidation of graphite is not needed and that the critical reagents ($KMnO_4$ and concentrated H_2SO_4) are required to facilitate Hummer's-type oxidations. Also, the use of less than 5 vol.% of water was found to facilitate the formation of single-layer GO.[76]

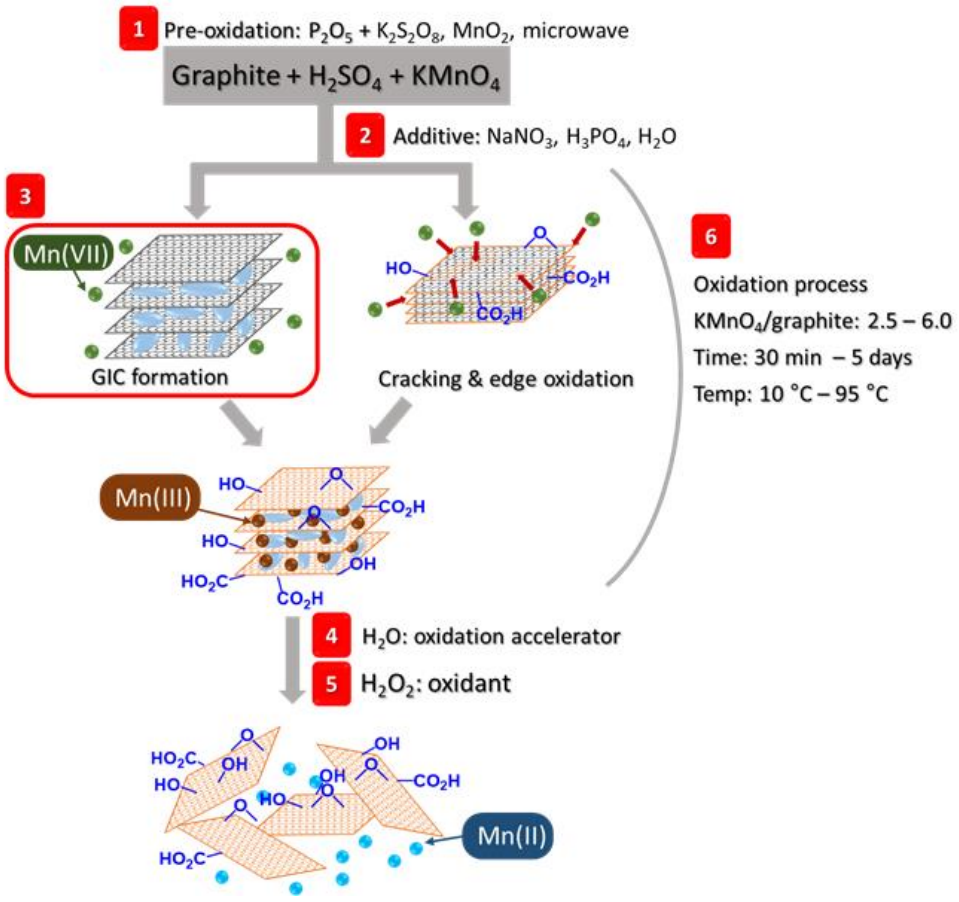

***Figure 1.4**: Summary of various synthesis methods of GO from graphite and remarks.*

Due to the high quantity of the oxygen functional groups on GO and the reactivity of the oxygenated functional groups, GO can inevitably undergo decomposition and aging under catalytic conditions. To tailor the properties of GO on purpose, enormous research has been done to remove the oxygenated functional groups from GO (Table 1.1).[77,78] Various methods and techniques, such as chemical agents,[79] electrochemistry,[80,81] UV irradiations,[82,83] microwave irradiations,[84] micro-organisms,[85] ion bombardment,[86] or thermal treatments,[80,82,87] were developed to tune the properties of rGO. The material design includes the C/O ratio, selective removal of the oxygenated functional groups such as hydroxyl, carboxyl, and epoxy, healing of the surface defects to maintain and improve the properties which are required for carbocatalyst.[98,99] the proposed structure of rGO is presented in the below (Scheme 1.4). Please note that this is only an example; there is no definitive structure of GO, as no stoichiometric definition so far).

Table 1.1*: Summary of various reduction methods of GO to rGO.*

Method	**Characteristics**
Chemical agent	The reduction is performed in liquid. Commonly used chemical agents are as follows. Borohydride: mainly reducing carbonyl groups. Aluminum hydride: removing carboxylic acid and ester. Hydrohalic acid: removing hydroxy and epoxide.
Electrochemical reduction	The reduction of GO occurs at the cathode, avoiding the use and contamination of chemical agents.
UV irradiation	Elimination of hydroxy and carbonyl functional groups occurs.
Microwave irradiation	Solid-state microwave irradiation not only removes oxygen-containing groups but also repair defects of the graphene sheets. Microwave removes C=O efficiently.
Micro-organism	Elimination of epoxy and alkoxy functionalities occurs.
Ion bombardment	Epoxy and carbonyl could be retained mainly.
Thermal treatment	High-temperature treatment results in much higher degree reduction as compared to chemical reduction.

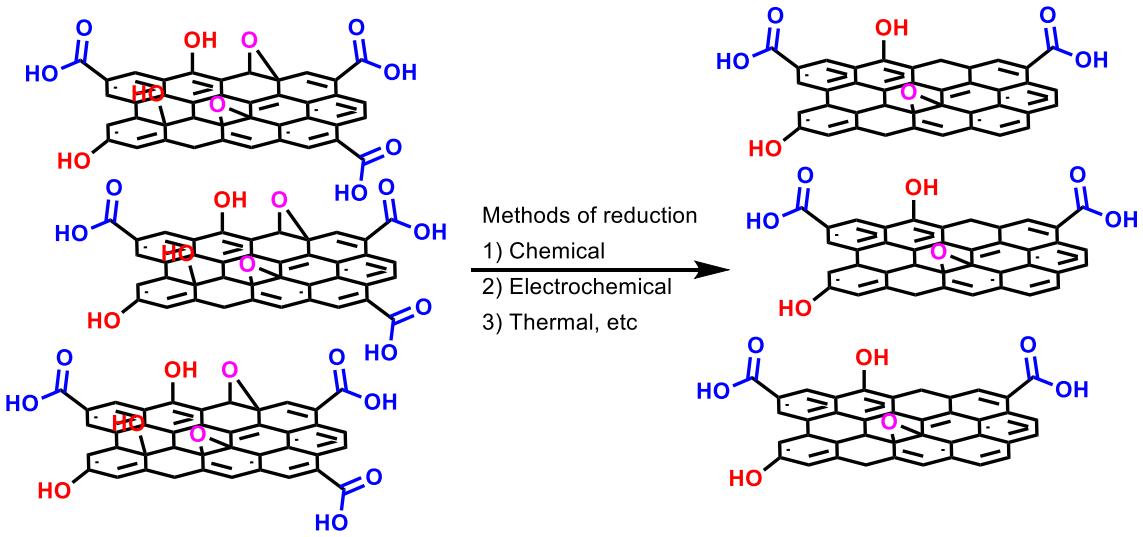

Scheme 1.4: *Synthesis of rGO with various methods.*

1.3.1 Doping of graphene-based materials

One of the prospects to incorporate the active site on graphene materials is to replace one carbon atom by other elements, e.g., nitrogen, sulfur, etc., leading to doped graphene-based materials. The most widely utilized dopant elements are B and N, recently doping with S, P have also been reported.[90,91] Definitely, the dopant of heteroatoms having empty and full orbitals will be of large potential in the field of catalysis, because of that the variety of Lewis acidic and basic sites of having strength in solid catalysts that can catalyze a large number of organic reactions.[92,93]

The parameters with impact in catalysis, for the doped or functionalized graphene, are the loading of the dopant element and its dispersion through different types according to their bond structure. The dopant element also influences the electronic and geometrical properties of the graphene oxide, causing around the dopant element a remarkable deviation from the local electronic density, planarity, and bond angles of the ideal graphene materials.[94] Among other considerations, dopant elements can also introduce Lewis acid or basic sites depending on the number of electrons or orbitals acquaint by the heteroatom and may work as FLP sites. Theoretical

studies have shown that working with simple models, the presence of heteroatoms on graphene generates a gap between the empty and full frontier orbitals, and accordingly, doped graphene exhibits behavior as a semiconductor in contrast to the conductive properties of the ideal graphene materials. There are various possibilities to synthesize doped graphene oxide, as presented below (Scheme 1.5).

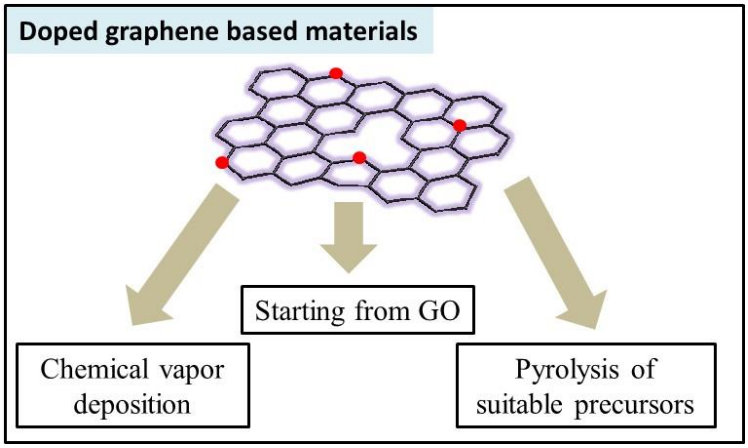

Scheme 1.5: *Synthesis methods to obtain doped graphene-based materials.*

Another approach for preparing doped graphene starts with GO that reacts, generally in the liquid phase, with a specific substrate of the dopant element, such as NH_3 or urea. The oxygenated functional groups (epoxy or hydroxy, etc.) of GO react with precursors (dopant element) by substitution, nucleophilic, or condensation reaction leading to doped GO, in which the dopant element is bonded to the carbon of graphene materials. This method is very convenient because of the easy availability of GO, its high solubility in various solvents, and its high reactivity with different nucleophilic substrates. In principle, the loading levels that are accomplished from GO can be substantial, seeing the proportion of functional groups. For example, alginate, a polysaccharide of mannuronic and guluronic acids, may be esterified with boric or phosphoric acids.[95] The OH group of sugars tend to generate esters with inorganic acid and carboxylic acids. Pyrolysis of these modified esters of inorganic acids gives graphene containing heteroatom, for instance, B, N, S, and P. Furthermore, if chitosan, already containing N, is modified with boric

acid to generate the corresponding borate ester, then pyrolysis of this modified chitosan leads to the formation of B and N codoped graphene.[93]

1.4 Typical liquid-phase reaction catalyzed by carbocatalyst

Since Bielawski and co-workers[33] demonstrated the ability of graphene-based materials to facilitate a number of synthetically useful transformations, the concept of "carbocatalysis" being widely explored and considered as an intriguing new direction in chemistry and materials science, the surface-bound oxygenated functional groups on the aromatic scaffold of GO is believed to allow ionic and nonionic interactions with a series of atoms and molecules. Numerous organic transformations, such as oxidation of alcohols and alkenes into their respective aldehydes and ketones, and the hydration of alkynes, carbon-carbon coupling reaction, have been carried out using graphene-based materials as a carbocatalyst. Here in this thesis, we will briefly review the catalytic performance of the graphene-based materials as carbocatalyst.

1.4.1 Oxidation reaction

The selective oxidation reaction of alcohols to carbonyls was traditionally accomplished in several ways, most of which need inorganic oxidants. The insertion of oxygen into organic substrates using oxidation or hydration transformations are generally achieved by TM based catalysts, which are quite expensive, toxic, difficult to remove, and are obtained from limited natural resources. Thus, the search for an alternative catalyst that combines the toxicological benefits of a metal-free synthesis with the convenience of heterogeneous setup, while maintaining high activity, is a continuing endeavor of critical importance.[96] Bielawski reported that the easily available and inexpensive carbon-based material as a catalyst for the generation of aldehydes or ketones from different alcohols, alkenes, and alkynes (Scheme 1.6).[33] These reactions were found under relatively mild reaction conditions and afforded the target products (aldehyde, ketone, or acid) in good yields. Notwithstanding, excellent chemoselectivity and activity were achieved, while a high GO loading (200 wt %) was needed.

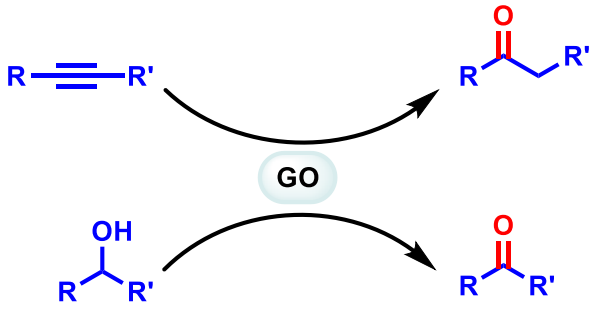

Scheme 1.6: *GO catalyzed oxidation reaction.*

Similarly, alcohol can be oxidized with N-doped graphene (N-Graphene) as carbocatalyst.[97] Wang and coworkers reported that the graphitic sp^2 nitrogenic sites are the active site for catalytic reactions based on a Langmuir-Hinshelwood mechanism through the possible generation of the sp^2 N-O_2 adduct transition state that shows high reactivity towards alcohols (Scheme 1.7). The non-catalytic conversion of the alcohols by carbene or electron-deficient defects on N-Gr was also speculated.

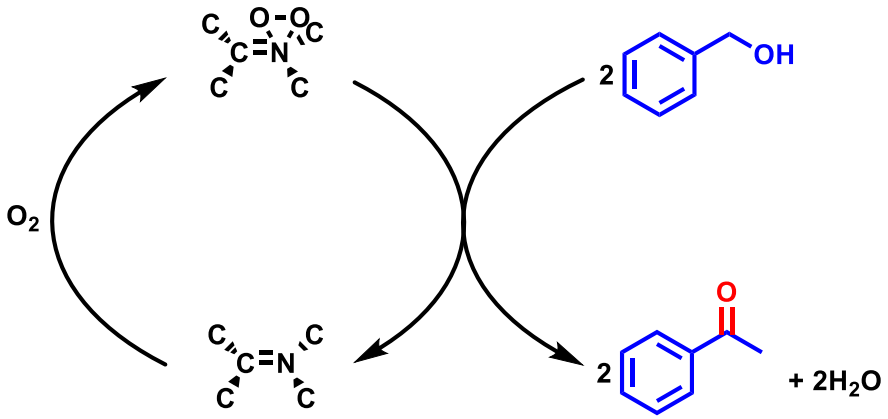

Scheme 1.7: *Proposed reaction pathway for aerobic alcohol oxidation over N-rGO.*

Kim prepared NrGO, which contained 6.3 at.% of N and was found to a significantly active for the oxidation of styrene, benzyl alcohol to the corresponding aromatic products through a free-radical pathway with tertbutylhydroperoxide (TBHP).[98] The inclusion of methanol yielded aromatic esters, while without the TBHP, aromatic ethers were observed instead. Moreover, using

a facile technique based on the microsonochemical method, and NrGO loading of only 30 wt % was needed to give high yield with high selectivity.

In addition, the oxidation reaction of alcohol, GO has also been utilized to activate the benzylic C(sp^3)−H and C(sp^2)−H bonds. This catalytic reaction was first reported with GO catalyst by Bielawski, who reported the corresponding ketone products in high yields, while a large quantity of the GO was required.[99] This method was found not suitable to obtain aldehyde product. Several other doped graphene materials were then investigated to prevent the limitations of GO. Ma and coworkers prepared NrGO starts from GO with acetonitrile as N source via a chemical vapor deposition process. Furthermore, the NrGO was utilized as a catalyst for the oxidation reaction of aryl alkanes, linear hydrocarbons, and cyclic paraffin to the corresponding oxidized compounds with TBHP oxidant.[100] Similar to the work above of Wang,[97] graphitic sp^2 nitrogen was assigned as the active site of the catalyst. Notably, the graphitic sp^2 nitrogen did not proceed with the catalytic process but changed the electronic properties of the neighboring carbon atoms and enhanced the generation of reactive oxygen species (peroxide radicals). Aside from that, Kim reported that the conversion of aliphatic chains into aliphatic ketones with N-rGO.[98] Moreover, N, B, co-doped-rGO (N 5.6 at.wt %, and B 2.1 at.wt %) and could selectively catalyze the oxidation reaction of cyclooctene and benzylic hydrocarbons to the corresponding ketones and alcohols (Scheme 1.8) with a low catalyst loading (0.1 wt %), with low conversion (50 %).[93] Control investigations were conducted with bare GO, B, and N-doped graphene, activated carbon, and MWCNTs showed much lower conversion rates. Besides, styrene was converted by N, B, co-doped-rGO into styrene oxide and benzaldehyde in low yields. Antonietti and coworkers investigated the synergistic effect of graphene/g-C_3N_4 nanocomposite for the cyclic saturated hydrocarbons oxidation reaction.[101] By this system, cyclohexane, a 12 % conversion with 94 % selectivity for cyclohexanone, was accomplished. Howbeit, the non-catalytic behavior toward n-hexane and DMSO highlighted the need for pre-adsorption of starting materials before the catalytic reaction may proceed over superoxide anion radicals.

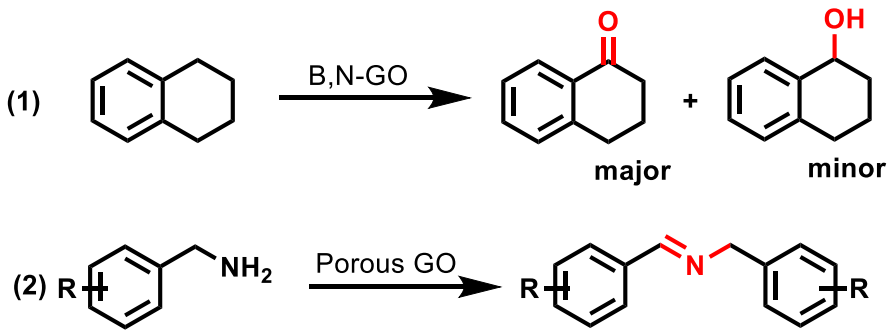

Scheme 1.8: 1*) Oxidation reaction of tetralin to the corresponding alcohol and ketone catalyzed by B, N, co-dopedrGO,* ***2****) Aerobic oxidative coupling reaction amine to imine utilizing porous GO as a catalyst.*

GO was also found active the oxidation of thiol to disulfides without over oxidation and with high conversion rates, which are generally achieved only with TM catalysts (Fe, Mo, and Pd) as reported by Bielawski (Scheme 1.9).[102] The catalytic performances of other carbons such as activated carbon, graphite, and hydrazine-reduced GO paled compared to that of GO. The reactivity of arene-functionalized substrates bettered that of alkyl-functionalized substrates. Furthermore, the application of GO was extended as a catalyst for the oxidation reaction of sulfide to the sulfoxide, which is conventionally catalyzed by Ru and Fe catalysts. This was, however, only possible with a GO loading of 300 wt %. GO worked as an oxidant and was reduced throughout the reactions.

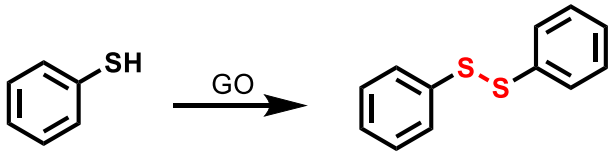

Scheme 1.9: *GO catalyzed oxidation of thiophenol.*

The catalytic oxidation reaction of amines to imines using molecular oxygen as an oxidant was also demonstrated with GO (Scheme 1.8) reported by Fan.[103] Natural flake graphite, MWCNTs, activated carbon, and rGO were reported lower to GO for this catalytic reaction. The effect of trace metal in GO catalyzed reaction measured with ICP-MS, and found 30 ppb of manganese, while the other trace metals were found below the detection limit. Primary and

secondary amines have also been oxidized with high yields, but aliphatic amines and amines lacking a hydrogen atom at the α-carbon position was not reactive. Furthermore, the syntheses of asymmetrical and cyclic imines were also attained. Loh synthesized porous GO by several acids and base treatments, without metallic impurities, while additional defects and pores were introduced into the graphene framework. Furthermore, the author utilized GO as a catalyst for aerobic oxidative coupling of amines to imines with porous GO catalyst.[104] The appearance of the ovoids was found to provide a high amount of edges with localized spins and found effective with the combination of carboxylic acid groups on the porous GO. This study clarified the functional groups of GO materials that gave rise to their catalytic effects. Ma and coworkers showed the synthesis method of the thiuram disulfide from secondary amines and carbon disulfide with rGO, which is one-pot synthesis bis(aminothiocarbonyl)disulfides (Scheme 1.10). The rGO can be recycled at least four times without any loss of catalytic activity and selectivity.[105]

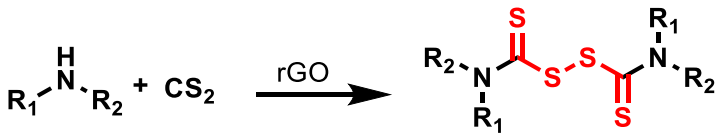

Scheme 1.10: *rGO catalyzed the bis(aminothiocarbonyl)disulfides in one-pot.*

Alkylamine and cyclic secondary amines were transformed into the thiuram disulfide in high yields. However, secondary aromatic amines were reported less reactive and required a strong base to facilitate the reaction. The authors also claimed that the unpaired electrons at the edges of the graphene might activate the O_2 to superoxide anion radicals, which further initiate a coupling reaction with dithiocarbamic acids to generate thiuram disulfide.

1.4.2 Hydrogenation reaction

One of the most important catalytic reactions in the petrochemical industry is the hydrogenation of multiple C−C bonds, which often require transition noble metals (Pt, Pd, Ni, Rh, and Fe) as a catalyst. The ability of graphene-based materials to act as a catalyst for the hydrogenation reaction and will contribute to this challenging area of chemistry. Bao utilized rGO as a catalyst for the hydrogenation reaction of nitrobenzene to aniline (Scheme 1.11),[106] the results reveal that the electronic properties of rGO are effective and the rGO can be a new alternative metal-free catalysts. The zig-zag edges of rGO may act as active catalytic sites to facilitate the activation of a reactant molecule. Garcia and coworkers also reported the selective hydrogenation of acetylene and other alkenes catalyzed by graphene-based materials as metal-free alternatives catalyst.[107]

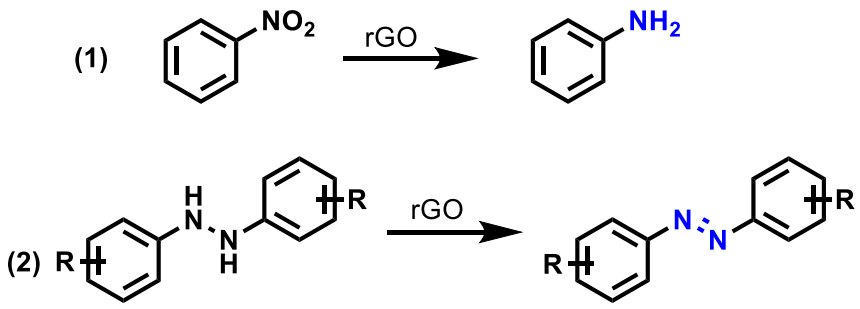

Scheme 1.11: ***1****) Hydrogenation of nitrobenzene to aniline using rGO,* ***2****) aerobic oxidative dehydrogenation reaction of hydrazo compounds with rGO.*

Defective graphene can also catalyze the oxidative degradation of C=C in conjugated alkenes (Scheme 1.12). Strizhak explored the catalytic activity of thermally reduced GO (TrGO) and nitrogen-doped thermally reduced GO (N-TrGO) for the hydrogenation of acetylene, while in the temperature range of 50 to 400 °C.[89] The author hypothesized that the doping of the nitrogen in the graphene framework decreases the total activity for acetylene hydrogenation and the selectivity for ethylene. While the oxygen-containing functional groups like ketone and hydroxyl groups may also contribute to catalytic activity, but they did not explore with characterization.

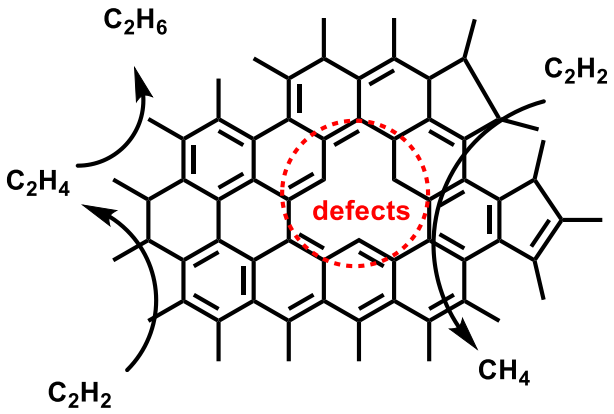

Scheme 1.12: *rGO catalyzed the hydrogenation reaction of acetylene.*

Hydrothermally treated GO has been reported as a new metal-free catalyst for the activation of $NaBH_4$, which further reduces the 4-nitrophenol to 4-aminophenol.[108] Generally, carbon material donates electron density to the metal center and enhances the hydride transfer. The experimental and theoretical studies suggested that pores and defects in the carbon sheet formed by acidic hydroxyl groups benefit this activity, meaning FLP structure sites can be assigned.

1.4.3 C–C coupling reaction

1.4.3.1 Oxidative and reductive coupling reaction

Loh and coworkers improved the activity of GO by a sequential base and acid treatment and obtained a 98 % yield of imine at a five wt % catalyst loading.[104] This means that there is great potential to improve the catalytic performance of the graphene catalyst. However, the amount of catalyst used was still higher than that of the metal catalyst. A model molecule (1-Pyrenecarboxylic acid) was used as a catalyst and found that the origin of the activity was attributed to the synergistic effect of the carboxyl group on the edge and unpaired electrons next to the COOH group of an adjacent benzene ring (Scheme 1.13).

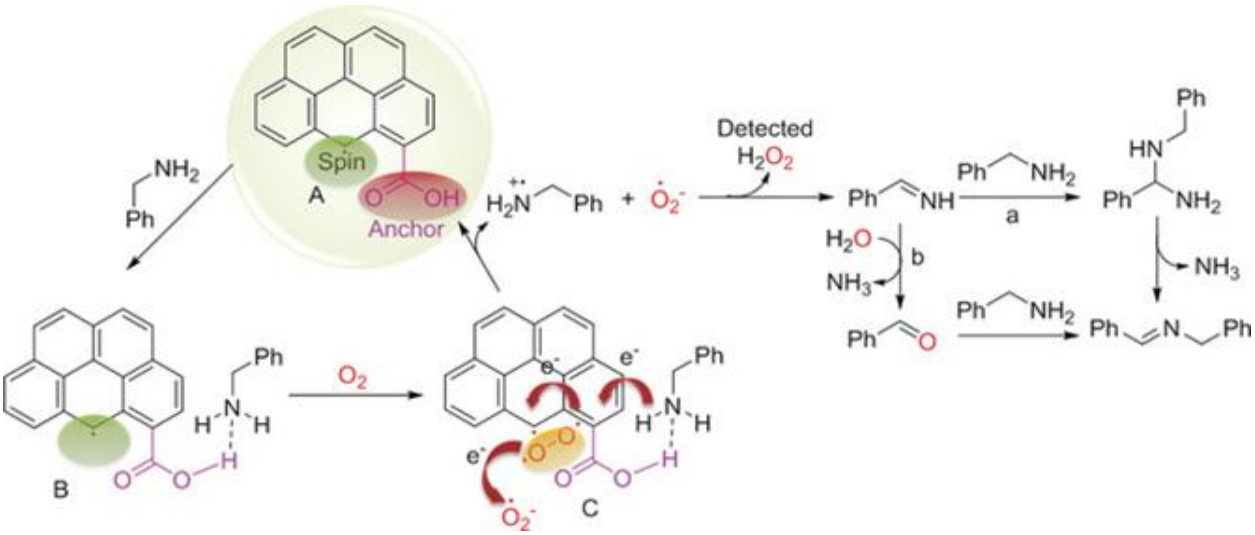

***Scheme 1.13**: Oxidative coupling reaction of amines to imines over GO. Reprinted with permission from ref.*[104]*.Copyright 2007 American Chemical Society.*

GO can also catalyze the Claisen-Schmidt coupling reactions of a series of alkynes or methyl ketones with alcohols and aldehydes to generate chalcones related compounds.[109] The reactions occur via in a tandem process: GO first proceed the hydration or oxidation of various alkynes or alcohols to their corresponding methyl ketones or aldehydes, respectively, and then these species further undergoes to the coupling reactions.

The oxidative homo-coupling reaction of β-naphthols gives binaphthols, which are widely utilized as ligands and DNA cross-linking reagents.[110,111] Commonly, binaphthols are synthesized by Fe,[112] Cu,[113] and V[114] catalysts. To overcome these limitations, Ranganath utilized GO as an efficient catalyst for the oxidative coupling of 2-naphthols.[115] It was observed that solvent plays an essential role in this reaction; when the reaction was performed in aqueous media, which leads to polymerization of the product, while in organic solvents, the reactants go selectively to binaphthol (Scheme 1.14). Furthermore, to arbitrate the effect of GO, various carbon materials such as graphite, carbon nanotubes, functionalized CNTs, and activated charcoal were utilized as catalysts under the optimized reaction conditions, but lower product yields were observed. Additives such as NaOH or KOH was required to generate the product in >90% yield; without the additive, only 20% of the target product was obtained. The GO catalyst could be recycled three times, but the active site and the effect of solvents is not clear at this stage.

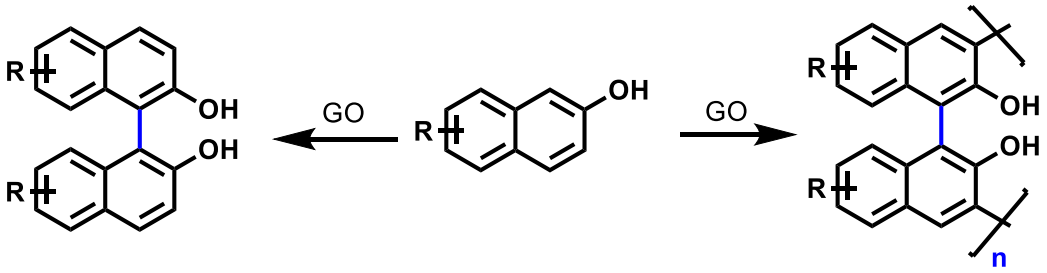

Scheme 1.14: *Oxidative coupling of β-naphthol catalyzed by GO.*

Gong investigated the active catalytic center on GO using various small molecules with various oxygen functional groups, such as hydroxy, carbonyl, epoxide, and carboxylic acid, and different π-conjugated systems.[116] Albeit, no product was observed, indicating that only a single functional group does not attribute to the catalytic property of GO. Other carbon-based materials, such as activated carbon, graphite, acetylene black, and rGO, were also tested, but all were found inactive. These findings indicate that the catalytic activity of GO was irrelevant to the π-conjugated system. Thus, the author proposes that the unpaired electrons on the GO might play a crucial role in the coupling reaction, which is already presented in the hydrogenation reaction[104] (Scheme 1.15). In this context, hydrogen may be captured by the unpaired electron on the GO edge, and the aromatic radical is generated. Finally, the radical coupling reaction subsequently occurs with the coupling partner, and the desired product can be generated. Oxidative carbocatalysis has the potential to replace several TM catalyzed or stoichiometric oxidative reactions. It should be commented that further experiments are needed to rule out the possibilities of metal-induced catalysis, because contamination of ppm level of metal species may not be prevented in the most of the carbon materials.[117]

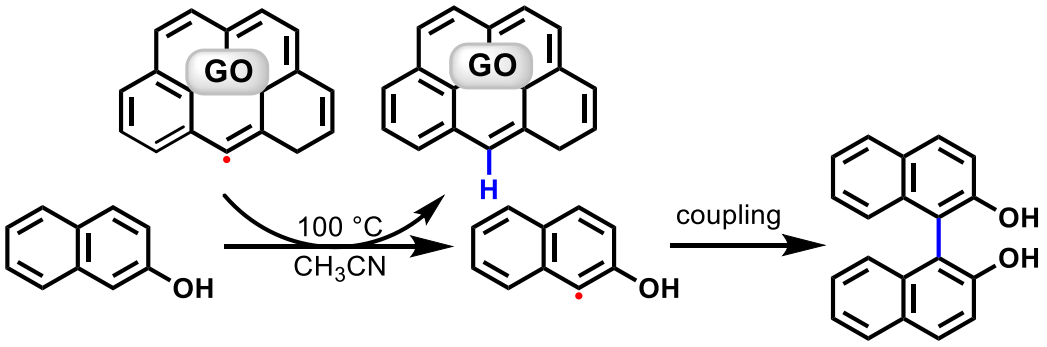

Scheme 1.15: *Mechanism of homo-coupling of β-naphthol catalyzed by GO.*

We reported a radical coupling reaction between aryldiazonium salts and electron-rich five-membered heterocycles catalyzed by rGO (Scheme 1.16).[118] The reaction provides rapid access to 2-arylfurans, pyrroles, and thiophenes under mild conditions, and the rGO catalysts can be reused several times. The localized radicals on the surface of rGO play a vital role in the coupling reaction.

Scheme 1.16: *GO catalyzed the coupling reaction between aryldiazonium salts and five-membered heterocycles.*

1.4.3.2 Aldol-type reaction

The aldol reaction is one of the essential methods of forming carbon-carbon bonds. The products, chalcone derivatives, are precursors for the biosynthesis of flavonoids and isoflavonoids.[119] The capability of GO as a catalyst was also examined for aldol reaction over various electron-withdrawing and electron-donating aromatic aldehydes with acetophenone under the condition solvent-free (Scheme 1.17).[120] In this study, the authors reported that GO works as a base catalyst. In contrast, Zali modified the surface of carbon materials with $-SO_3H$, which showed higher catalytic activity than sulfuric acid.[121] Asphaltene oxide (AO) produced by the Hummer's type oxidation of asphaltene also catalyze aldol reaction.[122] The origin of catalytic activity was examined by changing various parameters such as the effect of elemental composition, the dosage of catalyst, and particle size. In the presence of a base (i.e., pyridine), the product was not observed due to a neutralization reaction. Thus, the catalytically active sites are acidic sites on the carbocatalyst. GO catalyzed reactions are sometimes argued because of the contamination of metal species, removal of its oxygenated groups, and residual acids/oxidants.[123]

Cid developed a bifunctional amine catalyst, in which piperazine was grafted on to rGO.[124] The presence of two nitrogen atoms in piperazine provides a possible route to iminium and basic ammonium activation for aldol reaction. In the case of aldol reaction, the rGO support did not offer

any noticeable stabilization effect for the catalyst. The bared rGO was utterly inactive for aldol reaction.

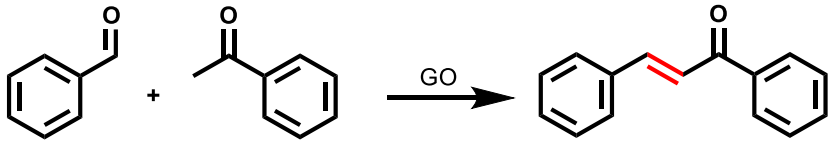

Scheme 1.17: *Aldol condensation reaction between acetophenone and benzaldehyde catalyzed by GO.*

1.4.3.3 Freidel-Crafts-type reaction

The alkylation of arenes is generally catalyzed by TM catalysts to get pharmaceutical component and fine chemicals. Interestingly, graphene-based materials was also found effective that catalyze the direct Friedel-Crafts alkylation reaction of arenes with styrene and alcohols.[125] The surface electrons of graphene are considered to affect the electrophilic intermediate. In this context, Kumar and Rao utilized GO as a catalyst for the Friedel-Crafts-type alkylation reaction of indoles to α,β-unsaturated ketones, or nitrostyrene (Scheme 1.18).[127]

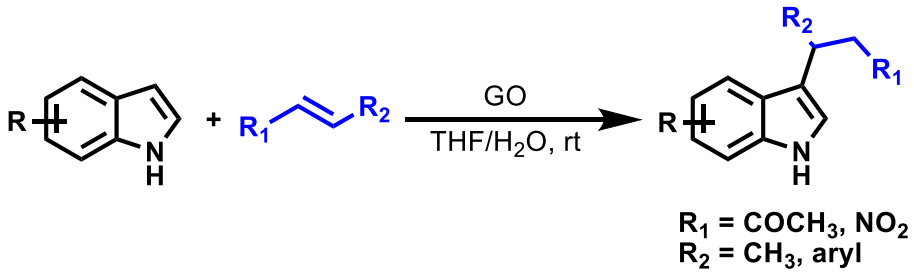

Scheme 1.18: *Friedel-Crafts addition of indoles to α,β-unsaturated substrate catalyzed by GO.*

Guerra reported GO as catalyst for the Friedel-Crafts reaction between indole and epoxides (Scheme 1.19).[128] graphite and carbon were used as catalysts for comparison, but showed negligible yield, suggesting the activity of GO is probably due to the carboxylic and hydroxy groups. The product was obtained regioselectively with complete inversion, indicating that the

GO-catalyzed reaction was S_N2 fashion. This reaction is typically catalyzed by nanocrystalline TiO_2,[129] Fe_3O_4 or $CuFe_2O_4$.[130]

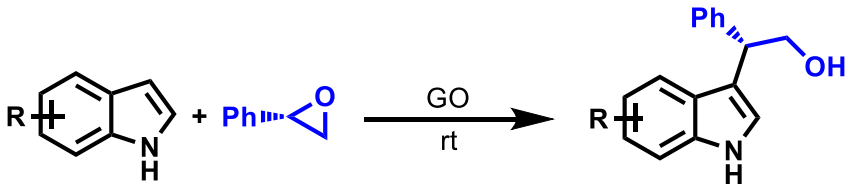

Scheme 1.19: *Regioselective ring-opening reaction of styrene oxide with indole catalyzed by GO.*

1.4.3.4 CH−CH homocoupling reactions

The activation of C−H bonds by carbocatalysts to form C−C bonds has recently emerged as a hot topic in carbocatalysis. The development of metal-free carbocatalysts for CH−CH type coupling, one of the most difficult chemical transformations, has rarely been reported.[131] We reported the use of GO as a catalyst for the formation of the C−C bond of anisoles and derivatives, of which mechanism was clarified as a free radical pathway.[132] The reaction conditions were initially optimized in the oxidative coupling of 3,4-dimethoxytoluene to the corresponding dimer. It was found that GO, in conjunction with $BF_3{\cdot}OEt_2$ afforded the biaryl product in excellent yield; however, GO was reduced and lost its activity after the reaction (Scheme 1.20). It was demonstrated that the developed conditions are superior to those using hypervalent iodine reagent, $PhI(OAc)_2$. Impressively, the substrate scope was shown to include halogen-containing substrates, which could be used as handles for traditional cross-coupling reactions. The reaction mechanism was investigated by adding a radical scavenger (TEMPO) and monitered the reaction by electron spin resonance (ESR), confirming the presence of radical species in situ.

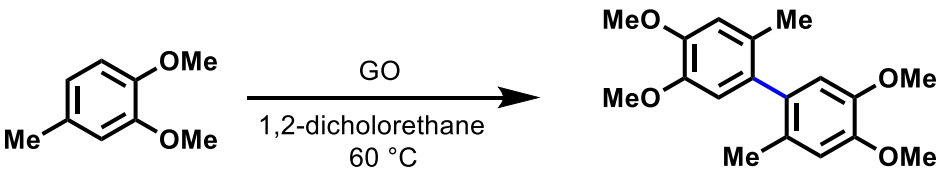

Scheme 1.20: *GO catalyzed the homocoupling of anisole derivatives.*

1.4.3.5 CH−CH cross-coupling reactions

CH−CH cross-coupling is one of the most challenging reactions. Recently, fine-tuning the substrates and reaction conditions enabled the selective functionalization of C−H bonds. Loh and Su carried out the cross-coupling of xanthenes or thioxanthene with arenes in the presence of GO with $TsOH{\cdot}H_2O$, yielding 85 % of the corresponding CH−CH cross-coupling products with high selectivity (Scheme 1.21).[133] The mechanistic study showed that the reactivity of GO was corresponded to the concentration of quinone type species (C=O) but had no apparent relationship with the content of epoxide and hydroxy groups. The use of small-molecules analogs allowed mimicking the active site of the catalyst. Molecular analogs such as benzyl alcohol, hydroxy, epoxides, and carboxy groups were not effective. Whereas their zig-zag edges counterpart, such as tetracene and pentacene, afford higher reactivity (54 %). Anthraquinone, which incorporates both the zig-zag edges and the C=O species, furnished the best performance (76 %) among all the tested small-molecule analogs.

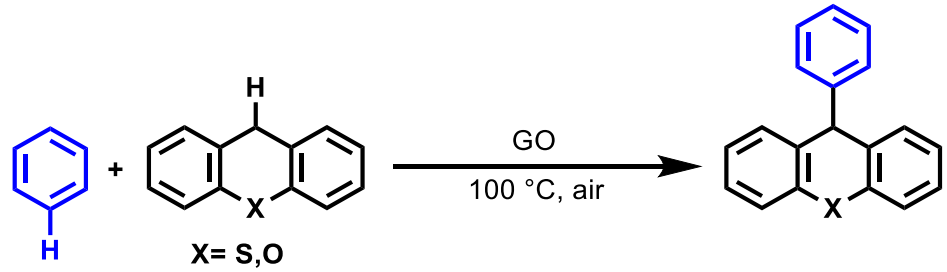

Scheme 1.21: *GO catalyzed CH−CH cross-coupling of xanthene with arenes.*

1.5 Objective and scope of the present study

Based on the aforementioned problems associated with the metal-based catalysts, the present study provides an effective response to them. In general, this study attempts to design and functionalized highly active, durable, and easily recyclable carbocatalyst for organic transformations such as coupling and reduction reactions. Based on the previous discussion, graphene materials have the highest surface area (2630 m^2/g) in comparison to the rest of the nanostructures carbonaceous materials (100 to 1000 m^2/g). Additionally, for example, in the case

of graphene oxide, the high degree of oxygen functional groups present on the structure allows as easy covalent and non-covalent functionalization of the materials. The feature makes graphene materials ideal candidates ina new sustainable heterogeneous catalytic system. Nishina is working in graphene-based materials for various applications, also started this material for catalyst application Figure 1.5.

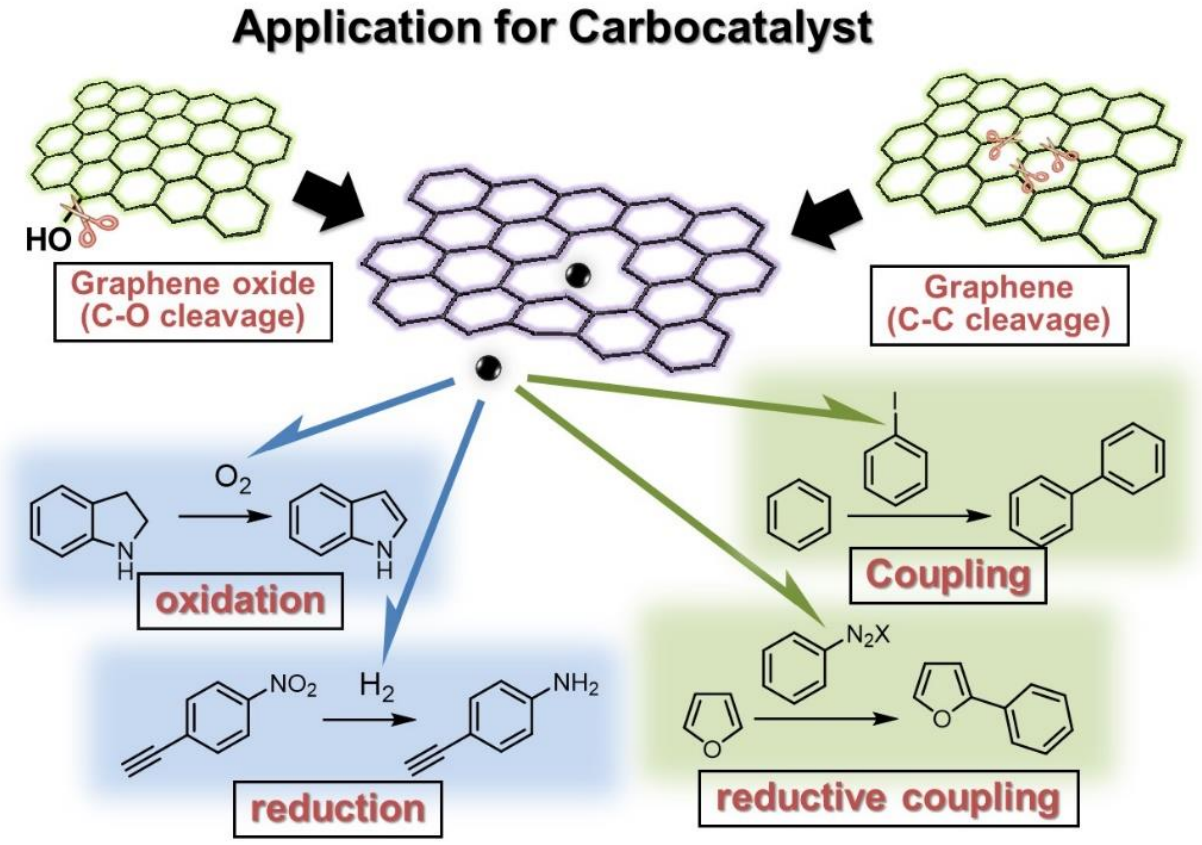

Figure 1.5: *Unpaired electron on nanocarbon for catalysis.*

Graphene and graphene-based materials have been developed over the last ten years as carbocatalsyts, and it is doubtless that such materials can catalyze many liquid phase reactions in organic chemistry. Although the actual mechanisms and the active sites of the carbon catalysts remain issues to be solved, the activity of carbon catalysts may be improved by optimizing the catalyst preparation and reaction conditions.

Now lets recall that in the first part of this chapter, talking about catalysis, we usually spontaneously think about transition metals, either as molecular species or as colloidal objects. Some of these transition metals are rare, and questions of sustainability do the search for alternatives a mandatory endeavor. In addition, many metals are not tolerant against functionality or are sensitive, e.g., against water and sulfur compounds, and especially the growing fields of modern biorefinery and biomass processing are strictly limited by the use of catalysts that can satisfy these criteria. In the last few years, it turned out that (metal-free) carbon-based materials, with large specific surface areas, are indeed effective as heterogeneous catalysts and have the potential to circumvent the described problems. Carbocatalysis for liquid-phase reactions, especially for organic synthesis, is an emerging research discipline and has undergone rapid development in recent years, Nishina reviews this topic up to somehow very recently in 2020.[134]

The intrinsic acidity and basicity of carbon materials as catalysts are related to the oxygenated functional groups or doped heteroatoms. Still, the distribution of acid/base functionalities is not well described in most of the studies reviewed here. More importantly, minor components may have any influence on the catalytic performance. In particular, when graphene oxide, which is prepared from graphite in H_2SO_4 and $KMnO_4$, is used, it always contains impurities by insufficient purification. One of the major motivation of this thesis is to overcome such problems in designing metal-free carbocatalyst, which will give the activity similar to or better than the metal catalyst. This dissertation also aims to provide an in-depth understanding of how the carbocatalyst works.

1.6 Thesis outline

As already seen, chapter 1 consists of an introduction relevant to the thesis work and the overall project objectives. We also discussed the synthesis methods of carbocatalyst and various effects of the strong oxidant, along with this, we also give a brief touch to the reduction of graphene oxide by various methods. Finally, the Overview of graphene-based materials as catalyst, also presents a comprehensive literature review of carbocatalysis.

In chapter 2 comprise the synthesis of nitrogen-doped reduced graphene oxide and its activity for CH functionalization reactions. The active catalytic sits are considered, and the mechanistic study was discussed.

Chapter 3 provides details of the catalytic activity of the carbocatalyst in terms of challenging chemoselective hydrogenation reactions, and the role of radicals was explored. The main conclusion resulting in this project are summarized in chapter 4, possible future work of research is also included.

In chapter 4, comprise the reaction mechanism of the alkylation of ketone with alcohol is still a matter of debate, is it a Meerwein-Ponndorf-Verley like process, or is hydrogen borrowing process by transition metals? Here, the alkylation reaction of ketones with benzylic alcohols via a radical pathway has been developed, where base treated graphene works as an initiator of radical reaction. Mechanistic study support that the radical anion of the benzylic alcohol is proposed to be the key intermediate, which further undergoes coupling with ketones via aldol condensation to form a new C−C bond with water the only byproduct. Chapter 5 concludes the work covered in this thesis.

1.7 References

[1] J. Matthey, The Early History of Catalysis, https://www.technology.matthey.com/article/19/2/64-69/, (accessed June 18, 2020).
[2] G. Bond and the late David Thompson, *Gold Bull.*, 2009, **42**, 247–259.
[3] I. M. Campbell, *Catalysis at Surfaces*, Springer Netherlands, 1988.
[4] J. Meurig Thomas and R. Raja, *Annu. Rev. Mater. Res.*, 2005, **35**, 315–350.
[5] P. T. Anastas and J. C. Warner, *Green Chemistry: Theory and Practice*, Oxford University Press, Oxford, 2000.
[6] H. Hu, J. H. Xin, H. Hu, X. Wang and Y. Kong, *Appl. Catal. Gen.*, 2015, **492**, 1–9.
[7] S. Navalon, A. Dhakshinamoorthy, M. Alvaro and H. Garcia, *Coord. Chem. Rev.*, 2016, **312**, 99–148.
[8] D. Astruc, F. Lu and J. R. Aranzaes, *Angew. Chem. Int. Ed.*, 2005, **44**, 7852–7872.
[9] L. Ackermann, R. Vicente and A. R. Kapdi, *Angew. Chem. Int. Ed.*, 2009, **48**, 9792–9826.
[10] D. Sempere, S. Navalon, M. Dančíková, M. Alvaro and H. Garcia, *Appl. Catal. B Environ.*, 2013, **142–143**, 259–267.
[11] J. Lee, O. K. Farha, J. Roberts, K. A. Scheidt, S. T. Nguyen and J. T. Hupp, *Chem. Soc. Rev.*, 2009, **38**, 1450.
[12] E. A. B. Kantchev, C. J. O'Brien and M. G. Organ, *Angew. Chem. Int. Ed.*, 2007, **46**, 2768–2813.
[13] D. Nair, J. T. Scarpello, L. S. White, L. M. Freitas dos Santos, I. F. J. Vankelecom and A. G. Livingston, *Tetrahedron Lett.*, 2001, **42**, 8219–8222.
[14] J. Rivera-Utrilla, I. Bautista-Toledo, M. A. Ferro-García and C. Moreno-Castilla, *Carbon*, 2003, **41**, 323–330.
[15] C. E. Garrett and K. Prasad, *Adv. Synth. Catal.*, 2004, **346**, 889–900.
[16] A. Gansäuer and H. Bluhm, *Chem. Rev.*, 2000, **100**, 2771–2788.
[17] C. Wang and Z. Xi, *Chem. Soc. Rev.*, 2007, **36**, 1395–1406.
[18] J. Oxgaard, W. J. Tenn, R. J. Nielsen, R. A. Periana and W. A. Goddard, *Organometallics*, 2007, **26**, 1565–1567.
[19] Y. Boutadla, D. L. Davies, S. A. Macgregor and A. I. Poblador-Bahamonde, *Dalton Trans.*, 2009, 5887–5893.
[20] Y. Boutadla, D. L. Davies, S. A. Macgregor and A. I. Poblador-Bahamonde, *Dalton Trans.*, 2009, 5820–5831.
[21] L. Ackermann, *Chem. Rev.*, 2011, **111**, 1315–1345.
[22] D. Lapointe and K. Fagnou, *Chem. Lett.*, 2010, **39**, 1118–1126.
[23] P. J. Dunn, *Chem. Soc. Rev.*, 2012, **41**, 1452–1461.
[24] C.-J. Li and B. M. Trost, *Proc. Natl. Acad. Sci.*, 2008, **105**, 13197–13202.
[25] M.-M. Titirici, R. J. White, N. Brun, V. L. Budarin, D. S. Su, F. del Monte, J. H. Clark and M. J. MacLachlan, *Chem. Soc. Rev.*, 2014, **44**, 250–290.
[26] F. Rodríguez-reinoso, *Carbon*, 1998, **36**, 159–175.
[27] E. K. Rideal and W. M. Wright, *J. Chem. Soc. Trans.*, 1925, **127**, 1347–1357.
[28] E. Keightley Rideal and W. Mary Wright, *J. Chem. Soc. Resumed*, 1926, **129**, 1813–1821.
[29] J. F. Keegel, W. A. Suruda and C. Schwob, *J. Am. Chem. Soc.*, 1938, **60**, 2483–2486.
[30] L. E. Cadus, L. A. Arrua, O. F. Gorriz and J. B. Rivarola, *Ind. Eng. Chem. Res.*, 1988, **27**, 2241–2246.
[31] F. Lücking, H. Köser, M. Jank and A. Ritter, *Water Res.*, 1998, **32**, 2607–2614.

[32] H. J. H. Fenton, *J. Chem. Soc. Trans.*, 1894, **65**, 899–910.
[33] D. R. Dreyer, H.-P. Jia and C. W. Bielawski, *Angew. Chem. Int. Ed.*, 2010, **49**, 6813–6816.
[34] J.-H. Yang, G. Sun, Y. Gao, H. Zhao, P. Tang, J. Tan, A.-H. Lu and D. Ma, *Energy Environ. Sci.*, 2013, **6**, 793–798.
[35] J. Luo, H. Yu, H. Wang, H. Wang and F. Peng, *Chem. Eng. J.*, 2014, **240**, 434–442.
[36] K. Savaram, M. Li, K. Tajima, K. Takai, T. Hayashi, G. Hall, E. Garfunkel, V. Osipov and H. He, *Carbon*, 2018, **139**, 861–871.
[37] Q. Wei, F. Qin, Q. Ma and W. Shen, *Carbon*, 2019, **141**, 542–552.
[38] M. S. Ahmad, H. He and Y. Nishina, *Org. Lett.*, 2019, **21**, 8164–8168.
[39] J. Xi, Q. Wang, J. Liu, L. Huan, Z. He, Y. Qiu, J. Zhang, C. Tang, J. Xiao and S. Wang, *J. Catal.*, 2018, **359**, 233–241.
[40] X. Hu, Y. Liu, H. Huang, B. Huang, G. Chai and Z. Xie, *Green Chem.*, , DOI:10.1039/C9GC03781K.
[41] B. Jurca, C. Bucur, A. Primo, P. Concepción, V. I. Parvulescu and H. García, *ChemCatChem*, 2019, **11**, 985–990.
[42] E. G. Gordeev, E. O. Pentsak and V. P. Ananikov, *J. Am. Chem. Soc.*, , DOI:10.1021/jacs.9b10887.
[43] D. S. Su, G. Wen, S. Wu, F. Peng and R. Schlögl, *Angew. Chem. Int. Ed.*, 2017, **56**, 936–964.
[44] Y. Zhai, Z. Zhu and S. Dong, *ChemCatChem*, 2015, **7**, 2806–2815.
[45] A. Schaetz, M. Zeltner and W. J. Stark, *ACS Catal.*, 2012, **2**, 1267–1284.
[46] P. Serp, M. Corrias and P. Kalck, *Appl. Catal. Gen.*, 2003, **253**, 337–358.
[47] M. J. Ahmed, *J. Environ. Chem. Eng.*, 2016, **4**, 89–99.
[48] Z. Li, Z. Liu, H. Sun and C. Gao, *Chem. Rev.*, 2015, **115**, 7046–7117.
[49] A. Hirsch and C. Backes, *Angew. Chem. Int. Ed.*, 2010, **49**, 1722–1723.
[50] M. Wang, Z.-H. Huang, Y. Bai, F. Kang and M. Inagaki, *Curr. Org. Chem.*, 2013, **17**, 1434–1447.
[51] C. N. R. Rao, U. Maitra and H. S. S. R. Matte, in *Graphene*, John Wiley & Sons, Ltd, 2012, pp. 1–47.
[52] A. K. Geim and K. S. Novoselov, *Nat. Mater.*, 2007, **6**, 183–191.
[53] X.-C. Dong, H. Xu, X.-W. Wang, Y.-X. Huang, M. B. Chan-Park, H. Zhang, L.-H. Wang, W. Huang and P. Chen, *ACS Nano*, 2012, **6**, 3206–3213.
[54] V. Presser, M. Heon and Y. Gogotsi, *Adv. Funct. Mater.*, 2011, **21**, 810–833.
[55] E. Pérez-Mayoral, V. Calvino-Casilda and E. Soriano, *Catal. Sci. Technol.*, 2016, **6**, 1265–1291.
[56] S. Filippone, E. E. Maroto, Á. Martín-Domenech and N. Martín, in *Advances in Organometallic Chemistry and Catalysis*, John Wiley & Sons, Ltd, 2013, pp. 459–472.
[57] B. Qiu, M. Xing and J. Zhang, *Chem. Soc. Rev.*, 2018, **47**, 2165–2216.
[58] Z.-S. Wu, Y. Sun, Y.-Z. Tan, S. Yang, X. Feng and K. Müllen, *J. Am. Chem. Soc.*, 2012, **134**, 19532–19535.
[59] C. N. R. Rao, A. K. Sood, K. S. Subrahmanyam and A. Govindaraj, *Angew. Chem. Int. Ed.*, 2009, **48**, 7752–7777.
[60] T. Kuila, S. Bose, A. K. Mishra, P. Khanra, N. H. Kim and J. H. Lee, *Prog. Mater. Sci.*, 2012, **57**, 1061–1105.
[61] L. Chen, Y. Hernandez, X. Feng and K. Müllen, *Angew. Chem. Int. Ed.*, 2012, **51**, 7640–7654.

[62] A. W. Robertson and J. H. Warner, *Nano Lett.*, 2011, **11**, 1182–1189.
[63] L. Wang, X. Zhang, H. L. W. Chan, F. Yan and F. Ding, *J. Am. Chem. Soc.*, 2013, **135**, 4476–4482.
[64] B. C. Brodie, *Philos. Trans. R. Soc. Lond.*, 1859, **149**, 249–259.
[65] L. Staudenmaier, *Berichte Dtsch. Chem. Ges.*, 1898, **31**, 1481–1487.
[66] U. Hofmann and E. König, *Z. Für Anorg. Allg. Chem.*, 1937, **234**, 311–336.
[67] W. S. Hummers and R. E. Offeman, *J. Am. Chem. Soc.*, 1958, **80**, 1339–1339.
[68] R. K. Singh, R. Kumar and D. P. Singh, *RSC Adv.*, 2016, **6**, 64993–65011.
[69] N. I. Kovtyukhova, P. J. Ollivier, B. R. Martin, T. E. Mallouk, S. A. Chizhik, E. V. Buzaneva and A. D. Gorchinskiy, *Chem. Mater.*, 1999, **11**, 771–778.
[70] J. Sun, N. Yang, Z. Sun, M. Zeng, L. Fu, C. Hu and S. Hu, *ACS Appl. Mater. Interfaces*, 2015, **7**, 21356–21363.
[71] Z. Luo, Y. Lu, L. A. Somers and A. T. C. Johnson, *J. Am. Chem. Soc.*, 2009, **131**, 898–899.
[72] D. C. Marcano, D. V. Kosynkin, J. M. Berlin, A. Sinitskii, Z. Sun, A. Slesarev, L. B. Alemany, W. Lu and J. M. Tour, *ACS Nano*, 2010, **4**, 4806–4814.
[73] J. Chen, Y. Zhang, M. Zhang, B. Yao, Y. Li, L. Huang, C. Li and G. Shi, *Chem. Sci.*, 2016, **7**, 1874–1881.
[74] J. H. Kang, T. Kim, J. Choi, J. Park, Y. S. Kim, M. S. Chang, H. Jung, K. T. Park, S. J. Yang and C. R. Park, *Chem. Mater.*, 2016, **28**, 756–764.
[75] L. Yang, R. Zhang, B. Liu, J. Wang, S. Wang, M.-Y. Han and Z. Zhang, *Angew. Chem. Int. Ed Engl.*, 2014, **53**, 10109–10113.
[76] N. Morimoto, H. Suzuki, Y. Takeuchi, S. Kawaguchi, M. Kunisu, C. W. Bielawski and Y. Nishina, *Chem. Mater.*, 2017, **29**, 2150–2156.
[77] N. Morimoto, T. Kubo and Y. Nishina, *Sci. Rep.*, 2016, **6**, 1–8.
[78] S. Pei and H.-M. Cheng, *Carbon*, 2012, **50**, 3210–3228.
[79] C. K. Chua and M. Pumera, *Chem. Soc. Rev.*, 2013, **43**, 291–312.
[80] D. R. Dreyer, S. Park, C. W. Bielawski and R. S. Ruoff, *Chem. Soc. Rev.*, 2009, **39**, 228–240.
[81] O. Ö. Ekiz, M. Ürel, H. Güner, A. K. Mizrak and A. Dâna, *ACS Nano*, 2011, **5**, 2475–2482.
[82] S. Park and R. S. Ruoff, *Nat. Nanotechnol.*, 2009, **4**, 217–224.
[83] W. Gao, Ed., *Graphene Oxide: Reduction Recipes, Spectroscopy, and Applications*, Springer International Publishing, 2015.
[84] D. Voiry, J. Yang, J. Kupferberg, R. Fullon, C. Lee, H. Y. Jeong, H. S. Shin and M. Chhowalla, *Science*, 2016, **353**, 1413–1416.
[85] E. C. Salas, Z. Sun, A. Lüttge and J. M. Tour, *ACS Nano*, 2010, **4**, 4852–4856.
[86] P. Šimek, Z. Sofer, O. Jankovský, D. Sedmidubský and M. Pumera, *Adv. Funct. Mater.*, 2014, **24**, 4878–4885.
[87] Z.-S. Wu, W. Ren, L. Gao, J. Zhao, Z. Chen, B. Liu, D. Tang, B. Yu, C. Jiang and H.-M. Cheng, *ACS Nano*, 2009, **3**, 411–417.
[88] A. T. Smith, A. M. LaChance, S. Zeng, B. Liu and L. Sun, *Nano Mater. Sci.*, 2019, **1**, 31–47.
[89] A. A. Abakumov, I. B. Bychko, O. V. Selyshchev, D. R. T. Zahn, X. Qi, J. Tang and P. E. Strizhak, *Carbon*, 2020, **157**, 277–285.

[90] X. Wang, X. Li, L. Zhang, Y. Yoon, P. K. Weber, H. Wang, J. Guo and H. Dai, *Science*, 2009, **324**, 768–771.
[91] Z. Yang, Z. Yao, G. Li, G. Fang, H. Nie, Z. Liu, X. Zhou, X. Chen and S. Huang, *ACS Nano*, 2012, **6**, 205–211.
[92] Y. Xue, D. Yu, L. Dai, R. Wang, D. Li, A. Roy, F. Lu, H. Chen, Y. Liu and J. Qu, *Phys. Chem. Chem. Phys.*, 2013, **15**, 12220–12226.
[93] A. Dhakshinamoorthy, A. Primo, P. Concepcion, M. Alvaro and H. Garcia, *Chem. – Eur. J.*, 2013, **19**, 7547–7554.
[94] S. S. Chauhan, P. Srivastava and A. K. Shrivastava, *Appl. Nanosci.*, 2014, **4**, 461–467.
[95] M. Latorre-Sánchez, A. Primo and H. García, *Angew. Chem. Int. Ed.*, 2013, **52**, 11813–11816.
[96] Y. Chen, D. M. Ho and C. Lee, *J. Am. Chem. Soc.*, 2005, **127**, 12184–12185.
[97] J. Long, X. Xie, J. Xu, Q. Gu, L. Chen and X. Wang, *ACS Catal.*, 2012, **2**, 622–631.
[98] A. K. Singh, K. C. Basavaraju, S. Sharma, S. Jang, C. Pil Park and D.-P. Kim, *Green Chem.*, 2014, **16**, 3024–3030.
[99] H.-P. Jia, D. R. Dreyer and C. W. Bielawski, *Tetrahedron*, 2011, **67**, 4431–4434.
[100] Y. Gao, G. Hu, J. Zhong, Z. Shi, Y. Zhu, D. S. Su, J. Wang, X. Bao and D. Ma, *Angew. Chem. Int. Ed.*, 2013, **52**, 2109–2113.
[101] X.-H. Li, J.-S. Chen, X. Wang, J. Sun and M. Antonietti, *J. Am. Chem. Soc.*, 2011, **133**, 8074–8077.
[102] D. R. Dreyer, H.-P. Jia, A. D. Todd, J. Geng and C. W. Bielawski, *Org. Biomol. Chem.*, 2011, **9**, 7292–7295.
[103] H. Huang, J. Huang, Y.-M. Liu, H.-Y. He, Y. Cao and K.-N. Fan, *Green Chem.*, 2012, **14**, 930.
[104] C. Su, M. Acik, K. Takai, J. Lu, S. Hao, Y. Zheng, P. Wu, Q. Bao, T. Enoki, Y. J. Chabal and K. Ping Loh, *Nat. Commun.*, 2012, **3**, 1298.
[105] M. Wang, X. Song and N. Ma, *Catal. Lett.*, 2014, **144**, 1233–1239.
[106] Y. Gao, D. Ma, C. Wang, J. Guan and X. Bao, *Chem Commun*, 2011, **47**, 2432–2434.
[107] A. Primo, F. Neatu, M. Florea, V. Parvulescu and H. Garcia, *Nat. Commun.*, 2014, **5**, 1–9.
[108] M.-M. Trandafir, M. Florea, F. Neaţu, A. Primo, V. I. Parvulescu and H. García, *ChemSusChem*, 2016, **9**, 1565–1569.
[109] H.-P. Jia, D. R. Dreyer and C. W. Bielawski, *Adv. Synth. Catal.*, 2011, **353**, 528–532.
[110] D. Verga, M. Nadai, F. Doria, C. Percivalle, M. Di Antonio, M. Palumbo, S. N. Richter and M. Freccero, *J. Am. Chem. Soc.*, 2010, **132**, 14625–14637.
[111] S. N. Richter, S. Maggi, S. C. Mels, M. Palumbo and M. Freccero, *J. Am. Chem. Soc.*, 2004, **126**, 13973–13979.
[112] H. Egami and T. Katsuki, *J. Am. Chem. Soc.*, 2009, **131**, 6082–6083.
[113] T. Temma, B. Hatano and S. Habaue, *Tetrahedron*, 2006, **62**, 8559–8563.
[114] S. Takizawa, T. Katayama, C. Kameyama, K. Onitsuka, T. Suzuki, T. Yanagida, T. Kawai and H. Sasai, *Chem. Commun.*, 2008, 1810–1812.
[115] M. Shaikh, A. Sahu, A. K. Kumar, M. Sahu, S. K. Singh and K. V. S. Ranganath, *Green Chem.*, 2017, **19**, 4533–4537.
[116] J. Fang, Z. Peng, Y. Yang, J. Wang, J. Guo and H. Gong, *Asian J. Org. Chem.*, 2018, **7**, 355–358.
[117] S. I. El-Hout, Y. Zhou, J. Kano, Y. Uchida and Y. Nishina, *Catal. Lett.*, , DOI:10.1007/s10562-019-02951-z.

[118] N. Morimoto, K. Morioku, H. Suzuki, Y. Nakai and Y. Nishina, *Chem. Commun.*, 2017, **53**, 7226–7229.
[119] R. Mestres, *Green Chem.*, 2004, **6**, 583–603.
[120] S. M. Islam, A. S. Roy, R. C. Dey and S. Paul, *J. Mol. Catal. Chem.*, 2014, **394**, 66–73.
[121] A. Zali, K. Ghani, A. Shokrolahi and M. H. Keshavarz, *Chin. J. Catal.*, 2008, **29**, 602–606.
[122] H. Jung and C. W. Bielawski, *Commun. Chem.*, 2019, **2**, 1–9.
[123] S. Presolski and M. Pumera, *Angew. Chem. Int. Ed.*, 2018, **57**, 16713–16715.
[124] E. Rodrigo, B. G. Alcubilla, R. Sainz, J. L. G. Fierro, R. Ferritto and M. B. Cid, *Chem. Commun.*, 2014, **50**, 6270–6273.
[125] G. A. Sereda, V. B. Rajpara and R. L. Slaba, *Tetrahedron*, 2007, **63**, 8351–8357.
[126] M. Rueping and B. J. Nachtsheim, *Beilstein J. Org. Chem.*, 2010, **6**, 6.
[127] A. Vijay Kumar and K. Rama Rao, *Tetrahedron Lett.*, 2011, **52**, 5188–5191.
[128] M. R. Acocella, M. Mauro and G. Guerra, *ChemSusChem*, 2014, **7**, 3279–3283.
[129] M. L. Kantam, S. Laha, J. Yadav and B. Sreedhar, *Tetrahedron Lett.*, 2006, **47**, 6213–6216.
[130] R. Parella, Naveen and S. A. Babu, *Catal. Commun.*, 2012, **29**, 118–121.
[131] S. Navalon, A. Dhakshinamoorthy, M. Alvaro and H. Garcia, *Chem. Rev.*, 2014, **114**, 6179–6212.
[132] K. Morioku, N. Morimoto, Y. Takeuchi and Y. Nishina, *Sci. Rep.*, 2016, **6**, 25824.
[133] H. Wu, C. Su, R. Tandiana, C. Liu, C. Qiu, Y. Bao, J. Wu, Y. Xu, J. Lu, D. Fan and K. P. Loh, *Angew. Chem. Int. Ed.*, 2018, **57**, 10848–10853.
[134] M. S. Ahmad and Y. Nishina, *Nanoscale*, , DOI:10.1039/D0NR02984J.

CHAPTER 2

Investigation of active sites for C−H functionalization on carbon-based catalyst: Effect of nitrogen-containing functional groups and radicals

Transition metal-catalyzed carbon-carbon bond formation reactions have become important transformations in organic synthesis. In this study, we have explored a general strategy of transition metal-free carbocatalytic carbon-hydrogen (C−H) functionalization. A carbon-based catalyst bearing nitrogen functional groups can facilitate the C−H functionalization of unactivated arenes to obtain biaryl products. We propose the active sites on the catalyst by analyzing its chemical composition before and after the reaction, in-situ FT-IR, ESR, and density functional theory calculation. As a result, stable NH groups and radicals were found to be effective for the reaction, providing high recyclability of the catalyst. The present methodology offers a diverse substrate scope without any dry or inert conditions, thus opening the door for an alternative to the conventional metal-based coupling reactions.

2 Introduction

The direct carbon-hydrogen (C−H) bond transformation is a promising and ideal method for the synthesis of complex molecules compared with conventional organic chemistry techniques because of the limited formation of by-products.[1] During the past decades, prodigious efforts have been devoted to the carbon-carbon (C−C) bond formation via C−H bond transformation for the synthesis of pharmaceuticals,[2] agrochemicals,[3] natural products,[4] and light-emitting materials.[5] C−H bond transformation was first developed using a stoichiometric amount of metallic reagent,[6,7] then evolved into a catalytic manner using organometallic compounds.[8,9] Although the metal-catalyzed reactions are excellent in terms of reaction efficiency and reactivity, the preparation of metal catalysts requires a lot of costs and processes which are less environmentally benign. Another serious issue of the metal catalyst is the contamination of the metal components in the products.[10] Driven by the increasing interest in the utilization of ubiquitous elements that are abundant and nontoxic, Fe,[11] Mn,[12] and Ni[13] catalysts have become a growing area of research. For the greener catalytic system, the metal catalysis should be switched to metal-free catalysis.[14]

C−H transformation reactions using homogeneous organo-catalysts have been explored recently.[15] For example, nitrogen-containing organic molecules, such as ethylene diamines,[10,16] and phenanthrolines,[17,18] were used in the presence of a strong base for the direct C−H bond transformations. In contrast, the heterogeneous metal-free catalyst for C−H bond transformation has remained limited (Figure 2.1). The promising candidate is carbon-based catalysts (carbocatalyst), which are eco-friendly, biocompatible, stable, readily available, and renewable.[19-22] From now on, different allotropes of carbon have been developed as carbocatalysts.[23] Among them, we have focused on 2-dimensional nanocarbons, namely graphene analogs, because of its high surface area and chemically tunable functional groups[24,25] and structures.[26] Graphene analogs have been used for various organic transformation reactions, such as Friedel-Crafts alkylation, [27] Michael addition,[28] oxidation,[29,30] reduction,[31] and others.[32]

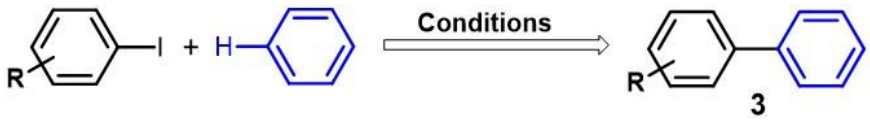

	Previous works [16, 18]		This work
Activation mechanism	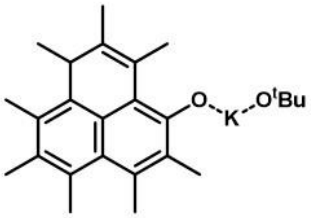 Graphene oxide	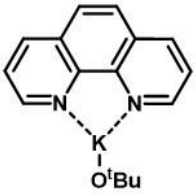 N-containing molecule	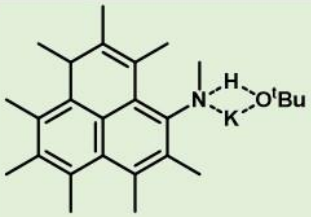 N-doped graphene
Reactivity	General	High	High
Stability	Low	N.D.	High
Separation	Easy	Difficult	Easy

Figure 2.1: *Comparison of the previous works with this work.*

The introduction of heteroatoms on graphene can enhance the catalytic activity, electrical conductivity, and affinity with polar molecules, [33] therefore, nitrogen-doped graphene has been used for electrode applications. [34-36] For example, nitrogen-doped graphene shows a superior catalytic activity than commercial platinum-supported carbon catalysts. [37] In addition, nitrogen-doped graphene shows better catalytic performance than non-doped graphene for oxidation reactions.[38-40] However, it has not been applied for C−C bond formation via C−H bond transformation. In this study, we have developed nitrogen-doped graphene as a catalyst for such type of organic reaction. We also determined the catalytically active site to establish a guideline for high-performance carbon-based catalysts.

2.1Results and discussion

Oxygen functional groups on carbon can promote C−C bond formation via C−H bond transformation. [41] Therefore, graphene oxide (GO), one of the highest oxygen-containing and high surface area carbon material, has been used as a catalyst in the coupling reaction of aryl iodides with aromatic compounds. [16] However, due to the instability of the oxygen functional groups on GO, the catalyst performance and recyclability were not satisfactory; we conducted a reproduction

experiment according to the reported reaction and found that the structure of GO dramatically changed after the reaction (Figure 2.2(i) (a) and (b)). This structural change is caused by the cleavage of fragile C−O bonds on GO. To overcome such a structural change, heteroatoms should be embedded in the graphene framework by multiple bonds, in other words, doping. Great efforts have been done for the preparation of nitrogen-doped graphene using GO as a source of the graphene framework. [27,42,43] During the nitrogen doping, GO is simultaneously reduced; therefore, the product is nitrogen-doped reduced graphene oxide (NrGO). Among various techniques of nitrogen doping, we selected hydrothermal method using guanidine, [44] ammonia, [45] and urea [46] as the source of nitrogen, and we call the products as NrGO(G), NrGO(A), and NrGO(U), respectively (Table 2.1). As shown in (Figure 2.2(ii) (a) and (b)), C 1s regions of XPS spectra before reaction and after the reaction is almost similar, which suggests that GO catalyst containing large amount of oxygen was less stable then NrGO.

Table 2.1: *Nitrogen-containing compound used in the synthesis of NrGO.*

Compound name	**Structure**	**Symbol**
Guanidine carbonate	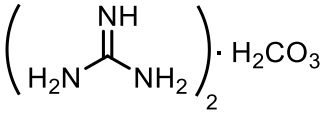	G
Ammonia	NH_3	A
Urea	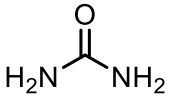	U

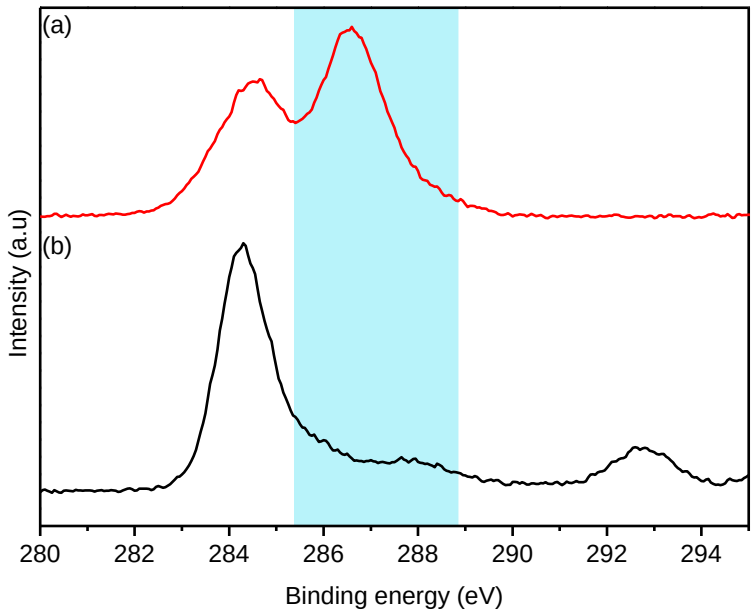

Figure 2.2(i): *XPS analysis of C1s, (**a**) GO fresh before reaction, and (**b**) GO recovered after the reaction.*

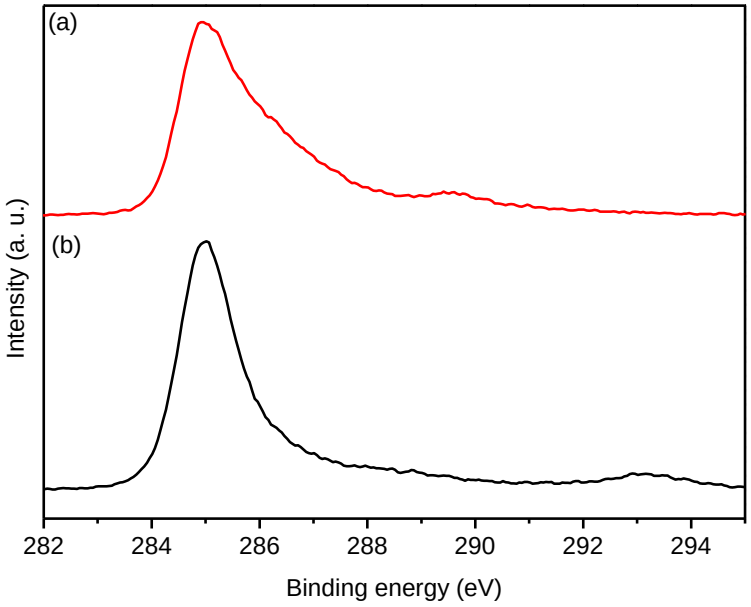

Figure 2.2(ii): *XPS C1S spectra of (**a**) NrGO fresh before reaction and (**b**) NrGO recovered after the reaction.*

2.1.1 Characterization

The morphology of the NrGO(G) was analyzed by scanning electron microscopy (SEM) and transmission electron microscopy (TEM), revealing that it was composed of several layers of graphene (Figure 2.3a). [47] The chemical bonding state was characterized by X-ray photoelectron spectroscopy (XPS). The XPS survey spectra showed peaks at 285, 399, and 533 eV, which were assigned as C 1s, N 1s, and O 1s, respectively (Figure 2.4). This confirms that the nitrogen atoms were successfully doped on the surface of graphene from the nitrogen-containing molecules. The atomic percentages of NrGO, rGO and GO determined by XPS were listed in (Table 2.2).

Table 2.2: *Elemental composition of NrGOs.*[a]

Catalyst	C / at%	N/ at%				O/ at%
		pyridinic	NH	quaternary	N-oxide	
NrGO(A)	83.19	1.59	2.5	0.62	0.79	11.76
NrGO(G)	79.73	0.69	4.5	--	--	15.08
NrGO(G)-2[b]	80.99	0.93	6.19	--	--	11.89
NrGO(U)	84.05	1.54	1.28	0.79	--	13.21
rGO	85.11	--	--	--	--	14.89

[a]Atomic ratio was determined by XPS. [b]NrGO(G)-2 was prepared by adding 1.2 g of nitrogen source was dissolved in 100 ml of 0.1 wt% GO aqueous dispersion, while the rest method was the same as mention above in experimental section.

The XPS narrow spectra for N 1s region can be deconvoluted into pyridinic, pyrrolic, or amino group (NH group), quaternary, and N-oxide. [48] Depends on doping reagents, the chemical state of nitrogen changed (Figure 2.5), and in the case of NrGO(G), NH groups were predominant (Figure 2.3b). The functional groups on NrGO(G) were further analyzed by Fourier transform infrared spectroscopy (FT-IR). A peak at 3410 cm^{-1} is attributed to OH and/or NH groups. [49] The presence of NH groups was supported by comparing the FT-IR spectra with a standard spectrum

of pyrrole and guanidine. Other characteristic peaks at 1660, 1575, 1180, and 1113 cm^{-1} were assigned for −C=O, C=C, epoxy, and C−N groups, respectively (Figure 2.3c). [50]

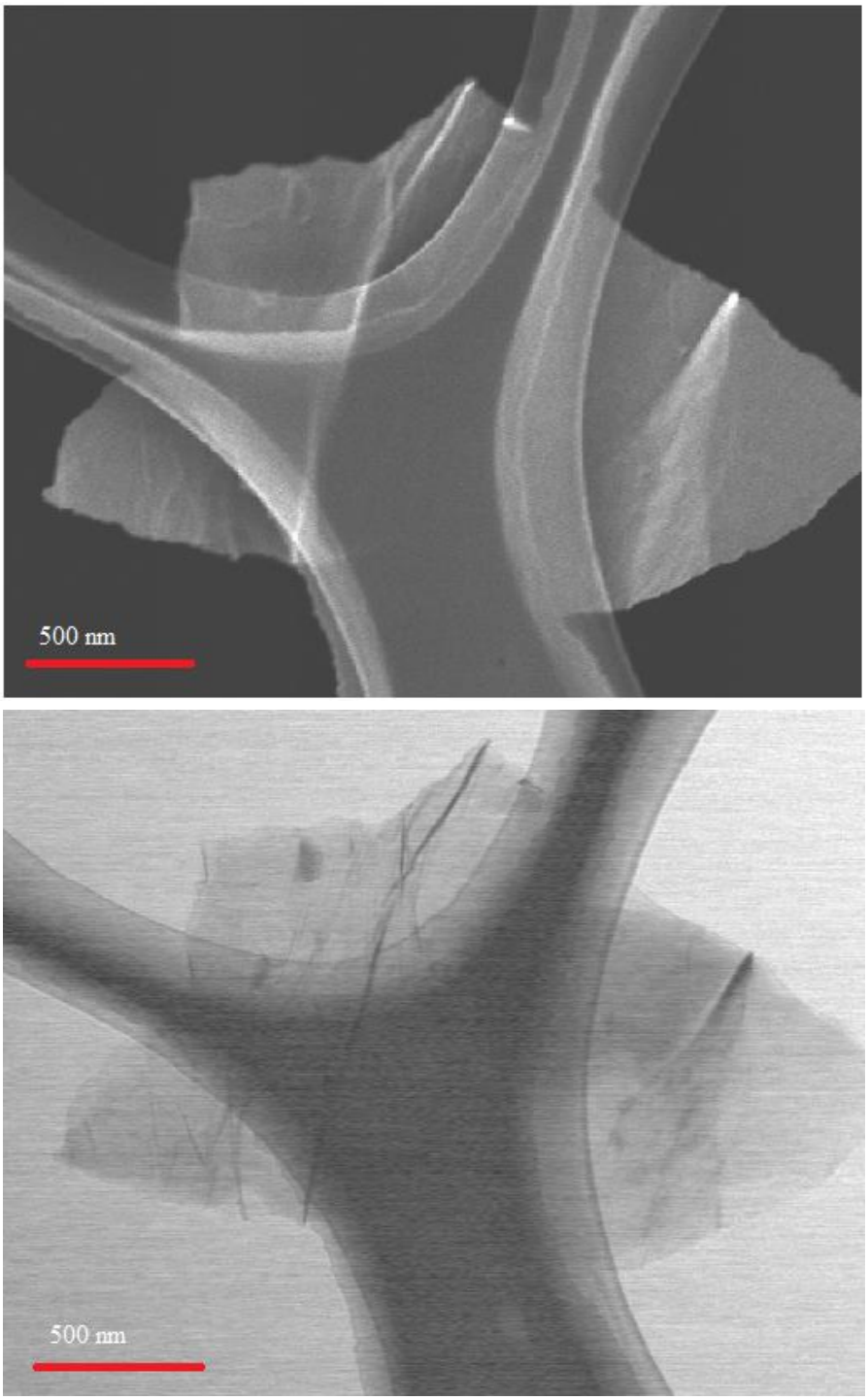

Figure 2.3a: *The upper is the SEM image of the NrGO; below is the TEM image of the NrGO.*

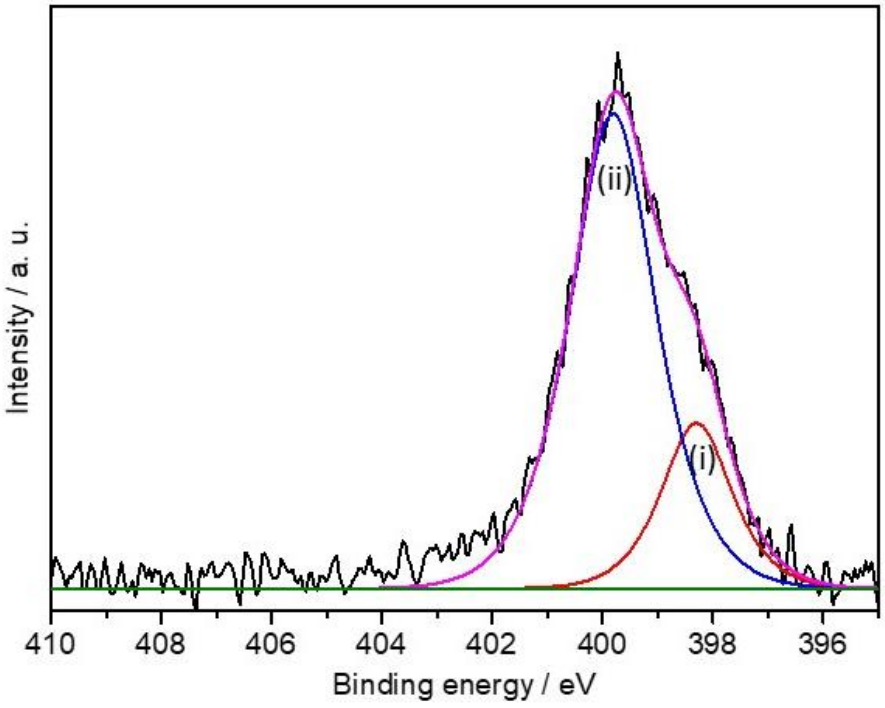

Figure 2.3b: *XPS spectra of the N1s, deconvolution was performed for XPS spectra, and* ***(i)*** *pyridinic and* ***(ii)*** *NH group were observed.*

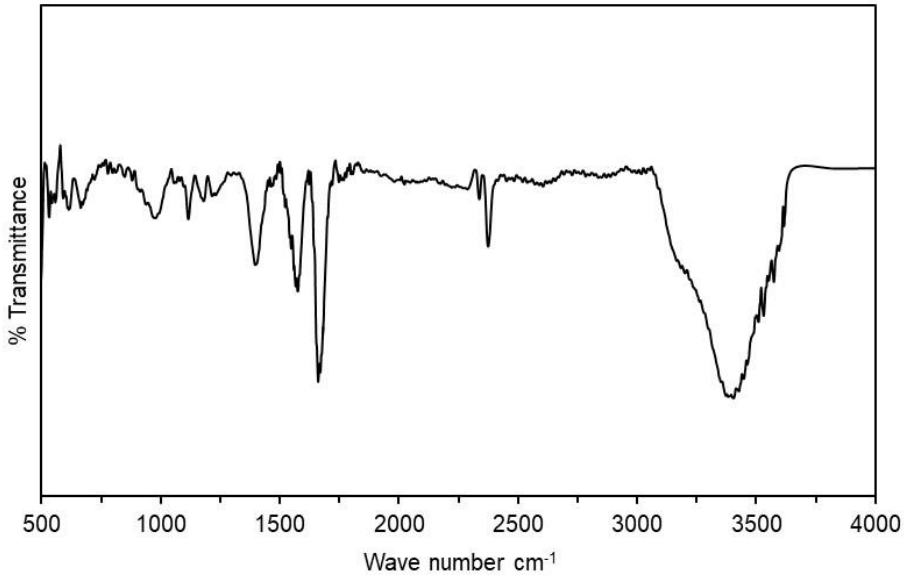

Figure 2.3c: *FT-IR analysis of NrGO(G).*

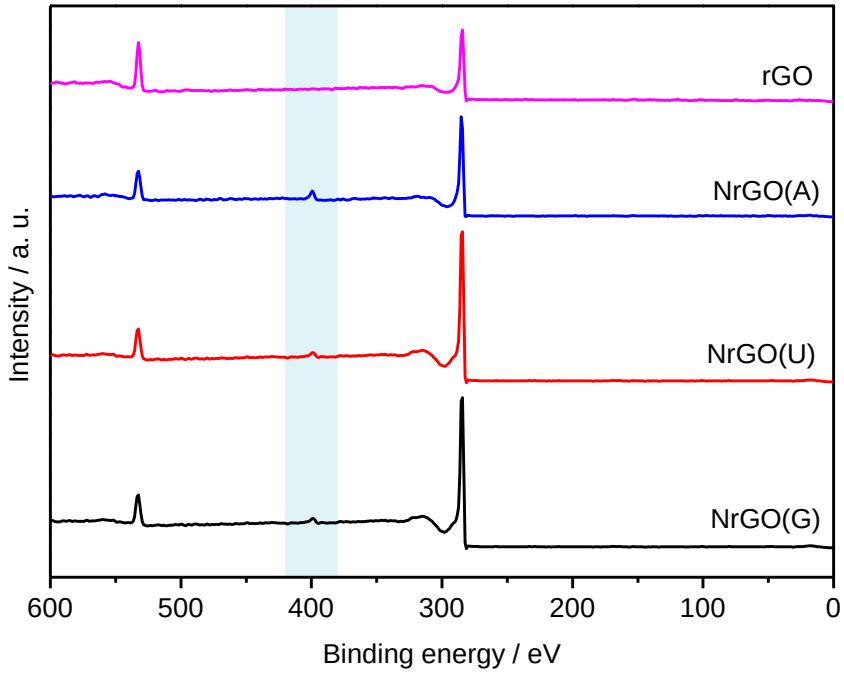

Figure 2.4: *XPS survey spectra of rGO and different NrGOs.*

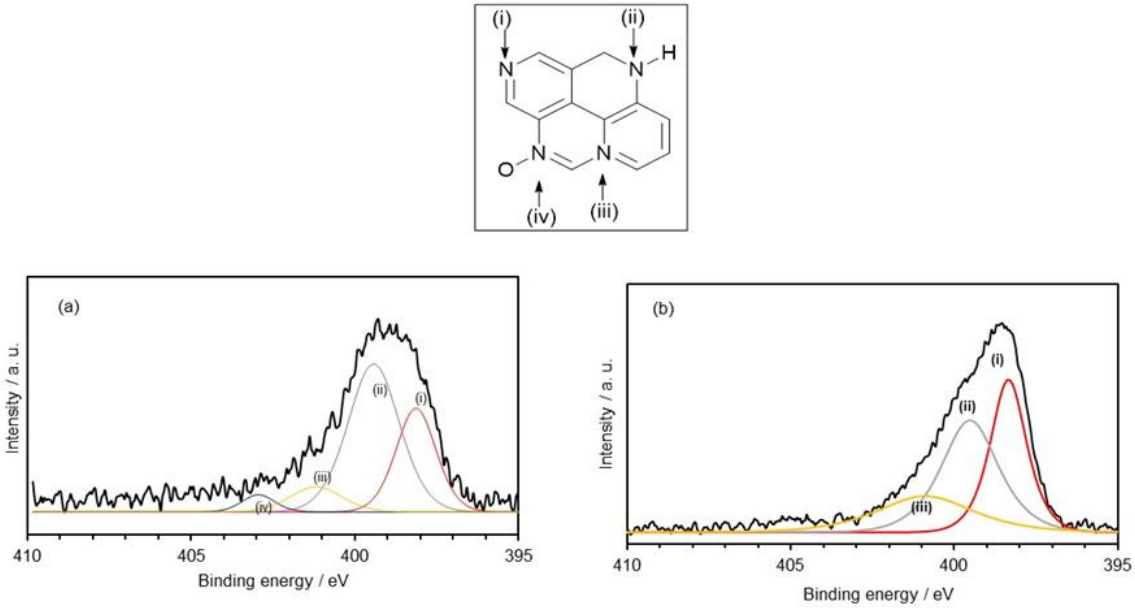

Figure 2.5: *XPS spectra of nitrogen species of different catalysts. (a) NrGO(A) and (b) NrGO(U).*

2.1.2 Catalytic activity of NrGOs and optimization of the reaction

The NrGOs were tested as a catalyst for the coupling reaction with iodobenzene (**1a**) and benzene (**2a**) in the presence of ^{t}BuOK. Among them, NrGO(G) showed the highest yield of 85% (Table 2-3, Entry 1). Other nitrogen-doped catalysts, NrGO(A) and NrGO(U), showed a lower yield of 66% and 60%, respectively (Table 2.3, Entries 2 and 3). Without catalyst under the same reaction, the condition gave 9% yield of **3a** (Table 2.3, Entry 4), which was also observed in the previous research. [14] In addition, GO and rGO prepared by the same procedure without nitrogen source were tested, and 35% 44% of **3a** was obtained, respectively (Table 2.3, Entries 5 and 6).

Table 2.3: *Catalyst screening* [a].

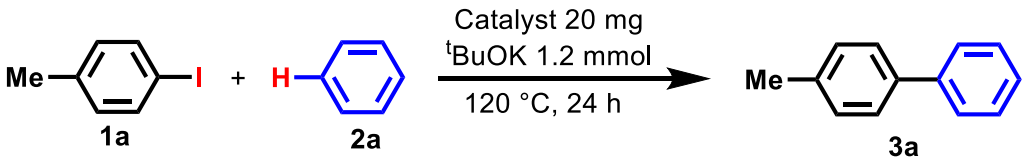

Entry	Catalyst	Yield / %[b]
1	NrGO(G)	85
2	NrGO(A)	66
3	NrGO(U)	60
4	-	9
5	GO	35
6	rGO	44
7	NrGO(G) + TEMPO[c]	N.D

[a]**Reaction conditions**: **1a** (0.4 mmol), **2a** (4 mL), catalyst (20 mg), ^{t}BuOK (1.2 mmol) 120 °C, 24 hours. [b]Yields were determined by GC using dodecane as an internal standard. [c]TEMPO (0.4 mmol) was added.

Initially, we choose benzene and 4-iodoanisole as the model substrates (Table 2.4). Almost no product was detected when the reaction was conducted with other solvents such as DMSO, or THF (Entry 2 and 3). Bases other than ^{t}BuOK, such as KOH, Cs_2CO_3, K_2CO_3, and NaOH, were found inactive. Almost no coupling products were formed when the reaction was performed at elevated temperatures.

***Table 2.4**. Reaction optimization.*[a]

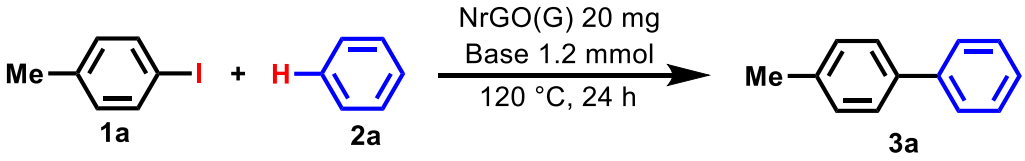

Entry	Base	Catalyst	Solvent	Yield / %[b]
1	^{t}BuOK	NrGO(G)	Benzene	85
2	^{t}BuOK	NrGO(G)	DMSO	N.D
3	^{t}BuOK	NrGO(G)	THF	N.D
4	KOH	NrGO(G)	Benzene	2
5	Cs_2CO_3	NrGO(G)	Benzene	N.D
6	K_2CO_3	NrGO(G)	Benzene	1
7	NaOH	NrGO(G)	Benzene	N.D
8	^{t}BuONa	NrGO(G)	Benzene	N.D
10	^{t}BuOK	NrGO(G)	Benzene	≤10[c]
9	-	NrGO(G)	Benzene	11

[a] **Reaction conditions: 1a** (0.4 mmol), **2a** (4 mL), catalyst (20 mg), base (1.2 mmol) 120 °C, 24 hours.; [b] Yields were determined by GC using dodecane as an internal standard.; [c] the coupling reaction of chlorobenzene and benzene were performed at 140 °C.

These results confirm that nitrogen doping plays an important role in the catalysis. Compared with the previous reports using metal-based catalysts, such as Co, [51,52] Ir, [53,54] Rh, [55,56] Fe, [11,57] and metal-free catalysts, such as GO, [16] phenanthroline, [18] and DMEDA, [58] our NrGO catalysts showed higher or comparable performance compared with the above conditions (Table 2.5).

Table 2.5: *Catalytic performance of NrGOs and other reported catalysts for the cross-coupling reactions of iodobenzene and benzene.*

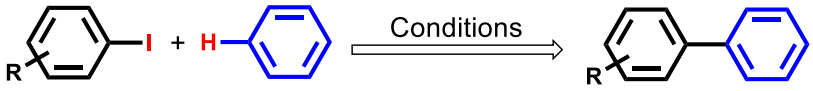

3

Catalyst	**Reaction conditions**	**Yield / %**	**Ref.**
Cobalt acetylacetonato complex (15 mol%)	Iodobenzene (0.5 mmol), LiHMDS (3 equiv), benzene (6 mL), 80 °C, 48 h	72	[51]
Cobalt porphyrin complex (5 mol%)	Iodobenzene (0.224 mmol), benzene (2.0 mL) KOH (2.24 mmol), ^{t}BuOH (2.24 mmol), 200 °C	70	[52]
Iridium Cp* complex (5 mol%)	Iodobenzene (0.50 mmol), benzene (20 mmol), ^{t}BuOK (1.65 mmol), 80 °C, 30 h	72	[53]
Fluorous ethylenediamine	Iodobenzene (0.5 mmol), benzene (6 mL), ^{t}BuOK (5 equiv), ligand (3 equiv), 120 °C, 24 h	70	[54]
1,10-Phenanthroline Derivative (10 mol%)	Iodobenzene (0.225 mmol), benzene (27 mmol), ^{t}BuONa (0.450 mmol), 185 °C, 6h	65	[18]
NrGO(G) (20 mg)	Iodobenzene (0.4 mmol), benzene (4mL), ^{t}BuOK (1.2 mmol), 120 °C, 24 h	**85**	This work
NrGO(A) (20 mg)		66	
NrGO(U) (20 mg)		60	
rGO (20 mg)		44	
GO (20 mg)		35	
No Catalyst		9	

2.1.3 Determination of the active sites of the catalyst

It has been unclear about which site can work as a catalyst in nitrogen-doped carbons. As for electrocatalysts in oxygen reduction reaction, pyridinic sites are determined to be active sites. [59] However, determination of the active sites in liquid phase organic reactions are quite difficult; previous reports suggest that quaternary nitrogen sites are catalytically active, [60,61] while in other studies, pyridinic sites are effective. [62,63] To understand which type of nitrogen atoms contribute to the catalytic site, we plotted the ratio of nitrogen structure (pyridinic, NH group, quaternary, or N-oxide) versus product yield and found that there was a clear relationship between the amount of NH groups and product yield (Figure 2.6, and 2.7). Therefore, we hypothesized that NH groups contribute to the catalytic cycle. To confirm that NH groups interact with substrates during the reaction, we conducted in situ FT-IR analysis. A peak of the NH group of NrGO(G) at 3410 cm^{-1} (Figure 2.8a) shifted to a lower wavenumber by the reaction with ^{t}BuOK (Figure 2-8b), of which phenomena were also observed in the case of standard pyrrole molecule (Figure 2.8c and d). These results that NH groups contribute to the reaction were also supported by density functional theory (DFT) calculation. We compared the stabilization energy of pyridine and pyrrole for ^{t}BuOK and found that pyrrole showed a better stabilization effect (Figure 2.10). DFT calculation was performed by using the Gaussian 09 program (B3LYP/6–311++G(d,p)).

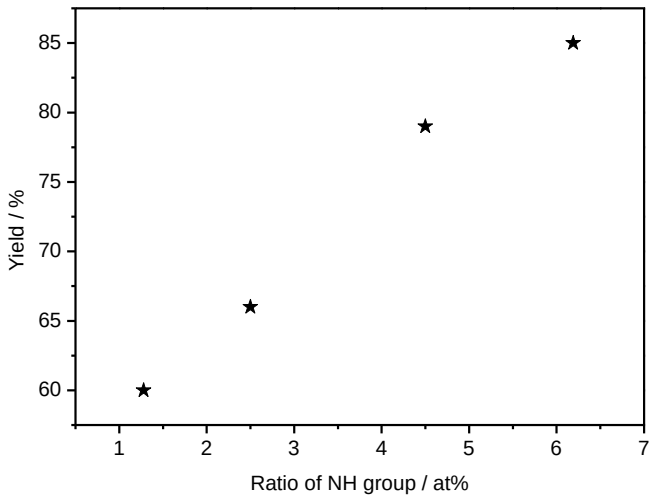

***Figure 2.6**: Relationship between the amount of NH groups and product yield.*

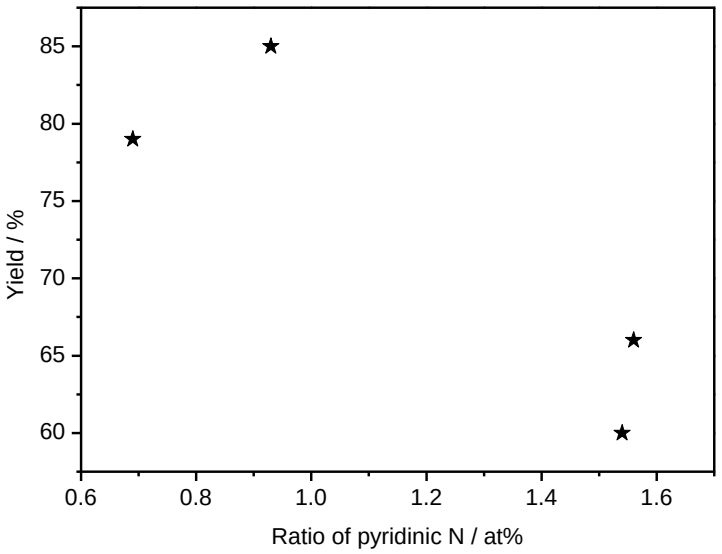

Figure 2.7: *Relationship between the amount of pyridinic nitrogen and product yield.*

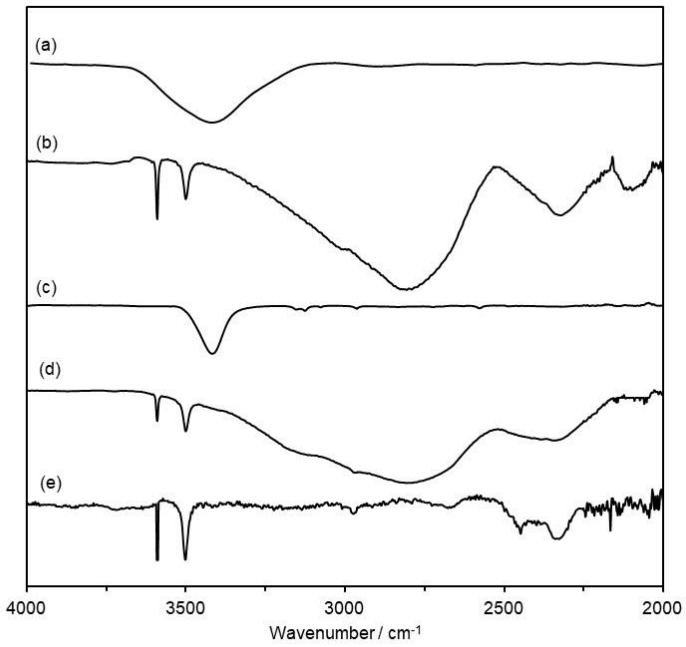

Figure 2.8: *FT-IR analysis of* ***(a)*** *NrGO(G),* ***(b)*** *NrGO(G) +* ^{t}*BuOK,* ***(c)*** *Pyrrole,* ***(d)*** *Pyrrole +* ^{t}*BuOK,* ***(e)*** ^{t}*BuOK.*

The presence of NH groups was supported by comparing the FT-IR spectra with a standard spectrum of pyrrole and guanidine (Figure 2.9).

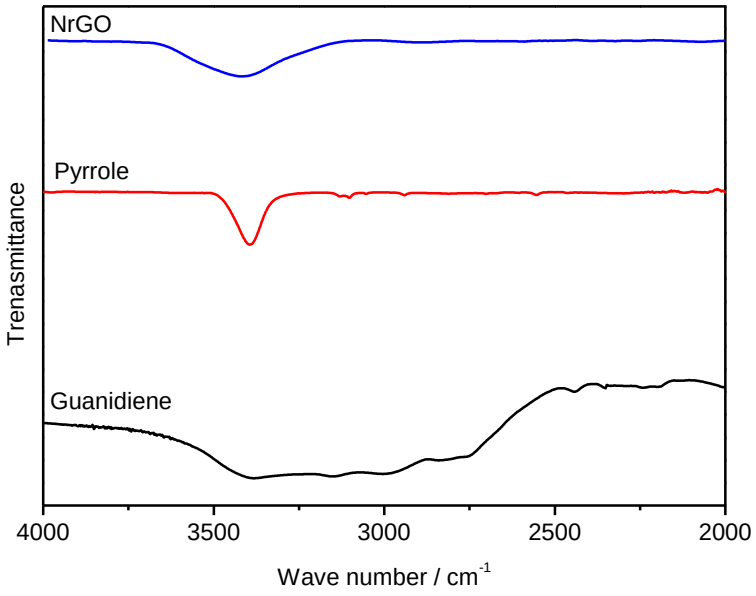

Figure 2.9: *FT-IR spectra of NrGO (G), pyrrole, and guanidine.*

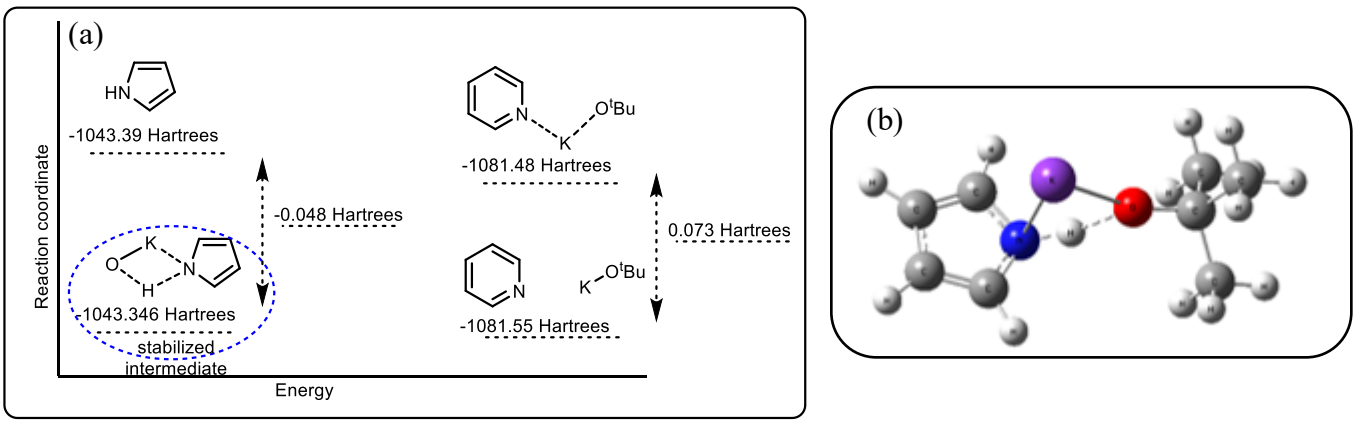

Figure 2.10: (a) *Comparison of the energies of pyridinic and pyrrolic,* ***(b)*** *Optimized structure of the catalytic intermediate of pyrrolic groups.*

2.1.4 Reaction scopes for C−H functionalization

To explore the scope of the NrGO(G) catalyzed reaction, a series of aryl halide and aromatic compounds were examined (Table 2.6). Iodobenzene (**1a**) and aryl iodides with an electron-donating substituent at the para position (**1b** and **1c**) successfully gave desired biaryl products (**3a, 3b,** and **3c**) (Table 2.6, Entries 1-3), while an aryl iodide with an electron-withdrawing substituent (**1d** and **1e**) did not give a product and both substrates were recovered (Table 2.6, Entries 4 and 5). The position of a substituent also influenced the product yield; ortho- and meta-methoxy iodobenzene (**1f** and **1g**) gave lower yields compared with their para-substituted analog (**1b**) (Table 2.6, Entries 4 and 5). Heteroaromatic iodides (**1h** and **1i**) and polyaromatic iodide (**1j**) could also be used as substrates (Table 2.6, Entries 6-8). Limitation of halogen atoms remains an issue; bromides (**1k** and **1l**) gave the products only 10% and 5% yields, respectively, and chloride did not give the product (Table 2.6, Entries 9-11). Heterobiaryls are core frameworks xin biologically active compounds. [64] Although the arylation of heteroarenes has not been explored by previous carbon-based catalysts, [16-18] we extended the potentials of NrGO catalyst to pyridine **2b** and indole **2c**, and desired products 2-phenyl pyridine (**3h**) and 3-phenylindole (**3k**) (Table 2.6, Entries 12 and 13). Such direct arylations of heteroarenes have only been accomplished with metal catalysts, such as palladium, rhodium, ruthenium, and platinum catalysts. [65]

Table 2.6: *Cross-coupling of aryl iodides/bromides/chlorides with arenes in the presence of NrGO(G) catalyst.*[a]

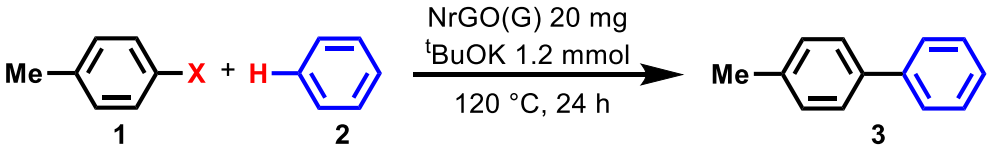

1 2 3

Entry	1		2	3	Yield / %[b]
	Ar	X			
1	C_6H_5 (**1a**)	I	C_6H_6 (**2a**)	**3a**	85
2	4-$MeOC_6H_4$ (**1b**)	I	C_6H_6 (**2a**)	**3b**	81
3	4-MeC_6H_4 (**1c**)	I	C_6H_6 (**2a**)	**3c**	75
4	4-$CF_3C_6H_4$ (**1d**)	I	C_6H_6 (**2a**)	**3d**	N.D.

5	3-$NO_2C_6H_4$ (**1e**)	I	C_6H_6 (**2a**)	**3e**	N.D.
4	2-$MeOC_6H_4$ (**1f**)	I	C_6H_6 (**2a**)	**3f**	60
5	3-$MeOC_6H_4$ (**1g**)	I	C_6H_6 (**2a**)	**3g**	28
6	2-pyridyl (**1h**)	I	C_6H_6 (**2a**)	**3h**	58
7	2-thiophenyl (**1i**)	I	C_6H_6 (**2a**)	**3i**	29
8	1-naphthyl (**1j**)	I	C_6H_6 (**2a**)	**3j**	48
9	C_6H_5 (**1k**)	Br	C_6H_6 (**2a**)	**3b**	10
10	4-$MeOC_6H_4$ (**1l**)	Br	C_6H_6 (**2a**)	**3a**	5
11	4-$MeOC_6H_4$ (**1m**)	Cl	C_6H_6 (**2a**)	**3a**	0
12	C_6H_5 (**1a**)	I	Pyridine(**2b**)	**3h**	66[c]
13	C_6H_5 (**1a**)	I	Indole (**2c**)	**3k**	57[d]

[a]**Reaction conditions: 1** (0.4 mmol), **2** (4 mL), NrGO(G) (20 mg), ^{t}BuOK (1.2 mmol) 120 °C, 24 hours.; [b]Yields were determined by GC using dodecane as an internal standard.; [c]The reaction was carried out in the presence of pyridine (3mL) instead of benzene.; [d]The reaction was carried out in the presence of DMSO, while the coupling partner was indole (0.2 mmol) instead of benzene.

2.1.5 KIE experiment

To understand the rate-determining step, we performed the competition experiment of **1b** with benzene (C_6H_6) and deuteriobenzene (C_6D_6) and evaluated the kinetic isotope effect (KIE) (Scheme 2.1). The reaction conditions are milder and shorter than the optimum to evaluate the reaction rate correctly. The observed low value of k_H/k_D (1.03) suggests that the C−H bond cleavage is not a rate-determining step, which is also proposed in the previous report.[58]

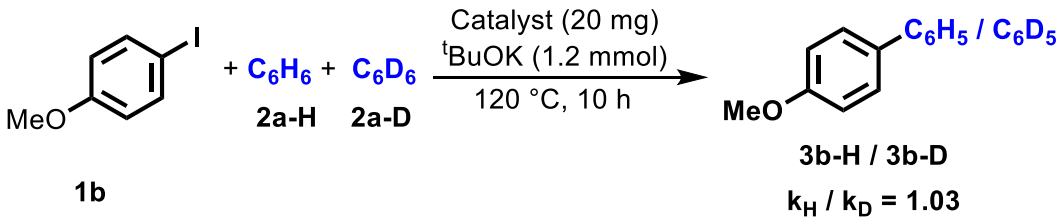

Scheme 2.1: *KIE experiment. The k_H/k_D value was determined by the ratio of* ***3b-H*** *and* ***3b-D*** *using ^1H NMR.*

2.1.6 Effect of radical scavenger

It was proposed that radical species contributed to the reaction [16]. In our NrGO system, radical species would also be formed, because in the presence of radical scavenger, 2,2,6,6-tetramethylpiperidine-1-oxyl (TEMPO), the reaction was completely suppressed (Table 2.1, Entry 7). Therefore, we tried to explain the higher activity of NrGO(G) by measuring the amount of radicals. As expected, the electron spin resonance (ESR) spectra of NrGO(G) showed larger amount of radical species than rGO (Figure 2.11).

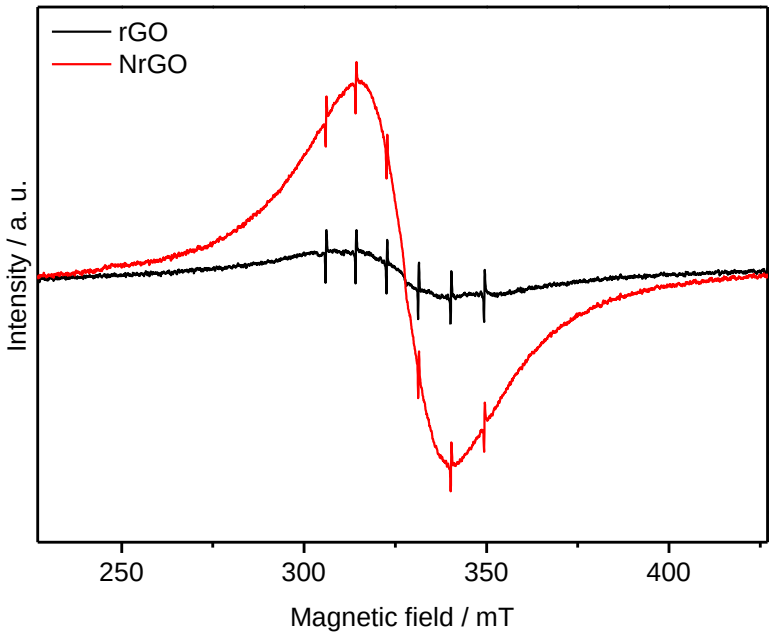

Figure 2.11: *ESR spectra of NrGO (G), and rGO.*

2.1.7 Plausible mechanism

Based on the current findings and conceived by the previous reports, we propose a plausible mechanism for the coupling reaction between iodobenzene and benzene under NrGO catalyst (Scheme 2.2). Potassium cation (K^+) was essential to this reaction as no coupling product was observed when other bases were used. The stabilization of K^+ by heteroatoms on the carbon catalyst occurs initially (Scheme 2.2i), [66] then efficiently activates the C–I bond of 1 and generates aryl radical species (Scheme 2.2ii).[67] The aryl radical reacts with a coupling partner to furnish a biaryl product (Scheme 2.2iii). The formation of specific radicals was supported by in situ ESR analysis (Figure 2.11). [68]

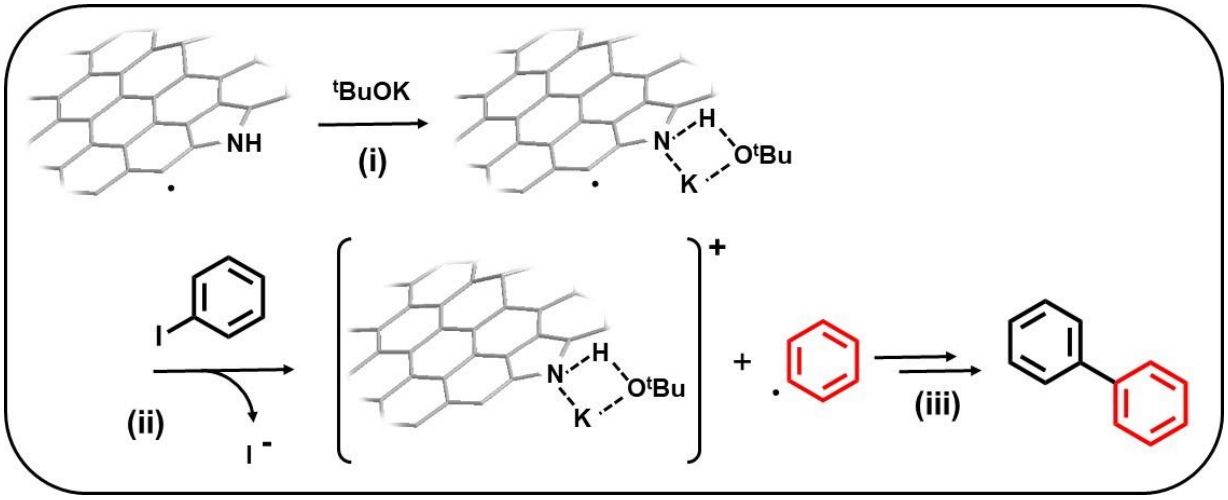

***Scheme 2.2**: Plausible mechanism.*

As a result of ESR analysis, NrGO(G) contained 10^{21}/g of radicals. Suppose that all the radicals are active, TON was calculated to be 0.2, and TOF was 0.008. These values are extremely low; therefore, we believe only a few specific radicals can contribute to the reaction since ESR spectra of NrGO is so broad, and after the addition of ^{t}BuOK, the ESR spectra has a sharp peak (Figure 2.12).

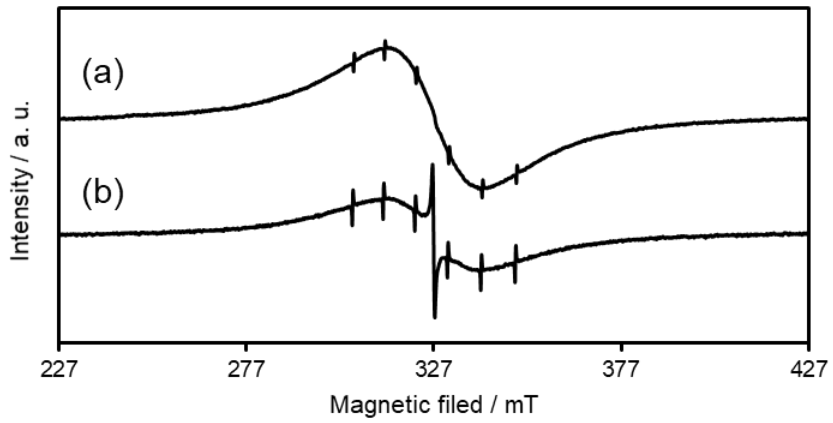

***Figure 2.12**: (**a**) ESR spectra of NrGO(G), and (**b**) in situ ESR spectra of NrGO(G)-catalyzed reaction. A new signal appeared at 327 mT, which is attributed to carbon radicals.*

2.1.8 Leaching and heterogeneity test

To explore the heterogeneity of the catalyst, leaching experiments were carried out. NrGO(G) catalyst was stirred in benzene and filtered, then iodobenzene and ^{t}BuOK were added to the filtrate and stirred under the same setup reaction condition. No more than 11 % of the biaryl product was detected. This product yield was similar to the reaction condition of without catalyst (Table 2.1, entry 4). Therefore, we concluded that the leaching of active species into the solution is limited. The recyclability of the catalysts was also examined (Figure 2.13). After completion of each run, the reaction mixture was cooled to room temperature and then filtered. The catalyst was washed thoroughly with ethanol, followed by water, and then dried. The dried catalyst was subjected again to another experimental run under the same conditions (**1a** (0.4 mmol), **2a** (4mL), ^{t}BuOK (1.2 mmol), at 120 °C for 24 h), and thus used for five cycles consecutively. The NrGO(G) showed high efficiency in recycling up to 3 runs, then slowly decreased. The decrease of the catalytic activity would derive from the loss of nitrogen atoms [69] and/or radical species (Figure 2.14).

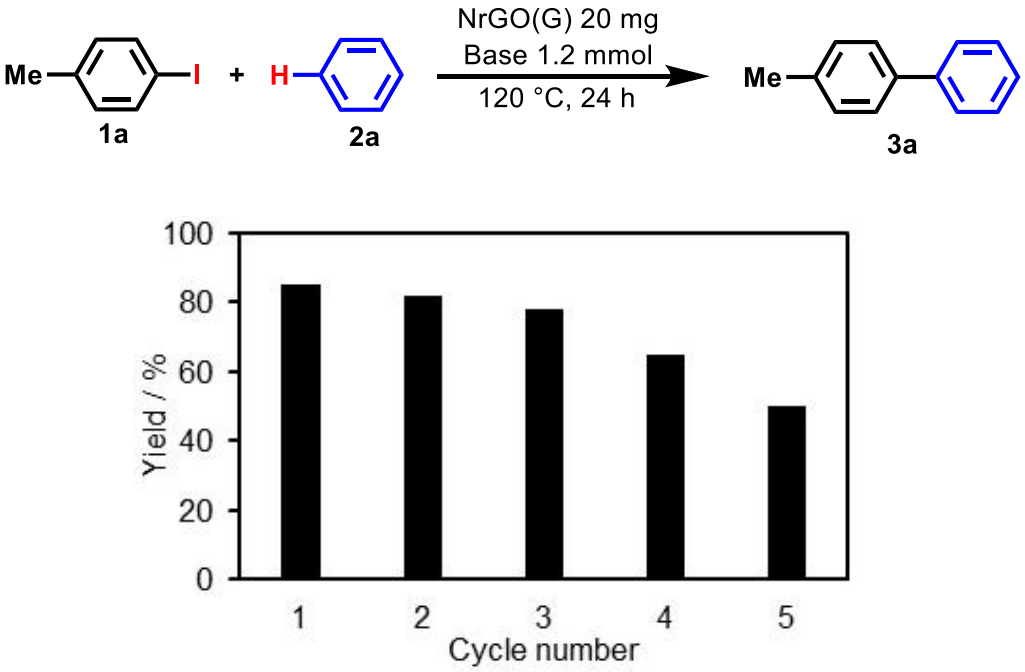

Figure 2.13: *Recyclability of NrGO(G) catalyst in the coupling reaction between* ***1a*** *and* ***2a****.*

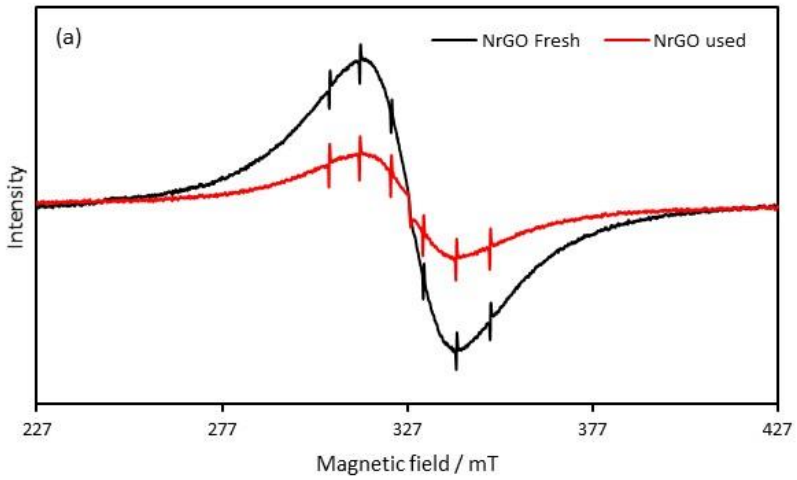

Figure 2.14: *ESR spectra of fresh and recovered catalyst (NrGO(G)).*

2.2 Experimental

2.2.1 General information

All the chemicals used in this study were purchased from commercial sources and used as such received or otherwise mentioned. The surface chemistry and elemental analysis of NrGOs were performed by X-ray photon spectroscopy (XPS) JPS-9030 with a pass energy of 20 eV. The morphology of NrGO was measured by transmission electron microscopy (TEM) JEOL JEM-2100F, while the functional groups on the surface of the prepared catalyst were recorded by Fourier transform infrared spectrometer (FT-IR SHIMADZU IR Tracer 100), the sample for FT-IR was dried and mixed with KBr, and then pressed up to 1.3 mm-diameter pellets. The ESR analysis was performed by an electron spin resonance spectrometer (JES-X310) with 9.542 GHz microwave frequency, 100 kHz modulation frequency, 1mW power, and 2 minutes of weep time. The products were quantified by gas chromatography GC (Shimadzu GC-2014 equipped with flame ionized detector FID detector).

2.2.2 Catalyst preparation

Graphite powder (100 g) was dispersed into concentrated H_2SO_4 (2.5 L). After cooling the mixture in an ice bath, $KMnO_4$ (300 g) was added, and the reaction mixture was kept below 55 °C. The mixture was stirred at 35 °C for two h to complete the oxidation process. Next, deionized water (5 L) was added slowly, and the temperature was kept below 50 °C with continuous stirring, then followed by the addition of H_2O_2 (30% aq., 250 mL) into the mixture. Finally, the brown crude graphite oxide was purified by performing 10 times centrifugation, and graphene oxide (GO) is prepared. The concentration of GO was measured by drying the GO dispersion under vacuum at 50 °C.

To dope nitrogen, 1 g of each nitrogen source (guanidine carbonate, ammonia, and urea) was dissolved in 100 ml of 0.1 wt% GO aqueous dispersion. The mixture was transferred into steel autoclave and performed hydrothermal treatment at 180 °C for 8 h. After cooling to room temperature, formed black precipitates were filtered and washed with deionized water five times and then followed by washing with isopropanol. Finally, the NrGO was dried in a freeze drier and

labeled as NrGO(G), NrGO(A), and NrGO(U), respectively. Reduced graphene oxide (rGO) without nitrogen was prepared by the same method without the addition of nitrogen sources.

2.2.3 Catalytic reaction

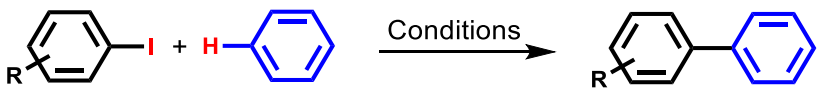

25 mL of screw-capped glass reactor was loaded with the catalyst (20 mg), aryl iodide (0.4 mmol), ^{t}BuOK (1.2 mmol), and benzene (4 ml). The reaction mixture was heated at 120 °C for 24 h. After completion of the reaction, the mixture was cooled to room temperature. To analyze the product yield by GC, 0.4 mmol of dodecane was added as an internal standard. To analyze the product by NMR, the mixture was purified by column chromatography using AcOEt: hexane = 1: 20 as an eluent.

2.2.4 Procedure for KIE experiment

A 25 mL of screw-capped glass reactor was charged with catalyst (20 mg), iodoanisole (0.4 mmol), ^{t}BuOK (1.2 mmol), benzene (C_6H_6, 2 mL) and deuteriobenzene (C_6D_6, 2 mL). Then the reaction mixture was stirred at 120 °C for 10 h. After the reaction mixture was cooled, quenched, and extracted with AcOEt, NMR analysis was performed to calculate the product ratio.

2.2.5 Method for the leaching experiment

25 mL of screw-capped glass reactor was charged with NrGO (20 mg) in benzene (4 mg) at 120 °C for 2.5 h, then filtered. Iodobenzene (0.4 mmol) and ^{t}BuOK (1.2 mmol) were added to the filtrate and stirred at 120 °C for 24 h. The product yield was analyzed by GC, 0.4 mmol of dodecane was added as an internal standard.

2.2.6 Method for the heterogeneity test

25 mL of screw-capped glass reactor was charged with the catalyst (20 mg), iodobenzene (0.4 mmol), ^{t}BuOK (1.2 mmol), and benzene (4 ml). The reaction mixture was then stirred at 120 °C for 24 h. After completion of the reaction, the mixture was cooled to room temperature,

and the catalyst was removed by filtration. To analyze the product yield by GC, 0.4 mmol of dodecane was added as an internal standard. The filtered catalyst was washed, dried, and subjected to a next experiment under the same conditions. The process was repeated up to five cycles, and the product yield was analyzed by GC.

2.3 References and notes

[1] D.A. Petrone, J. Ye, M. Lautens, *Chem. Rev.* **2016**, *116*, 8003-8104.
[2] D.J. Constable, P.J. Dunn, J.D. Hayler, G.R. Humphrey, G.R., J. L. Leazer Jr, R.J. Linderman, A. Zaks, *Green Chem.* **2007**, *9*, 411-420.
[3] M. Giannerini, M. –F, Mastral B.L. Feringa, *Nat. Chem.* **2013**, *5*, 667-672.
[4] J.W. Blunt, B.R. Copp, R.A. Keyzers, M.H. Munro, M.R. Prinsep, *Nat. Prod. Rep.* **2013**, *30*, 237-323.
[5] J.–W. Delord, F. Glorius, *Nat. Chem*. **2013**, *5*, 369.
[6] J. Chatt, M. Davidson, *J. Chem. Soc.* **1965**, 843.
[7] M.I. Bruce, M.Z. Iqbal, F.G.A. Stone, *J. Chem. Soc. A*, **1970**, 3204.
[8] P. Hong, H. Yamazaki, K. Sonogashira, N. Hagihara, *Chem. Lett.* **1978**, *7*, 535-538.
[9] S. Murai, F. Kakiuchi, S. Sekine, Y. Tanaka, A. Kamatani, M. Sonoda, N. Chatani, *Nature*, **1993**, *366*, 529.
[10] W. Liu, H. Cao, A. Lei, *Angew. Chem, Int. Ed*. **2010**, *122*, 2048-2052.
[11] R. Shang, L. Ilies, and E. Nakamura, *Chem. Rev.* **2017**, *117*, 9086-9139.
[12] W. Liu, L. Ackermann, *ACS Catal.* **2016**, *6*, 3743.
[13] S.Z. Tasker, E.A. Standleym, T.F. Jamison, *Nature*, **2014**, *509*, 299.
[14] F. Vallee, J.J. Mousseau, A.B. Charette, *J. Am. Chem. Soc.* **2010**, *132*, 1514-1516.
[15] Y. Qin, L. Zhu, S. Luo, *Chem. Rev.* **2017**, *117*, 9433-9520
[16] Y. Gao, P. Tang, H. Zhou, W. Zhang, H. Yang, N. Yan, D. Ma, *Angew. Chem. Int. Ed.* **2016**, *55*, 3124-3128.
[17] C.L. Sun, H. Li, D.G. Yu, M.A. Yu, X.A. Zhou, X.Y. Lu, K. Huang, S.F. Zheng, B.J. Li, Z.J. Shi, *Nat. Chem.*, **2010**, *2*, 1044-1049.
[18] E. Shirakawa, K.I. Itoh, T. Higashino, T. Hayashi, *J. Am. Chem. Soc.* **2010**, *132*, 15538-15539.
[19] A. Schaetz, M. Zeltner, W.J. Stark, *ACS Catal*. **2012**, *2*, 1267-1284.
[20] J. Zhang, S. Chen, F. Chen, W. Xu, G. Deng, H. Gong, *Adv. Synth. Catal.* **2017**, *359*, 2358-2363.
[21] M.M. Titirici, M. Antonietti, *Chem. Soc. Rev.* **2010**, *39*, 103-116.
[22] H. Hu, J.H. Xin, H. Hu, X. Wang, Y. Kong, *Appl. Catal. A: Gen.* **2015**, *492*, 1-9.
[23] Y. Cui, Y.H. Lee, J.W. Yang, *Sci. Rep.* **2017**, *7*, 3146.
[24] D.R. Dreyer, S. Park, C.W. Bielawski, R.S. Ruoff, *Chem. Soc. Rev.* **2010**, *39*, 228-240.
[25] C. Su, K.P. Loh, *Acc. chem. Res.* **2012**, *46*, 2275-2285.
[26] A. Primo, M. Puche, O.D. Pavel, B. Cojocaru, A. Tirsoaga, V. Parvulescu, H. Garcia, *Chem. Comm.* **2016**, *52*, 1839-1842.
[27] F. Hu, M. Patel, F. Luo, C. Flach, R. Mendelsohn, E. Garfunkel, M. Szostak, *J. Am. Chem. Soc.*, **2015**, *137*, 14473-14480.
[28] S. Verma, H.P. Mungse, N. Kumar, S. Choudhary, S.L. Jain, B. Sain, O.P. Khatri, *Chem. Comm*. **2011**, *47*, 12673-12675.
[29] M.A. Patel, F. Luo, M.R. Khoshi, E. Rabie, Q. Zhang, C.R. Flach, H. He, *ACS Nano*, **2016**, *10*, 2, 2305.
[30] A. Schaetz, M. Zeltner, W.J. Stark, *ACS Catal*. **2012**, *2*, 1269-2172.
[31] Y. Gao, D. Ma, C. Wang, J. Guan, X. Bao, *Chem. Commun*, **2011**, 47, 2432-2434.
[32] D.S. Su, G. Wen, S. Wu, F. Peng, R. Schlögl, *Angew. Chem. Int. Ed*. **2017**, *56*, 936-964.
[33] Z. Xing, Z. Ju, Y. Zhao, J. Wan, Y. Zhu, Y. Qiang, Y. Qian, *Sci. Rep*. **2016**, *6*, 26146.

[34] Y. Xue, J. Liu, H. Chen, R. Wang, D. Li, J. Qu, L. Dai, *Angew. Chem. Int. Ed.* **2012**, *51*, 12124-12127.
[35] T. Susi, J. Kotakoski, R. Arenal, S. Kurasch, H. Jiang, V. Skakalova, J.C. Meyer, *ACS Nano*, **2012**, *6*, 8837-8846.
[36] H. Sun, Y. Wang, S. Liu, L. Ge, L. Wang, Z. Zhu, S. Wang, *Chem. Comm.* **2013**, *49*, 9914-9916.
[37] D. Geng, Y. Chen, Y. Chen, Y. Li, R. Li, X. Sun, S. Knights, *Energ. Environ. Sci.* **2011**, *4*, 760-764.
[38] S.J. Vijaya, V. Subramanian, *Org. Lett*. **2013**, *15*, 5920-5923.
[39] J. Long, X. Xie, J. Xu, Q. Gu, L. Chen, X. Wang, *ACS Catal.* **2012**, *2*, 622-631.
[40] Y. Gao, G. Hu, J. Zhong, Z. Shi, Y. Zhu, D.S. Su, D. Ma, *Angew. Chem. Int. Ed.* **2013**, *52*, 2109-2113.
[41] N. Morimoto, Y. Takeuchi, Y. Nishina, *Chem. Lett*., **2015**, *45*, 21-23.
[42] X. Fan, C. Yu, J. Yang, Z. Ling, J. Qiu, *Carbon*, **2014**, *70*, 130-141.
[43] Y. Zhao, C. Hu, Y. Hu, H. Cheng, G. Shi, L. Qu, *Angew. Chem. Int. Ed.* **2012**, *51*, 11371-11537.
[44] B. Grzyb, S. Gryglewicz, A. Śliwak, N. Diez, J. Machnikowski, G. Gryglewicz, *RSC Adv*. **2016**, *6*, 15782-15787.
[45] X. Li, H. Wang, J.T. Robinson, H. Sanchez, G. Diankov, H. Dai, *J. Am. Chem. Soc.* **2009**, *131*, 15939-15944.
[46] L. Sun, L. Wang, C. Tian, T. Tan, Y. Xie, K. Shi, H. Fu, *RSC Adv.* **2012**, *2*, 4498-4506.
[47] L. Stobinski, B. Lesiak, A. Malolepszy, M. Mazurkiewicz, B. Mierzwa, J. Zemek, I. Bieloshapka, J. Electron. Spectrosc. Relat. Phenom. 2014, 195, 145-154.
[48] P. Chambrion, T. Suzuki, Z. Zhang, T. Kyotani, A. Tomita, Energy Fuel, 1997, 11, 681-685.
[49] Y. Lin, J. Jin, M. Song, J. Mater. Chem. A, 2011, 21, 3455-3461.
[50] M.P. Kumar, T. Kesavan, G. Kalita, P. Ragupathy, T.N. Narayanan, D.K. Pattanayak, RSC Adv. 2014, 4, 38689-38697.
[51] W. Liu, H. Cao, J. Xin, L. Jin, A. Lei, Chem. Eur. J. 2011, 17, 3588-3592.
[52] C.T. To, T.L. Chan, B.Z. Li, Y.Y. Hui, T.Y. Kwok, S.Y. Lam, K.S. Chan, Tetrahedron Lett. 2011, 52, 1023-1026.
[53] K.I. Fujita, M. Nonogawa, R. Yamaguchi, Chem. Comm. 2004, 0, 1926-1927.
[54] Y.W. Zhu Y.X. Shi, J. Fluor. Chem. 2016, 188, 10-13.
[55] S. Proch, R. Kempe, Angew. Chem. Int. Ed. 2007, 46, 3135-3138.
[56] J.C. Lewis, S.H. Wiedemann, R.G. Bergman, J.A. Ellman, Org. Lett. 2004, 6, 35-38.
[57] A. Correa, O.G. Mancheño, C. Bolm, Chem. Soc. Rev. 2008, 37, 1108-1117.
[58] W. Liu, H. Cao, H. Zhang, H. Zhang, K.H. Chung, C. He, A. Lei, J. Am. Chem. Soc. 2010, 132, 16737-16740.
[59] D. Guo, R. Shibuya, C. Akiba, S. Saji, T. Kondo, J. Nakamura, Science, 2016, 351, 361-365.
[60] J. Long, X. Xie, J. Xu, Q. Gu, L. Chen, X. Wang, ACS Catal. 2012, 2, 622-631.
[61] H. Watanabe, S. Asano, S.I. Fujita, H. Yoshida, M. Arai, ACS Catal., 2015, 5, 2886-2894.
[62] S. Li, W. Wang, X. Liu, X. Zeng, W. Li, N. Tsubaki, S. Yu, RSC Adv., 2016, 6, 13450-13455.
[63] S. van Dommele, K.P. de Jong, J.H. Bitter, Chem. Comm., 2006, 0, 48594861.
[64] L. Ackermann, R. Vicente, A.R. Kapdi, Angew. Chem. Int. Ed. 2009, 48, 9792-9826.
[65] M. Ye, G.L. Gao, A.J. Edmunds, P.A. Worthington, J.A. Morris, J.Q. Yu, J. Am. Chem. Soc. 2011, 133, 19090-19093.

[66] G.P. Yong, W.L. She, Y.M. Zhang, Y.Z. Li, Chem. Commun., 2011, 47, 11766-11768.
[67] R. Paira, B. Singh, P.K. Hota, J. Ahmed, S.C. Sau, J.P. Johnpeter, S.K. Mandal, J. Org. Chem. 2016, 81, 2432-2441.
[68] N. Morimoto, K. Morioku, H. Suzuki, Y. Nakai, Y. Nishina, Chem. Comm. 2017, 53, 7226-7229.
[69] C.V. Rao, C.R. Cabrera Y. Ishikawa, J. Phys. Chem. Lett. 2010, 1, 2622-2627.

CHAPTER 3

Selective Hydrogenation by carbocatalyst: The Role of Radicals

Selective hydrogenation of nitro moiety is a difficult task in the presence of other reducible functional groups such as alkene and/or alkyne. The carbon-based (metal-free) catalyst can be used to selectively reduce substituted nitro-groups using H_2 as a reducing agent, providing a great potential to replace noble metal catalysts and contributing to simple and greener strategies for organic synthesis.

3 Introduction

The development of transition-metal-free catalyses, such as carbocatalysis, would drastically alter the synthetic strategies and purification processes of various conventional organic syntheses. The use of carbocatalysis was first reported in 1867 for the oxidation of alcohols.[1] Since then, this catalytic route has also been applied to dehydrogenation,[2a,b] oxidation,[2c] and Friedel-Crafts reactions.[2d] Carbocatalysts have been increasingly employed in common organic reactions since 2010, including acid, oxidation, reduction, and coupling reactions.[3] Hitherto, however, the carbon-based catalyst has not been used in organic synthesis as alternatives to metal catalysts. We believe that this is due to the low activity, narrow substrate scope, and limited selectivity of the carbocatalysts as compared to metal-based catalysts. It is well-known that the pure carbon hexagonal structure is not catalytically active. Instead, the active sites are formed by defects, edges, and carbon atoms vicinal to the functional groups.[4] The limited number of such active sites in general carbon materials results in low activity. However, it is possible to introduce functional groups, defects, and pores, which can potentially work as catalytically active sites, by chemical treatments.[3b] Therefore, research on the use of chemically modified carbons as catalysts has recently become increasingly popular. Furthermore, several studies have employed additives along with carbon-based catalysts to expand the substrate scope. For example, graphene oxide (GO) has been used with $BF_3{\cdot}OEt_2$ in oxidative C−H coupling reactions,[5] with p-TsOH in the cross-coupling reactions of xanthenes with arenes,[6] and with ^{t}BuOK in C−H bond activation reactions.[7] It has been suggested that these additives generate active radical species on the surface of the carbon, thereby expressing its activity.[8]

In this study, we applied carbon as a selective catalyst for hydrogenation reactions, which are some of the most fundamental reactions in organic synthesis.[9] Although various methods of hydrogenation reactions have been developed over the last several decades, highly active catalytic systems have been achieved using conventional metal-based catalysts.[10] Yet, the selectivity of the metal-catalyzed reaction has long been a problem. In order to fulfill the requirement of fine chemical synthesis, selectivity is critical when two or more reactive groups are present.[12] However, metal catalysts such as Pt, Pd, and Ni, and their supported catalysts, in general, are not chemoselective.[13] Although the modification with alloy or partial poisoning has been reported to

improve the selectivity of noble metal catalysts, such treatments have also led to significantly reduced catalytic activity.[14] Therefore, there is a strong incentive to develop a chemoselective catalyst suitable for the reduction of multi-functionalized compounds in fine chemical synthesis.[15] Herein, we present a new strategy of the carbocatalytic system for the selective reduction of substituted nitro compounds in the presence of H_2, which acted as a reducing agent (Table 3.1). Similar reactivity has been achieved by Co catalyst supported on N-doped carbon materials.[16]

Table 3.1: *Hydrogenation reaction of nitrobenzene with another reducible functional group over different catalysts.*

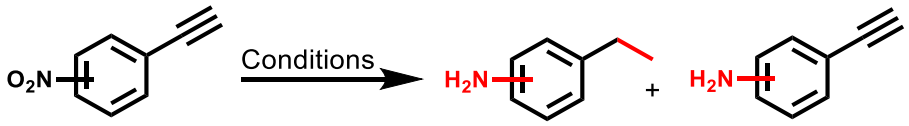

Catalyst	Activity	Selectivity	Ref.
Pd/Pt/Ni	High	No	[13]
Pt+Mo/C Ru:Co-PS Ni-NiO/NGr@C	Moderate	Low	[14]
Co/N-doped carbon	High	High	[16]
Carbocatalyst	High	High	This work

In addition to solving the issue of selectivity, our strategy is advantageous over the previously developed carbon-based catalysts using hydrazine, $NaBH_4$, and other reducing agents,[11] since H_2 is more cost-effective and atom economical.

3.1 Results and discussions

3.1.1 Optimization course

First, we optimized the reaction conditions for the hydrogenation of a nitro group using nitrobenzene (**1a**) as a model substrate (Table 3.2). Notably, no product was formed when the reaction was performed in the absence of a catalyst or base (Table3.2, entries 1 and 2). However, treating **1a** with ^{t}BuOK and nitrogen-doped reduced graphene oxide (NrGO)[‡] in an autoclave at 130 °C in DMSO under 1.5 MPa hydrogen afforded aniline (**2a**) in 58% yield (Table 3., entry 3).[†] The yield was improved by using isopropyl alcohol (IPA) as a solvent (Table 3.2, entry 4, and Table 3.3, entry 1), while other solvents such as THF, toluene, and 1,4-dioxane were not effective (Table 3.2, entries 5–12).

Table 3.2: *Screening results.*[a]

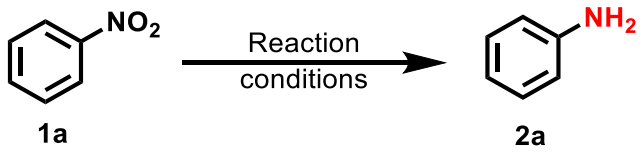

Entry	Base	Catalyst	Solvent	Yield [%]
1	--	NrGO	DMSO	14
2	^{t}BuOK	---	DMSO	11
3	^{t}BuOK	NrGO	DMSO	58
4	^{t}BuOK	NrGO	IPA	80
5	^{t}BuOK	NrGO	THF	39
6	^{t}BuOK	NrGO	Toluene	25
7	^{t}BuOK	NrGO	Ethanol	46
8	^{t}BuOK	NrGO	1,4-dioxane	15
9	^{t}BuOK	NrGO	Water	0

10	^{t}BuOK	NrGO	Pyridine	10
11	^{t}BuOK	NrGO	Acetonitrile	15
12	^{t}BuOK	NrGO	NMP	12
13	NaOH	NrGO	DMSO	26
14	^{t}BuONa	NrGO	DMSO	17
15	K_2CO_3	NrGO	IPA	30
16	Na_2CO_3	NrGO	IPA	12
17	Cs_2CO_3	NrGO	IPA	0
18	^{t}BuOK	NrGO	IPA	30[b]

[a]Reaction conditions: nitrobenzene (0.5 mmol), ^{t}BuOK (1 mmol), NrGO (20 mg), 2 h, 130 °C, H_2 (1.5 MPa). Yields were determined by GC using dodecane as an internal standard. [b]The reaction was performed without molecular hydrogen.

In addition, the decisive influence of the potassium cation was observed, with other bases such as Cs2CO3, NaOH, and ^{t}BuONa being ineffective (Table 3.2, entries 13–17). Furthermore, other carbon materials, such as reduced graphene oxide (rGO), graphene oxide (GO), carbon black (CB), activated carbon (AC), carbon nanotubes (CNTs), and ketjen black (KB) were found less active than NrGO (Table 3.3, entries 2–7).

Table 3.3: *Hydrogenation reaction of nitrobenzene over different catalysts.*[a]

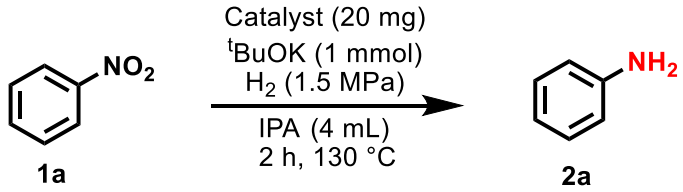

Entry	Catalyst	Yield [%][b]
1	NrGO	80

2	rGO	52
3	GO	46
4	Carbon black	<1
5	Activated carbon	19
6	CNTs	38
7	Ketjen black	21

[a] Reaction conditions: **1a** (0.5 mmol), catalyst (20 mg), ^{t}BuOK (1 mmol), H_2 (1.5 MPa), IPA (4 mL), 2 h, 130 °C. [b] Yields were detected by GC, using dodecane as an internal standard.

3.1.2 The role of radical in the hydrogenation reaction

The radical species of a carbon catalyst is reported to play an important role in promoting electron transferring to substrates, generating new radical intermediates.[17] In order to investigate the contribution of radicals on the NrGO in our hydrogenation system, we performed electron spin resonance (ESR) analysis. The amount of radicals was calculated by integrating the ESR spectra using TEMPOL (4-hydroxy-2,2,6,6-tetramethylpiperidine-1-oxyl) as a standard. As a result, we found a clear correlation between the amount of radicals and the yield of **2a** (Figure 3.1). In an effort to get a deeper insight into the reaction mechanism, we carried out a spin trapping experiment by ESR and confirmed the formation of H radicals *in situ* (Figure 3.2).

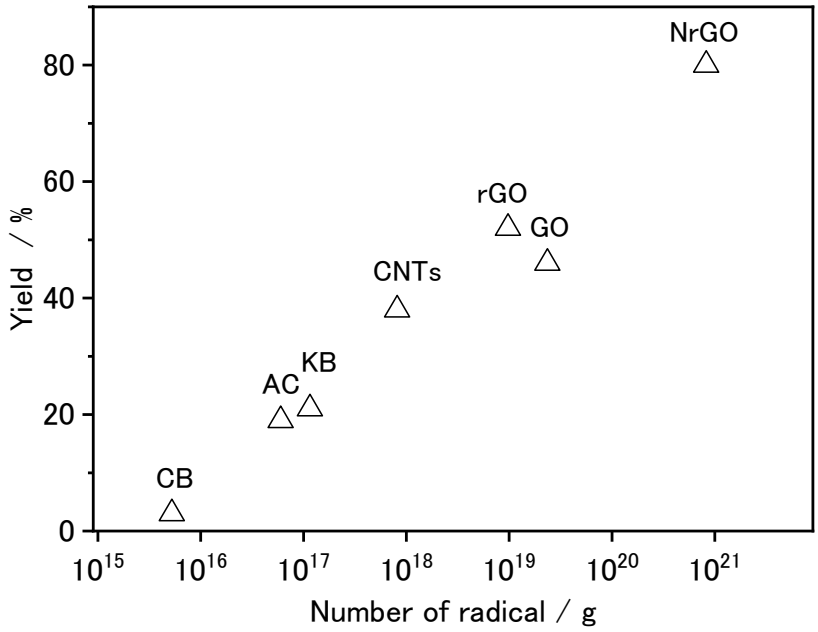

Figure 3.1: *The number of radicals on carbon versus product yield of* ***2a****. The reaction conditions were the same as the reactions shown in Table 3.3.*

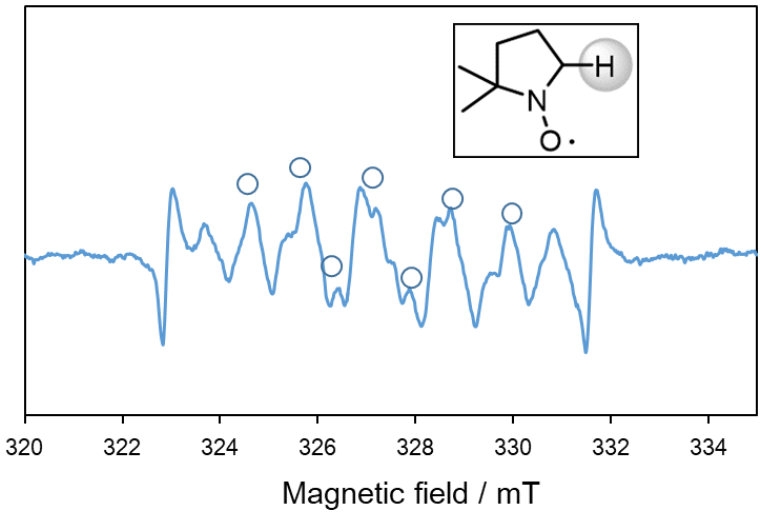

Figure 3.2*. In situ ESR analysis of the mixture of DMPO, NrGO, and* ^{t}*BuOK in IPA in the presence of* H_2*.*

3.1.3 Reaction scope

To manifest the general applicability of NrGO, we explored the reaction scope, testing a series of nitrobenzene compounds for hydrogenation reactions. Notably, the desired amine-containing products were obtained smoothly in good yields (Scheme 3.1). The steric effect of nitrobenzene had a small influence on the product yield; nitro compounds with a methyl group at different positions (ortho and para) gave **2c** and **2d** in similar yields. In addition, nitro compounds with electron-donating substituents gave the corresponding aniline products **2h**-**2k** in good to excellent yields. Furthermore, when both halogens (Br, Cl, or I) and nitro substituents coexist in a substrate, selective hydrogenation of the nitro group proceeded to form **2h**, **2i**, and **2k** without the formation of dehalogenation or homo-coupling product. This is in high contrast with the precious-metal-based catalysts such as Ru,[18a] $Pd(OAc)_2$/MHS,[18b] and S8/mild base systems;[18c] dehalogenation occurred with these catalysts.

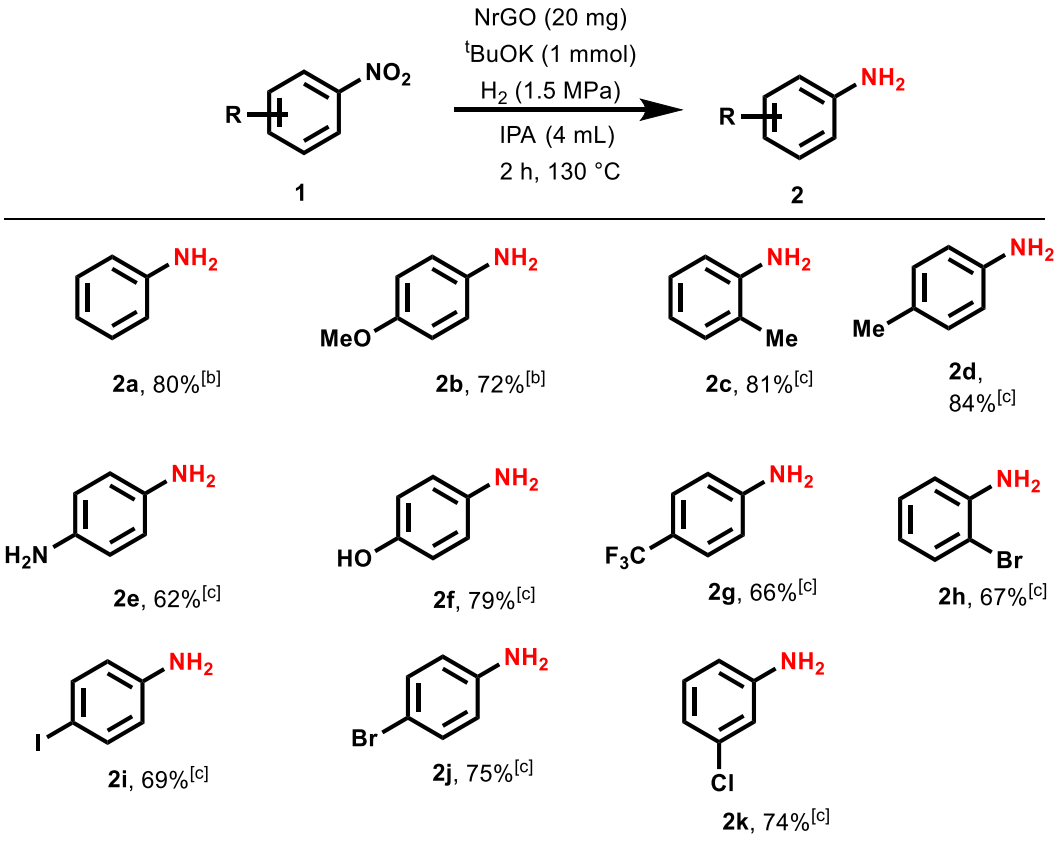

Scheme 3.1: Reaction conditions; **1** (0.5 mmol), catalyst (20 mg), ^{t}BuOK (1 mmol), H_2 (1.5 MPa), IPA (4 mL), 2 h, 130 °C. [b] Yields were detected by GC, using dodecane as an internal standard. [c] Yields were detected by ^{1}H-NMR, using 1,1,2,2-tetrachloroethane as an internal standard.

3.1.4 Mechanistic study

Generally, there are two reaction pathways for the catalytic hydrogenation of nitro compounds: direct and condensation (Scheme 3.2). In the direct pathway, nitrobenzene is reduced to aniline through nitrosobenzene and phenylhydroxylamine. In contrast, in the condensation pathway, nitrosobenzene reacts with phenylhydroxylamine to form azoxobenzene via condensation; azobenzene and hydroazobenzene are then formed before aniline is obtained.[19]

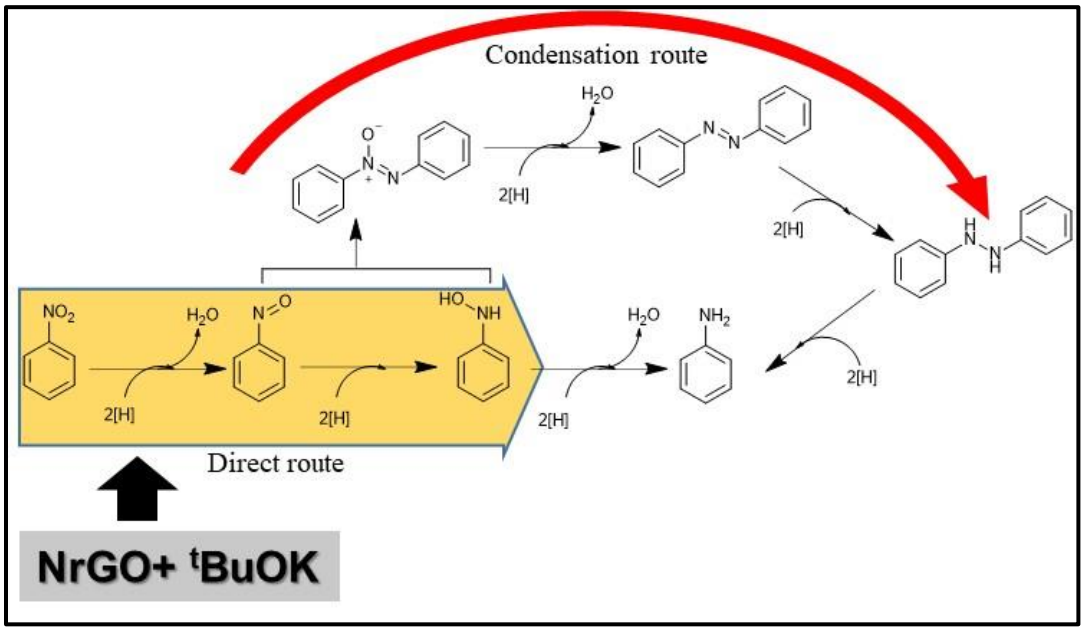

***Scheme 3.2**: Different mechanisms for the hydrogenation reaction of nitrobenzene to aniline, catalyzed by NrGO.*

In our system, 3% azobenzene (**3a**) was obtained as a by-product of the desired aniline (**2a**) (Scheme 3.3a), thereby indicating a condensation pathway. This was confirmed by the fact that the reaction of the possible intermediate, azobenzene (**3a**), under standard reaction conditions achieved full conversion to aniline (**2a**) (Scheme 3.3b).

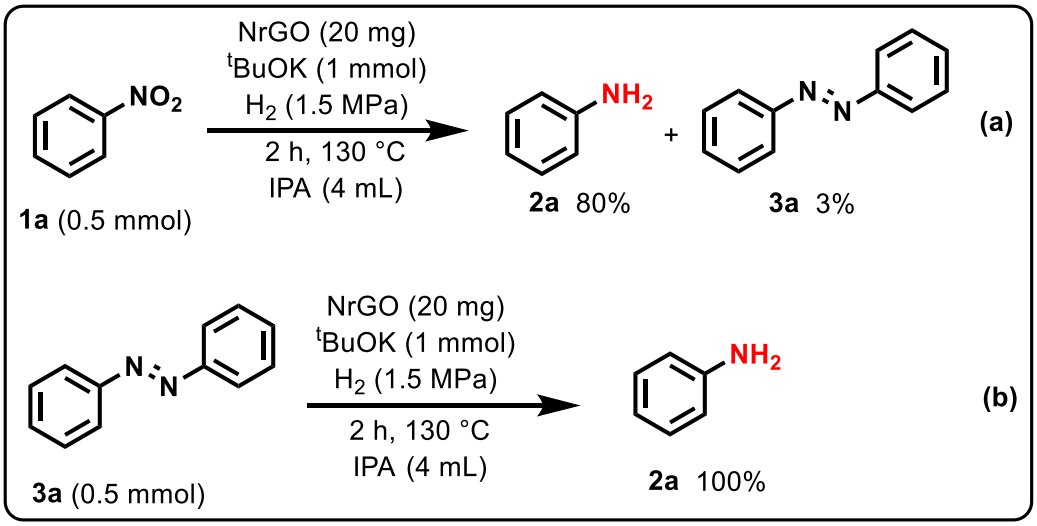

Scheme 3.3. *Reaction pathway analysis.*

3.1.5 Ketone hydrogenation

The scope of the NrGO-catalyzed hydrogenation was further extended to carbonyl compounds. Acetophenone derivatives (**3**) were hydrogenated effectively to form the corresponding alcohol (**4**) under identical conditions (Scheme 3.4).

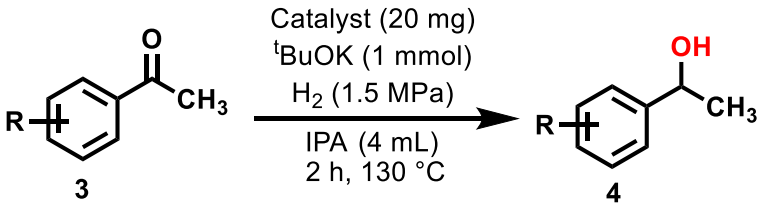

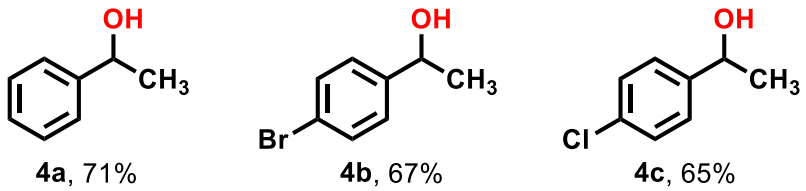

Scheme 3.4: Reaction conditions; **3** (0.5 mmol), NrGO (20 mg), ^{t}BuOK (1 mmol), H_2 (1.5 MPa), IPA (4 mL), 2 h, 130 °C. Yields were detected by ^{1}H NMR using 1,1,2,2-tetrachloroethane as an internal standard.

3.1.6 Chemoselective competitive hydrogenation

Next, we applied the carbocatalytic hydrogenation on a more challenging chemoselective competitive systems. The chemoselective reduction of the nitro group in the presence of an alkyne group was then studied through the hydrogenation of 4-ethynyl-4'-nitro-1,1'-biphenyl (**5**), as a result, the alkyne group was not reduced and only **6** was formed as a product, thereby confirming the chemoselectivity of NrGO (Table 3.4, entry 1). As a control, we also applied Pd/C as a catalyst to the same system; **5** was completely reduced to **7** (Table 3.4, entry 2). Yabe et al. reported a similar phenomenon in Pd-based nitrogen-containing molecules as heterogeneous catalytic systems.[20] In conclusion, NrGO catalyzed the hydrogenation of the nitro group faster than other reducible functionalities. This result further evidenced the excellent chemoselectivity of NrGO.

Table 3.4: *Chemoselective hydrogenation of the nitro group in the presence of NrGO and Pd/C.*

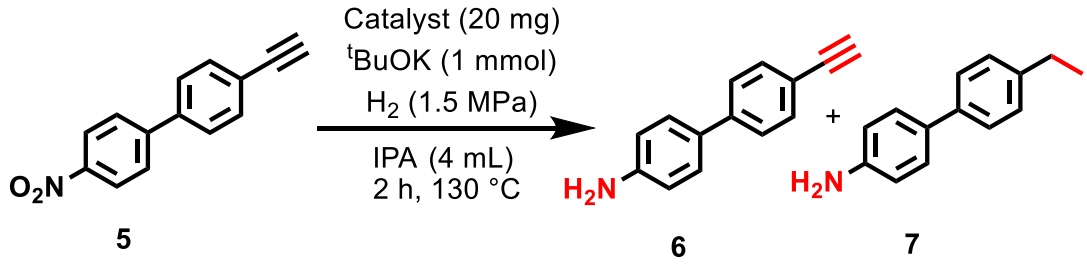

Entry[a]	Catalyst	Products yield [%][b]	
		6	**7**
1	NrGO	65	0
2	Pd/C	0	98

[a] **Reaction conditions**: **5** (0.5 mmol), NrGO (20 mg), ^{t}BuOK (1 mmol), H_2 (1.5 MPa), IPA (4 mL), 2 h, 130 °C. [b] Yields were detected by 1H NMR using 1,1,2,2-tetrachloroethane as an internal standard.

Furthermore, we proved that the nitro group could be selectively reduced even in the presence of a carbonyl moiety using NrGO via a reduction of 4-nitroacetophenone (**8**). The chemoselectivity of NrGO towards the nitro group was once again confirmed. Neither (4-nitrophenyl)ethan-1-ol nor (4-aminophenyl)ethan-1-ol (**10**) was detected when NrGO was used as a catalyst, and aminoacetophenone (**9**) was obtained exclusively (Table 3.5, entry 1). Interestingly, the use of Pd/C (Table 3.5, entry 2) led to the contrary result: the reduction of the nitro group with molecular hydrogen was not selective, and both functional groups were reduced to form **10**. Overall, NrGO differed drastically from previously reported hydrogenation reactions by transition-metal catalysts.[21]

Table 3.5: *Chemoselective hydrogenation of the nitro group in the presence of NrGO and Pd/C.*

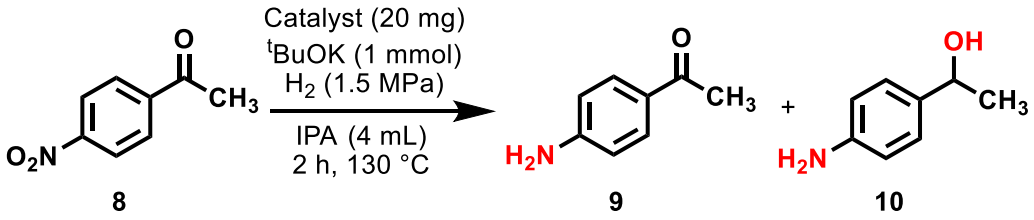

Entry[a]	Catalyst	Products yield (%)[b]	
		9	**10**
1	NrGO	68	0
2	Pd/C	0	92

[a] **Reaction conditions: 8** (0.5 mmol), catalyst (20 mg), ^{t}BuOK (1 mmol), H_2 (1.5 MPa), IPA (4 mL), 2 h, 130 °C. [b] Yields were detected by GC-MS using dodecane as an internal standard.

From these experimental pieces of evidence, we considered the following explanation for the chemoselectivity. The addition of ^{t}BuOK to NrGO promotes the neutralization of acidic functional groups (orange moiety in Figure 3.3a) and accelerates localization of radicals at the

basic sites (blue in Figure 3.3a). Molecular hydrogen and the radicals react to generate hydrogen radicals (blue in Figure 3.3b), which are confirmed by spin trap reaction (Figure 3.3c). Ionic moiety on NrGO (orange in Figure 3.3b) can interact strongly with polarized nitro groups than less polarized alkynes, alkenes, and carbonyls.[22] Such stronger interaction of nitro groups with the carbon-based catalyst promotes the selective reaction. Another explanation is that frustrated Lewis acid-base pairs on NrGO, such as oxygenated functional groups and amino groups, would activate hydrogen molecules by polarization and simultaneous formation of H^+ -like and H^- -like species.[23] Then, nitro groups located at the surface of NrGO react preferentially to be converted to amino groups.

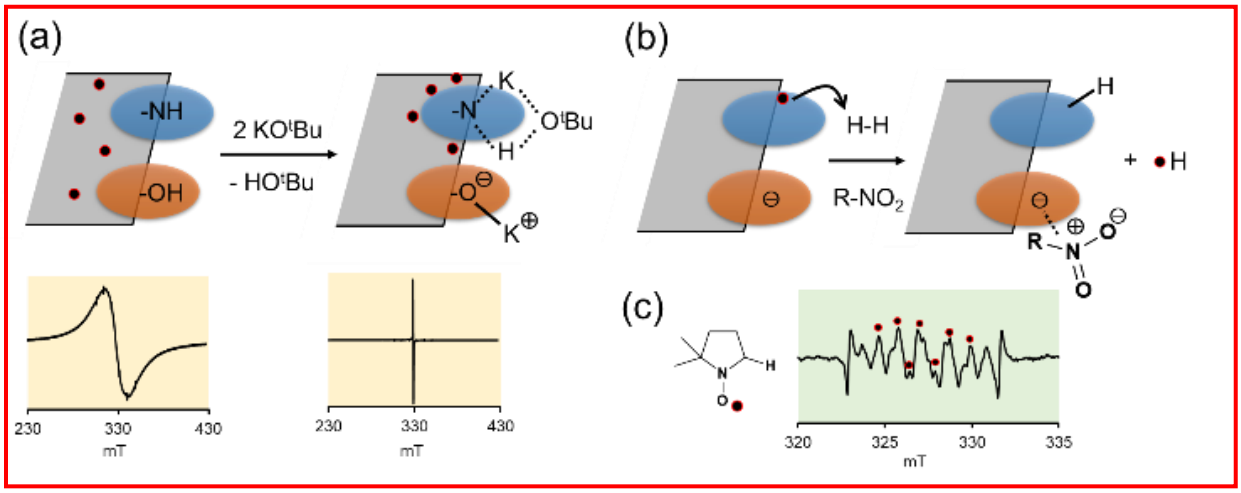

Figure 3.3: *Explanation of reaction mechanism; (a) reaction of NrGO with ^{t}BuOK, then (b) reaction with H_2, and (c) trapping of hydrogen radical with DMPO.*

3.1.7 Recyclability of the catalyst

Finally, we investigated the recyclability and stability of NrGO, which are very important indicators for the practical applicability of the catalyst. Notably, NrGO was recycled and reused five times without reactivation.‡ However, after the 4th recycling run, a slight decrease in the yield of (**2a**) was observed (Figure 3.4). In this case, longer reaction time (~4 h) was necessary to increase the product yield.

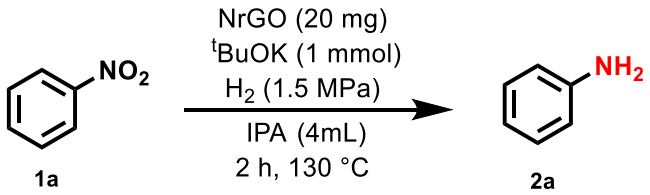

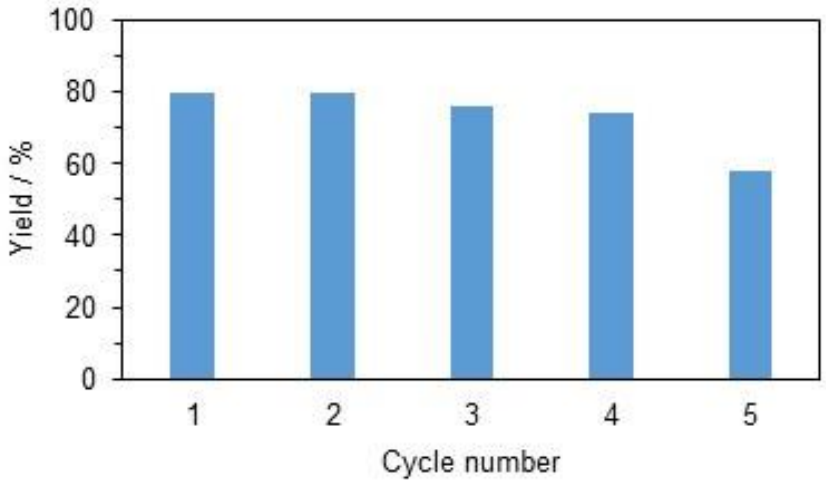

Figure 3.4: *Recyclability of NrGO for the hydrogenation of nitrobenzene.*

In conclusion, we developed a metal-free chemoselective system for the reduction of substituted nitroaromatic compounds using NrGO as a catalyst and molecular hydrogen as a reducing agent. Similar catalytic performances have been reported by metal catalysts supported on N-doped carbon materials.[16,17] We suggest that the selective hydrogenation reaction proceeds via a radical mechanism, in which the localized radicals of NrGO activate the hydrogen. Overall, our results revealed that the unconventional activity of NrGO has excellent potential for the selective hydrogenation reaction of multi-functionalized nitro compounds.

3.2 Experimental

Generally, graphite powder (100 g) was dispersed in 2.5 L of concentrated H_2SO_4. After cooling the mixture in an ice bath, $KMnO_4$ (300 g) was subsequently added and kept below 55 °C. The mixture was stirred at 35 °C for two h to complete the oxidation. The generated suspension was once again cooled down, after which 5 L of deionized water was added slowly as the temperature was adjusted below 50 °C with continuous stirring. Then, 250 mL of H_2O_2 (30% aq.) was added to the mixture. Finally, the generated brown crude graphite oxide was purified by centrifugation (10 times) to afford graphene oxide (GO). Nitrogen doping onto GO was conducted by dissolving 1 g of nitrogen source (guanidine carbonate) (Scheme 3.5) in 100 mL of 0.1 wt% GO solution to attain a 10:1 ratio of nitrogen source to GO. The mixture was transferred into a steel-based autoclave and subjected to hydrothermal treatment at 180 °C for 8 h. The autoclave was then allowed to cool down to room temperature naturally, after which the black precipitate was filtered and washed five times with deionized water and once with isopropanol. Finally, the product was dried in a freeze drier and labeled as NrGO, as presented in the scheme below (Scheme 3.5). For comparison, rGO was prepared according to the same method, without the addition of a nitrogen source.

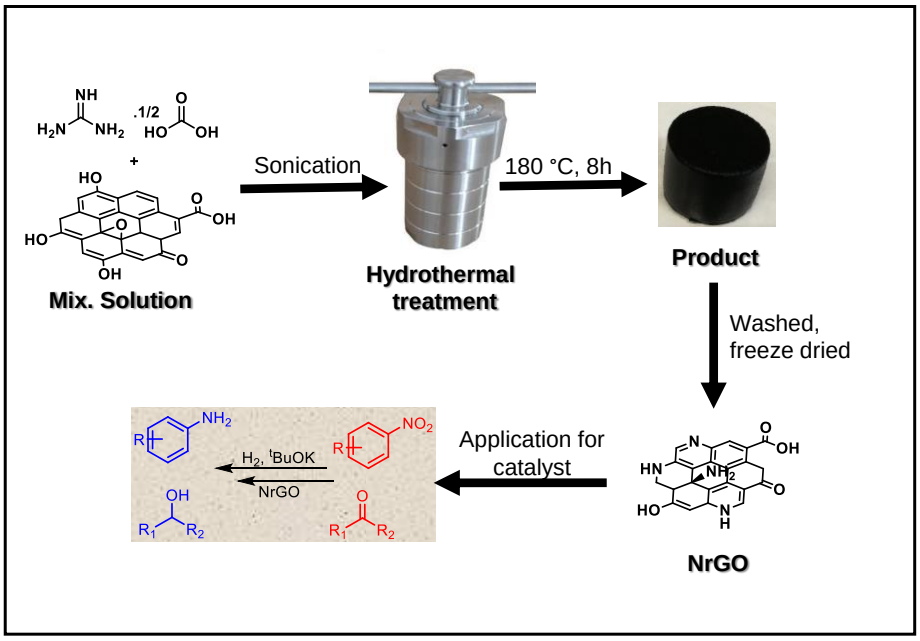

Scheme 3.5: *Schematic illustration of the synthesis of NrGO and its application in catalysis.*

3.2.1 Structural analysis of NrGO

For the structural analysis of NrGO, we performed Fourier-transform infrared (FT-IR) spectroscopy (Figure 3.6). A peak was observed at 3408 cm^{-1}, corresponding to –OH and/or –NH. The characteristic peaks at 1660 and 1548 cm^{-1} were assigned to the C=O and C=C stretching vibrations, respectively. Furthermore, the sharp peak at 1151 cm^{-1} may be attributed to C–N bond stretching.[24-26] The chemical composition was further examined by X-ray photoelectron spectroscopy (XPS). The XPS spectra showed peaks at 285, 400, and 532 eV, corresponding to the binding energies of C 1s, N 1s, and O 1s, respectively (Figure 3.6).[27,28]These results confirmed that the nitrogen atom was successfully doped on the graphene framework. Narrow XPS analysis at the N1s region showed a total nitrogen doping level of 5 at%, with NH groups mainly formed (Figure 3.6b). The morphology studies of NrGO using scanning electron microscopy (SEM) and transmission electron microscopy (TEM) revealed a layered structure, as reported by Gao *et al.* (Figure 3.6c).[29]

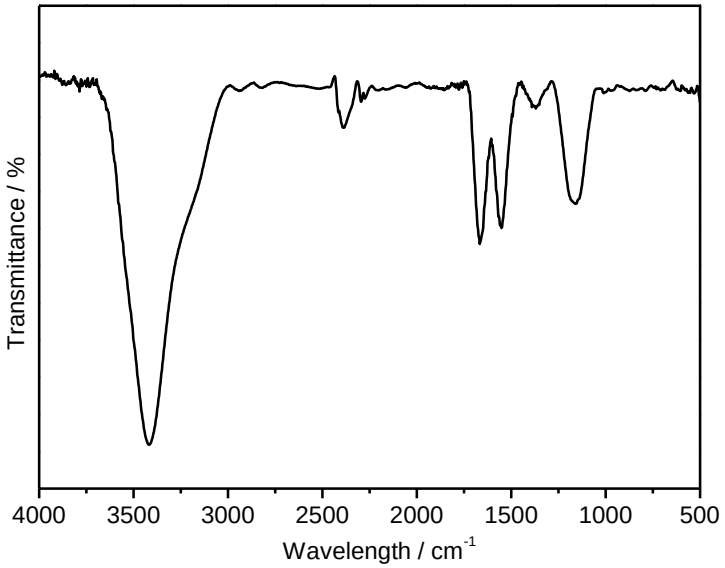

Figure 3.6a: *Structural analysis of NrGO the FT-IR spectra.*

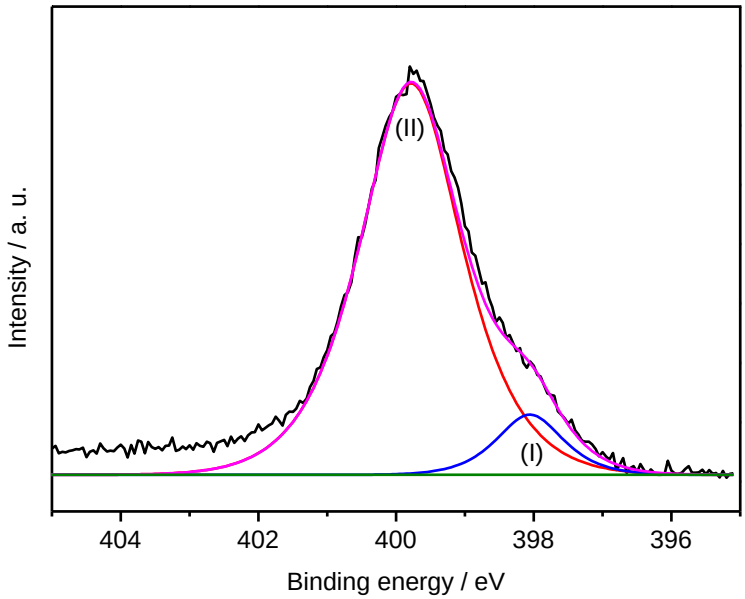

Figure 3.6b: *XPS N1s spectra: **(I)** pyridinic and **(II)** NH groups detected.*

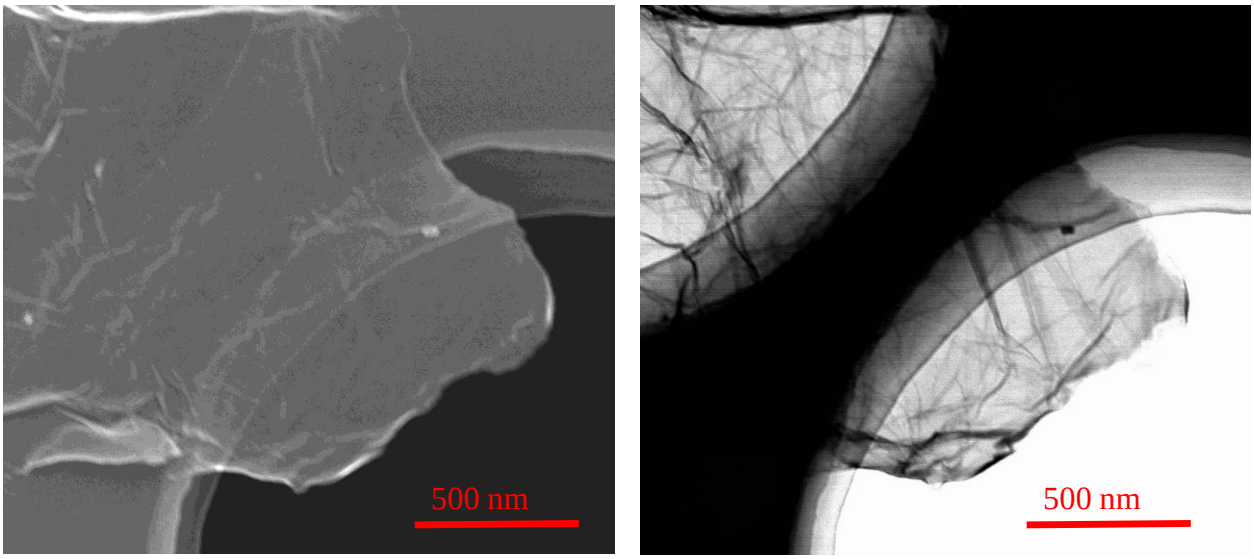

Figure 3.6c: *SEM image of the NrGO upper, while the TEM image of the NrGO below.*

Table 3.6*: Elemental composition of the catalysts, the atomic ratio was determined by XPS.*

	C / at %	**N / at %**	**O / at %**
NrGO	83.3	5.0	11.7
rGO	85.1	--	14.9
GO	65.3	--	34.7

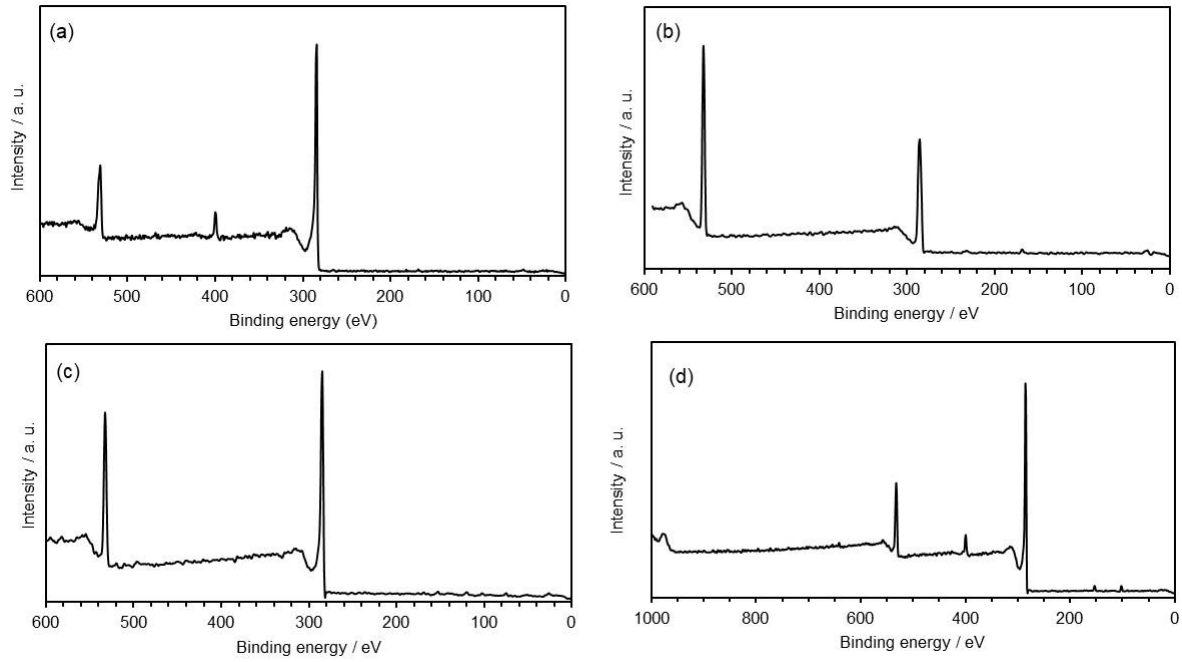

Figure 3.6: *XPS survey spectra of (**a**) NrGO, (**b**) GO, (**c**) rGO, and (**d**) wide range XPS of NrGO.*

3.2.2 General procedure for the hydrogenation of nitroarenes

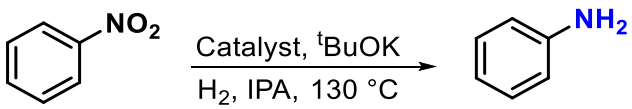

Nitroarenes (0.5 mmol), NrGO (20 mg), base (1.0 mmol), solvent (4 mL), and H_2 (1.5 MPa) were loaded into a glass tube equipped in a steel-based autoclave. The mixture was heated to 130 °C with continuous stirring for 2 h unless otherwise specified. After completion of the reaction, the mixture was cooled to room temperature. Furthermore, 0.5 mmol of dodecane, which

was used as an internal standard, was added. The product was analyzed by GC-MS and quantified by GC.

3.2.3 General procedure for the hydrogenation of ketones

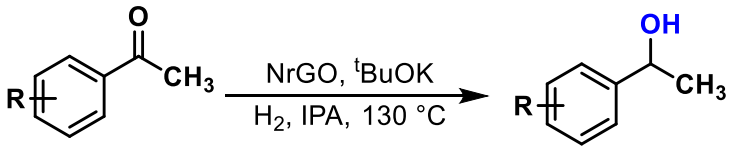

The method is similar to the one presented above for the hydrogenation of nitroarenes. A steel-based autoclave was charged with NrGO (20 mg), ketone (0.5 mmol), base (1.0 mmol), and solvent (4 mL). The autoclave was purged with H_2 (1.5 MPa) 3 times. The mixture was then stirred at 130 °C for the specified amount of time. After completion of the reaction run, the mixture was cooled down to room temperature, and 0.5 mmol of dodecane was subsequently added and used as an internal standard. The product was analyzed by GC-MS and quantified by ^{1}H NMR.

3.2.4 Selective competitive experiment

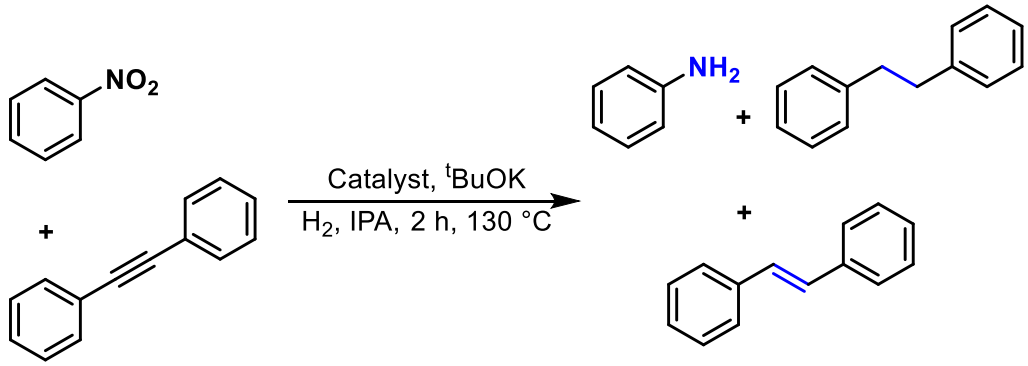

An equimolar mixture of nitrobenzene (0.5 mmol) and diphenylacetylene (0.5 mmol) was added into an autoclave, followed by the addition of NrGO (20 mg), IPA (4 mL), and ^{t}BuOK (1 mmol). The autoclave was then pressurized with H_2 to 1.5 MPa. The mixture was stirred continuously at 130 °C for a specified time. After cooling down to room temperature and releasing the hydrogen pressure in a fume hood, and 0.5 mmol of dodecane as an internal standard was subsequently added. The product was analyzed by GC-MS and quantified by ^{1}H NMR. The same experiment was performed under the Pd/C catalyst, and the product yields were compared.

3.2.5 Representative procedure

The stainless steel auto cleave (30 mL) fitted with an inner glass tube was charged with nitrobenzene (1 mmol), catalyst (40 mg), base (2.0 mmol), solvent (8 mL), and H_2 (3 MPa). The mixture was heated to 130 °C with continuous stirring for 2 h. After completion of the reaction, the mixture was cooled to room temperature. Furthermore, the catalyst (NrGO) was removed by filtration, and the filtrate was extracted with ethyl acetate, and concentrated under reduced pressure. The residue was purified by flash column chromatography on silica gel (hexane: ethyl acetate = 10 : 1), to afford the product **2a** in 85% yield (78.2 mg).

3.2.6 Product identification

Hydrogenation of nitroarenes was performed in 30 ml of stainless autoclave fitted with an inner glass tube. Upon completion of the reaction run, the catalyst (NrGO) was removed by filtration, and the filtrate was extracted with ethyl acetate. Evaporation of solvent followed by column chromatography, the purity of the compound was determined by 1H NMR analysis. All of these compounds are known and in good agreement with the reported literature. All these compounds are known compounds and were characterized by a comparison of their spectra with the reported data.

Aniline (2a): Purification by flash chromatography (hexane : ethyl acetate = 10 : 1) gave 80% (43.5 mg) of a colorless oil. ^{1}H NMR (400 MHz, $CDCl_3$): δ 7.19-7.15 (m, 2H), 6.80-6.76 (m, 1H), 6.71-6.69 (m, 2H), 3.48 (br s, 2H, -NH_2).[30]

4-Aminoanisole (2b): Purification by flash chromatography (hexane: ethyl acetate = 10: 1) gave 72% (44.2 mg) of pale purple crystals. ^{1}H NMR (400 MHz, DMSO-d_6): δ 6.6 (d, *J*= 9.2 Hz, 2H), 6.5 (d, *J*= 9.2 Hz, 2H), 4.5 (br s, 2H), 3.6 (s, 3H).[31]

2-Aminotoluene (2c): Purification by flash chromatography (hexane: ethyl acetate = 12: 1) gave 81% (51.3 mg) of a colorless oil. ^{1}H NMR (400 MHz, DMSO-d_6): δ 6.7 (m, 2H), 6.5 (m, 2H), 4.6 (br s, 2H), 3.6 (s, 3H).[32]

4-Aminotoluene (2d): Purification by flash chromatography (hexane: ethyl acetate = 10: 1) gave 84% (44.9 mg) of pale yellow crystals. ^{1}H NMR (400 MHz, DMSO-d_6): δ 6.8 (d, *J*= 9.2 Hz, 2H), 6.4 (d, *J*= 9.2, 2H), 4.7 (br s, 2H), 2.1 (s, 3H).[33]

1,4-Phenylenediamine (2e): Purification by flash chromatography (hexane: ethyl acetate = 8: 1) gave 62% (34.5 mg) of purple crystals. ^{1}H NMR (400 MHz, DMSO-d_6): δ 6.3 (s, 4H), 4.2 (br s, 2H).[34]

4-Aminophenol (2f): Purification done by flash chromatography (hexane: ethyl acetate = 8: 1) gave 79% (43.1 mg) of brown solid. ^{1}H NMR (400 MHz, DMSO-d_6): δ 8.4 (s, 1H), 6.5 (d, *J*= 8.8 Hz, 2H), 6.5 (d, *J* = 8.8 Hz, 2H), 4.4 (br s, 2H).[35]

4-Trifluromethylaniline (2g): Purification by flash chromatography (hexane: ethyl acetate = 8: 1) gave 66% (66 mg) of purple crystals. ^{1}H NMR (400 MHz, DMSO-d_6): δ 7.3 (d, *J*= 8.4 Hz, 2H), 6.6 (d, *J*= 8.4 Hz, 2H), 5.8 (br s, 2H).[36]

2-Bromoaniline (2h): Purification by flash chromatography (hexanes: ethyl acetate = 10: 1) gave 67% (57.6 mg) of pale yellow crystals. ^{1}H NMR (400 MHz, DMSO-d_6): δ 7.3 (dd, *J*= 8.0, 1.4 Hz, 1H), 7.1-7.0 (m, 1H), 6.8 (dd, *J*= 8.0, 1.4 Hz, 1H), 6.5-6.4 (m, 1H), 5.3 (br s, 2H).[37]

4-Iodoaniline (2i): Purification by flash chromatography (hexane: ethyl acetate = 10: 1) gave 69% (48.4 mg) of pale brown crystals, ^{1}H NMR (400 MHz, $CDCl_3$): δ 7.43 (d, *J*= 8.8 Hz, 2H), 6.47 (d, *J*= 8.8 Hz, 2H), 3.70 (br s, 2H).[38]

4-Bromoaniline (2j): Purification by flash chromatography (hexane: ethyl acetate = 10: 1) gave 75% (76.6 mg) of brown solid. ^{1}H NMR (400 MHz, DMSO-d_6): δ 4.3 (d, *J*= 8.8 Hz, 2H), 6.5 (d, *J*= 8.8 Hz, 2H), 3.6 (br s, 2H).[35]

3-chloroaniline (2k): Purification by flash chromatography (hexane: ethyl acetate = 10: 1) gave 74% (49.7 mg) of pale yellow crystals. ^{1}H NMR (400 MHz, DMSO-d_6): δ 7.05-7.01 (m, 1H), 6.62-6.50 (m, 1H), 6.5-6.4 (m, 2H), 5.4 (br s, 2H).[39]

3.2.7 ESR study

The ESR spectra of the samples were initially recorded using an electron spin resonance spectrometer (JES-X310) with 9.542 GHz microwave frequency, 100 kHz modulation frequency, 1 mW power, and 2 min of weep time. The samples (~1 mg each) were sealed in a 1-mm-internal-diameter, 50-mm-long quartz capillary tubes. Radical contents were calculated from the integration of ESR spectra using TEMPOL (4-hydroxy-2,2,6,6-tetramethylpiperidine-1-oxyl) as a standard. As can be seen from (Figure 3.7a), a pair of broad peaks were observed for NrGO, suggesting the presence of delocalized radical species. Upon the addition of ^{t}BuOK to NrGO, these peaks became narrower, thus implying that the delocalized radicals on the surface of NrGO have become localized (Figure 3.7b).

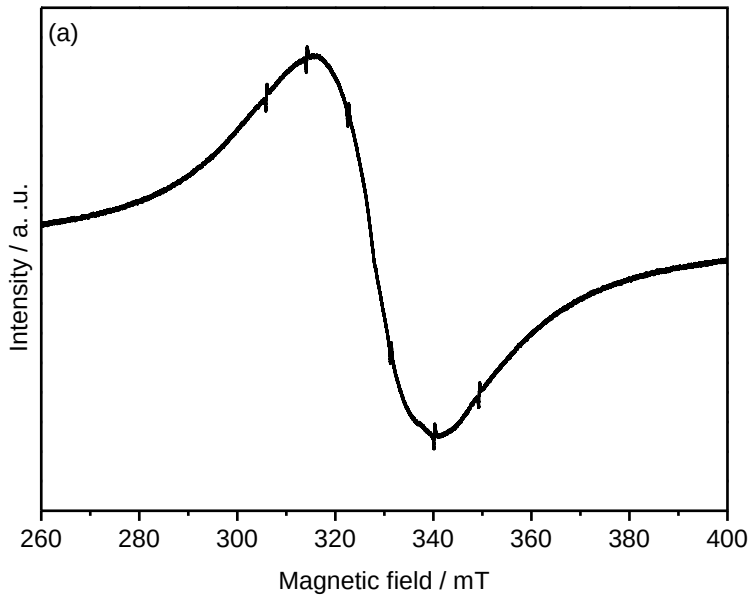

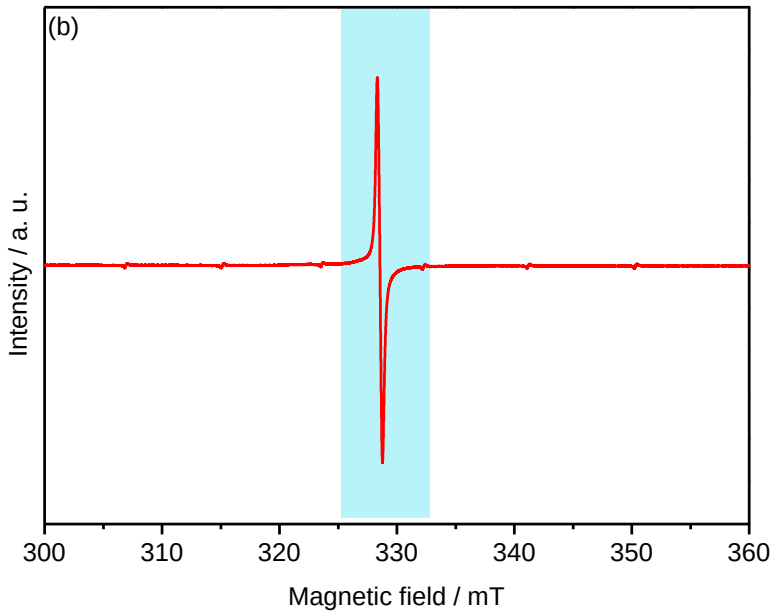

Figure 3.7: *(**a**) ESR spectrum of NrGO, while (**b**) ESR spectrum of NrGO after mixing with* ^{t}*BuOK.*

3.2.8 Spin trap experiments

1) NrGO (1 mg) was placed in an ESR tube, sealed, and analyzed.
2) NrGO (10 mg) and ^{t}BuOK (0.5 mmol) were mixed homogenously, 1 mg of the resulting mixture was immediately transferred to an ESR tube and analyzed.
3) NrGO (10 mg), IPA (2 mL), and a stir bar were loaded into an autoclave, together with 5,5-dimethyl-1-pyrroline N-oxide (DMPO). The reaction mixture was then stirred at 130 °C. After the completion of the reaction, the liquid mixture was taken and analyzed by ESR.
4) For the hydrogen trapping, the same method was used, while the autoclave was purged with 1.5 MPa H_2 before stirring at 130 °C. After releasing the hydrogen pressure, the liquid sample was taken up and directly measured by ESR.

3.2.9 Method for the recyclability test

Typically, a mixture of nitroarenes (0.5 mmol), NrGO (20 mg), ^{t}BuOK (1.0 mmol), IPA (4 mL), and H_2 (1.5 MPa) were loaded into a glass tube equipped in a steel-based autoclave. The mixture was heated to 130 °C with continuous stirring for 2 h. After completion of the reaction, the mixture was cooled to room temperature and filtered. Furthermore, 0.5 mmol of dodecane, which was used as an internal standard, was added. The product was analyzed by GC. The recovered catalyst was washed with water and then ethanol, subsequently dried before its use in the next reaction. The process was repeated up to the fourth cycle, and the yield was calculated by GC.

3.2.10 Surface characterization of the recycled catalyst

XPS analysis at C 1s region of GO before and after the hydrogenation reaction indicated a drastic decrease of C−O/C=O on the surface (Figure 3.8). In contrast, NrGO did not change before and after the reaction (Figure 3.9-3.11).

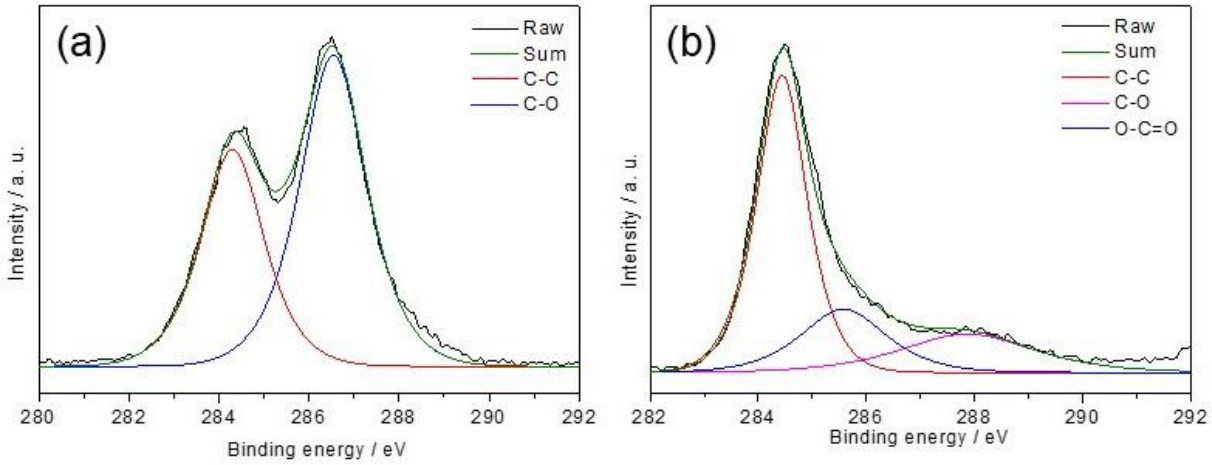

Figure 3.8: *XPS C 1s of GO (**a**) before and (**b**) after the hydrogenation reaction*.

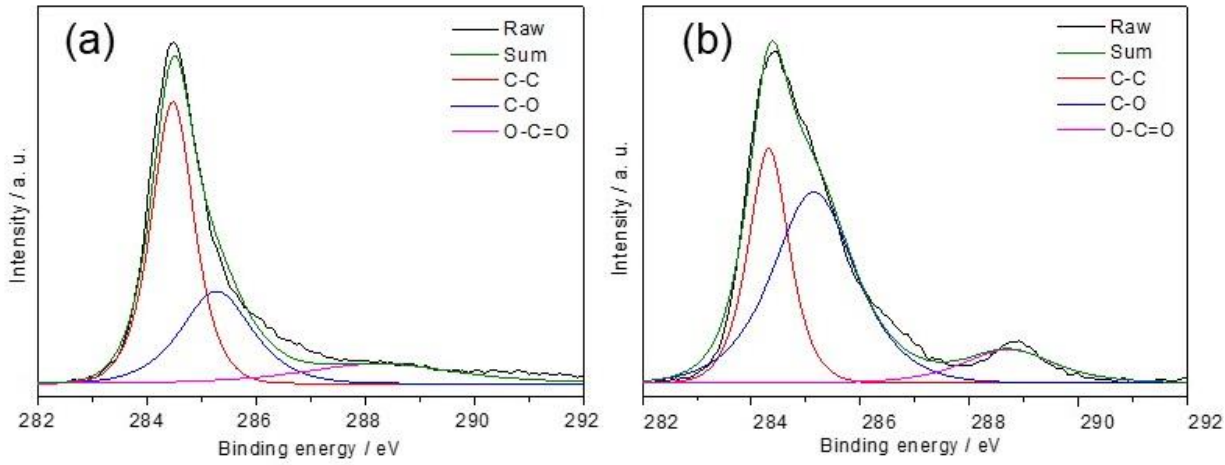

Figure 3.9: *XPS C 1s of rGO (**a**) before and (**b**) after the reaction.*

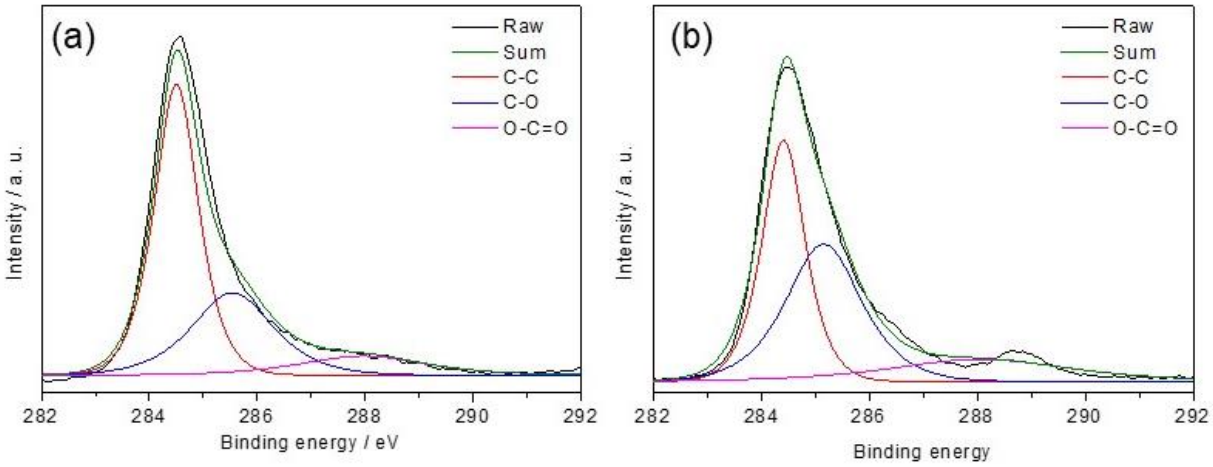

Figure 3.10: *XPS C 1s of NrGO (**a**) before and (**b**) after the reaction.*

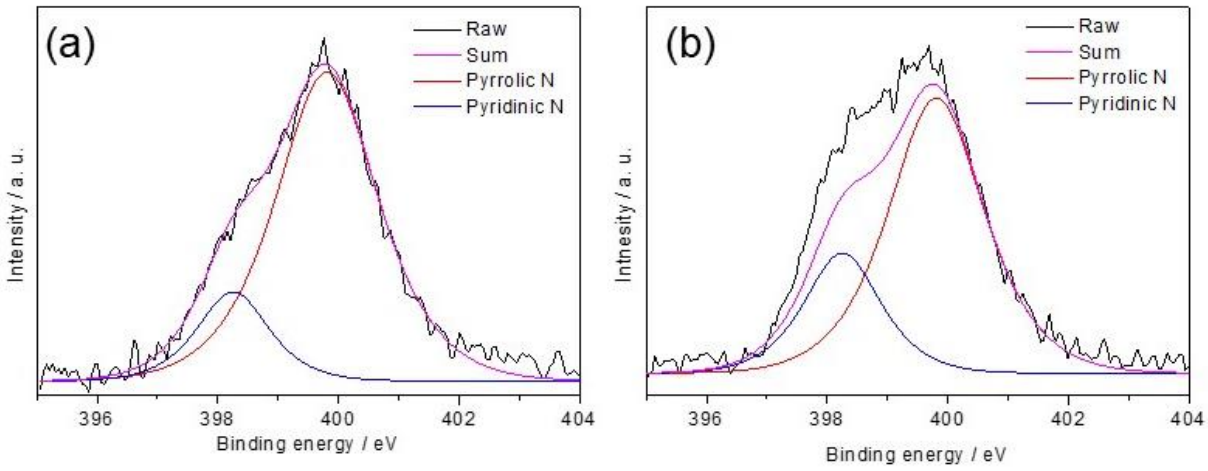

Figure 3.11: *XPS spectra of N 1s of NrGO (**a**) before and (**b**) after the reaction.*

3.3 References and Note

‡ NrGO was previously developed by the author's laboratory and used as a cross-coupling catalyst.[4b] The structure of NrGO was characterized by FT-IR, SEM, TEM, XPS analyses, and 1H NMR data, and the stability of NrGO after 5 cycles was evaluated using XPS analysis. (Figure 3-7 to 3-10).

† Initially, we utilized DMSO as a solvent in the hydrogenation reactions and obtained the product in acceptable yields. In addition, we confirmed that IPA could work as a hydrogen source but provided low product yields. In this case, the product yield was further enhanced by adding molecular hydrogen to the system. Thus, IPA was used as a solvent for further studies.

[1] Calvert, F. C. *J. Chem. Soc.* **1867**, 20, 293–296.

[2] (a) Iwasawa, Y. *J. Catal.* **1973**, 31 (3), 444–449. (b) Zhang, J.; Liu, X.; Blume, R.; Zhang, A.; Schlogl, R.; Su, D. S. *Science* **2008**, 322 (5898), 73–77. (c) Lücking, F.; Köser, H.; Jank, M.; Ritter. A. *Water Res.* **1998**, 9 (32) 2607-2614. (d) Kodomari, M.; Suzuki, Y.; Yoshida, K. *Chem. Commun*. **1997**, 0 (16), 1567–1568.

[3] (a) Su, C.; Loh, K. P. *Acc. Chem. Res.* **2013**, 46 (10), 2275–2285. (b) Navalon, S.; Dhakshinamoorthy, A.; Alvaro, M.; Garcia, H. *Chem. Rev.* **2014**, 114 (12), 6179–6212. (c) Su, D. S.; Wen, G.; Wu, S.; Peng, F.; Schlögl, R. *Angew. Chem. Int. Ed*. **2017**, 56 (4), 936–964.

[4] (a) Guo, D.; Shibuya, R.; Akiba, C.; Saji, S.; Kondo, T.; Nakamura, J. *Science* **2016**, 351 (6271), 361–365. (b) Sohail Ahmad, M.; Suzuki, H.; Wang, C.; Zhao, M.; Nishina, Y. *J. Catal*. **2018**, 365, 344–350.

[5] Morioku, K.; Morimoto, N.; Takeuchi, Y.; Nishina, Y. *Sci. Rep*. **2016**, 6, 25824.

[6] Wu, H.; Su, C.; Tandiana, R.; Liu, C.; Qiu, C.; Bao, Y.; Wu, J.; Xu, Y.; Lu, J.; Fan, D.; et al. *Angew. Chem. Int. Ed.* **2018**, 57 (34), 10848–10853.

[7] Gao, Y.; Tang, P.; Zhou, H.; Zhang, W.; Yang, H.; Yan, N.; Hu, G.; Mei, D.; Wang, J.; Ma, D. *Angew. Chem. Int. Ed.* **2016**, 55 (9), 3124–3128.

[8] Xie, J. *Carbon* **2017**, 121, 418–425.

[9] (a) Smith, M. B.; March, J. *John Wiley & Sons,* **2007**. (b) Andersson, P. G.; Munslow, I. J. *John Wiley & Sons,* **2008**.

[10] (a) Schäfer, C.; J. Ellstrom, C.; Cho, H.; Török, B. *Green Chem.* **2017**, 19 (5), 1230–1234. (b) Gribble, G. W.; Lord, P. D.; Skotnicki, J.; Dietz, S. E.; Eaton, J. T.; Johnson, J. *J. Am. Chem. Soc.* **1974**, 96 (25), 7812–7814. (c) Gribble, G. W.; Hoffman, J. H. *Synthesis* **1977**, 1977 (12), 859–860. (d) Schwob, T.; Kempe, R. A. *Angew. Chem. Int. Ed.* **2016**, 55 (48), 15175–15179. (e) Zaccheria, F.; Ravasio, N.; Ercoli, M.; Allegrini, P. *Tetrahedron Lett*. **2005**, 46 (45), 7743–7745. (f) Xu, S.; He, J.; Cao, S. *J. Mol. Catal. Chem*. **1999**, 147 (1), 155–158. (g) Strohmeier, W.; Weigelt, L. *J. Organomet. Chem.* **1978**, 145 (2), 189–194.

[11] (a) Wu, S.; Wen, G.; Wang, J.; Rong, J.; Zong, B.; Schlögl, R.; Su, D. S. *Catal. Sci. Technol.* **2014**, 4 (12), 4183–4187. (b) Gao, Y.; Ma, D.; Wang, C.; Guan, J.; Bao, X. *Chem Commun* **2011**, 47 (8), 2432–2434. (c) Savaram, K.; Li, M.; Tajima, K.; Takai, K.; Hayashi, T.; Hall, G.; Garfunkel, E.; Osipov, V.; He, H. *Carbon* **2018**, 139, 861–871.

[12] Corma, A. Chemoselective Hydrogenation of Nitro Compounds with Supported Gold Catalysts. *Science* **2006**, 313 (5785), 332–334.

[13] (a) Ding, Z.-C.; Li, C.-Y.; Chen, J.-J.; Zeng, J.-H.; Tang, H.-T.; Ding, Y.-J.; Zhan, Z.-P. *Adv. Synth. Catal.* **2017**, 359 (13), 2280–2287. (b) Wang, Y.; Zhong, H.; Li, L.; Wang, R. *ChemCatChem* **2016**, 8 (13), 2234–2240. (c) R. Morse, J.; F. Callejas, J.; J. Darling, A.; E. Schaak, R. *Chem. Commun*. **2017**, 53 (35), 4807–4810.

[14] (a)Beier, M. J.; Andanson, J.-M.; Baiker, A. *ACS Catal.* **2012**, 2 (12), 2587–2595. (b) Boymans, E.; Boland, S.; Witte, P. T.; Müller, C.; Vogt, D. *ChemCatChem* **2013**, 5 (2), 431–434. (c) Udumula, V.; Tyler, J. H.; Davis, D. A.; Wang, H.; Linford, M. R.; Minson, P. S.;

Michaelis, D. J. *ACS Catal*. **2015**, 5 (6), 3457–3462. (d) Pei, Y.; Qi, Z.; Goh, T. W.; Wang, L.-L.; Maligal-Ganesh, R. V.; MacMurdo, H. L.; Zhang, S.; Xiao, C.; Li, X.; (Feng) Tao, F.; et al. *J. Catal*. **2017**, 356, 307–314.

[15] Zhu, K.; Shaver, M. P.; Thomas, S. P. *Chem. Sci*. **2016**, 7 (5), 3031–3035.

[16] (a) Westerhaus, F. A.; Jagadeesh, R. V.; Wienhofer, G.; Pohl, M. M.; Radnik, J.; Surkus, A. E.; Rabeah, J.; Junge, K.; Junge, H.; Nielsen, M. Nat. Chem. 2013, 5, 537– 543. (b) Wang, X.; Li, Y. J. Mol. Catal. A: Chem. 2016, 420, 56– 65.

[17] (a) Morimoto, N.; Morioku, K.; Suzuki, H.; Nakai, Y.; Nishina, Y. *Chem. Commun*. **2017**, 53 (53), 7226–7229. (b) Alcántara, R.; Ortiz, G. F.; Lavela, P.; Tirado, J. L.; Stoyanova, R.; Zhecheva, E. *Chem. Mater*. **2006**, 18 (9), 2293–2301. (c) Paulus, G. L.; Wang, Q. H.; Strano, M. S. *Acc. Chem. Res*. **2012**, 46 (1), 160–170. (d) Seber, G.; Rudnev, A. V.; Droghetti, A.; Rungger, I.; Veciana, J.; Mas-Torrent, M.; Rovira, C.; Crivillers, N. *Chem. Eur. J.* **2017**, 23 (6), 1415–1421.

[18] (a) Schabel, T.; Belger, C.; Plietker, B. *Org. Lett.* **2013**, 15, 11, 2858-2861.(b) Rahaim, R. J.; Maleczka, R. E. P. *Org. Lett.* **2005**, 7 (22), 5087–5090.(c) McLaughlin, M. A.; Barnes, D. M. *Tetrahedron Lett*. **2006**, 47 (51), 9095–9097.

[19] Guo, X.; Qi, W.; Liu, W.; Liang, C.; Zheng, A.; Yi, X.; Su, D. *RSC Adv*. **2016**, 6 (101), 99570–99576.

[20] Yabe, Y.; Sawama, Y.; Monguchi, Y.; Sajiki, H. *Catal. Sci. Technol.* **2014**, 4 (2), 260–271.

[21] Liu, J.; Yang, S.; Tang, W.; Yang, Z.; Xu, J. *Green Chem*. **2018**, 20 (9), 2118–2124.

[22] Guo, L.; Hao, Y.; Li, P.; Song, J.; Yang, R.; Fu, X.; Xie, S.; Zhao, J.; Zhang, Y. *Sci. Rep.* **2018**, 8, 4918.

[23] Primo, A.; Neatu, F.; Florea, M.; Parvulescu, V.; Garcia, H. *Nat. Commun*. **2014**, 5, 5291

[24] Senthilnathan, J.; Rao, K. S.; Yoshimura, M. *J. Mater. Chem. A* **2014**, *2* (10), 3332–3337.

[25] Chua, C. K.; Pumera, M. *J. Mater. Chem. A* **2013**, *1* (5), 1892–1898.

[26] Zhang, Y.; Sun, Z.; Wang, H.; Wang, Y.; Liang, M.; Xue, S. *RSC Adv.* **2015**, *5* (14), 10430–10439.

[27] Kumar, M. P.; Kesavan, T.; Kalita, G.; Ragupathy, P.; Narayanan, T. N.; Pattanayak, D. K. *RSC Adv.* **2014**, *4* (73), 38689–38697.

[28] Nolan, H.; Mendoza-Sanchez, B.; Kumar, N. A.; McEvoy, N.; O'Brien, S.; Nicolosi, V.; Duesberg, G. S. *Phys. Chem. Chem. Phys.* **2014**, *16* (6), 2280–2284.

[29] Gao, Y.; Tang, P.; Zhou, H.; Zhang, W.; Yang, H.; Yan, N.; Hu, G.; Mei, D.; Wang, J.; Ma, D. *Angew. Chem. Int. Ed.* **2016**, *55* (9), 3124–3128.

[30] Vijaykumar, G.; Mandal, S. K. *Dalton Trans.* **2016**, *45* (17), 7421–7426.

[31] Xu, H.; Wolf, C. *Chem. Commun.* **2009**, No. 21, 3035.

[32] Vernekar, A. A.; Patil, S.; Bhat, C.; Tilve, S. G. *RSC Adv.* **2013**, *3* (32), 13243.

[33] Rahaim, R. J.; Maleczka, R. E. *Org. Lett.* **2005**, *7* (22), 5087–5090.

[34] Kumaran, E.; Sridevi, V. S.; Leong, W. K. *Organometallics* **2010**, *29* (23), 6417–6421.

[35] Yasuhara, A.; Kasano, A.; Sakamoto, T. *J. Org. Chem.* **1999**, *64* (7), 2301–2303.

[36] Takasaki, M.; Motoyama, Y.; Higashi, K.; Yoon, S.-H.; Mochida, I.; Nagashima, H. *Org. Lett.* **2008**, *10* (8), 1601–1604.

CHAPTER 4

Graphene catalyzed radical alkylation between benzylic alcohols and ketones to generate α-alkylated ketones

The reaction mechanism of the alkylation of ketone with alcohol is still a matter of debate, is it a Meerwein-Ponndorf-Verley like process, or are hydrogen borrowing process by transition metals? Here, the alkylation reaction of ketones with benzylic alcohols via a radical pathway has been developed, where base treated graphene works as an initiator of radical reaction. Mechanistic study support that the radical anion of the benzylic alcohol is proposed to be the key intermediate, which further undergoes coupling with ketones via aldol condensation to form a new C−C bond with water the only byproduct.

4 Introduction

Inspired by the demand for green and sustainable chemistry, synthetic chemists endeavor more effective ways to construct carbon-carbon (C−C) bonds, which is fundamental in organic synthesis.[1,2] Amongst C−C bond forming reactions, the α-alkylation of ketones with abundantly available alcohols as the substrate is still requiring precious metals (Ru,[3–14] Ir,[15–22] Rh,[23,24] Os,[25] Au,[26] Pd,[27–29] and Re[30]) or abundant transition metals (Ni, Mn, and Fe) [27,31–33] as catalysts (Scheme **1a**).[34–36] The metal catalysts are dehydrogenating the alcohol to the corresponding carbonyl compounds, which subsequently undergoes condensation with CH acidic compounds followed by hydrogen transfer to α-alkylated products, also called hydrogen borrowing methodology or hydrogen auto-transfer (Scheme 4.1a).[37–42] However, despite significant advancement in the metal-catalyzed α-alkylation of ketones with alcohols, these procedures still have limitations (i.e., functional group tolerance, the cost of the metal catalysts, complex handling technique in an inert atmosphere, metal contamination in the product, and the utilization of stoichiometric amount of base.[43,44] Therefore, methods that utilize more eco-friendly and inexpensive systems to construct C−C bonds are demanded.

Another approach, which is mechanistically different alkylation process, is Oppenauer oxidation,[45,46] which, after an aldol reaction followed by Meerwein-Ponndorf-Verley (MPV) reduction,[47,48] may generate the same products as the metal-catalyzed hydrogen borrowing or auto-transfer methodology. In this way, a transition or precious metal catalyst is not needed since the transformation can be initiated by a main group metal hydroxide or alkoxide.[32] The mechanism involves direct hydride transfer through a six-membered transition state, which is different from the transition metal-catalyzed system, example dihydrogen is not involved during this process (Scheme 4.1b).[46,49,50] For instance, the α-alkylation of ketones with primary alcohols and β-alkylation of secondary alcohols, which is reported to be catalyzed by alkali metal hydroxides and tert-butoxides.[32,33,51,52] These transformations with alcohol are advantageous because the stoichiometric amount of waste is not produced since water is often produced as the sole byproduct.

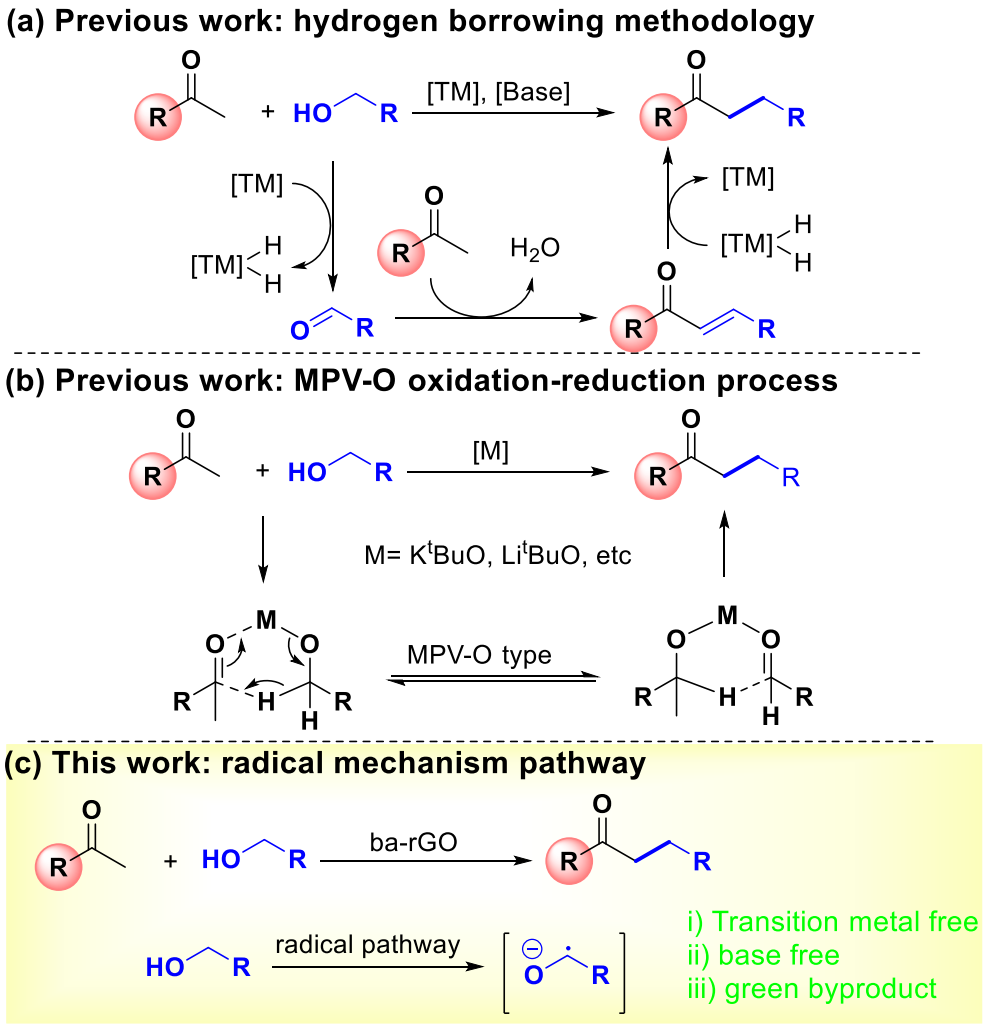

Scheme 4.1: (a) *Alkylation reaction via hydrogen borrowing strategy,* ***(b)*** *MPV-O mechanism of the alkylation reaction,* ***(c)*** *alkylation reaction of ketone with alcohol via radical pathway (This work).*

There is also the possibility of radical mechanisms pathway in the C−C bond forming reactions with alcohol. Example, The activation of benzylic alcohols with the stoichiometric amount of phosphorus or titanium reagents in the presence of metal catalysts has been reported to form benzylic radicals, which may further proceeds to cross-coupling reactions with aryl halides, and an addition reaction with strained alkenes as well.[53–55] Recently, the Milstein group reported the coupling of benzylic alcohol with aryl alkynes using potassium tert-butoxide to form the α-alkylated ketones. In this process, a ketyl radical is believed to be generated from the alcohol-based substrate, and the radical further reacts with the alkyne, followed by several hydrogen transfer reactions to produce the desired product.[56] Albeit potassium tert-butoxide working as a

mediator in this coupling, the alkoxide has also been reported to promote C−C coupling reactions via radical pathways such as the formation of biaryls from aryl halides and arens.[57–59]

Recently, tremendous progress has been made in the development and application of new graphene-based materials as a sustainable, benign, and readily available catalyst and the various possibilities that these materials offer to introduce active sites. In this context, we have developed a graphene-based catalyst for the C−H functionalization and selective hydrogenation reactions, while radical was found to be effective in these transformations.[60,61] In the present study, we questioned whether doped graphene-based materials could be employed as a benign catalyst to promote the alkylation reaction of ketone with alcohol.

4.1 Results and Discussion

4.1.1 Optimization course

Initially, no product was detected when a blank reaction of acetophenone with benzyl alcohol in toluene was performed at 130 °C for 24 h (Table 4.1, entry 1). Notably, when the same experiment was performed in the presence of potassium tert-butoxide as a catalyst smoothly afforded 1,3-diphenylpropan-1-one (**3a**) in 84% yield (Table 4.1, Entry 2). Thus, it was decided to optimize this alkylation reaction by investigating the influence of the base. When the transformation was performed in other bases, such as (K_2CO_3, Cs_2CO_3, NaOH, or KOH furnished the desired product, albeit in lower yields of 30, 10, 63, and 49%, respectively (Table 4.1, Entries 3-6). By changing the solvent, the nonpolar solvent, toluene, resulted in a higher product yield as compared to polar solvents such as DMF, dioxane, or acetonitrile (Table 4.1, Entries 7-9). The same reaction was carried out in the presence of (15 mg) of graphene oxide as a catalyst without base in toluene, yielded the product less than 10 %. Furthermore, we attempted to make doped graphene oxide (treated with base see Experiemtnal section) and extended its application as a catalyst to the α-alkylation of ketones with alcohol to form alkylated products (Scheme 4.1c). Interestingly, the best results were obtained with base treated graphene oxide, and more surprisingly, mechanistic studies indicated the alkylation to take place by a radical pathway. To confirm the actual sites and surface chemistry of the base treated graphene oxide catalyst, we then analyzed with the characterization technique.

Table 4.1: *Optimization of the reaction of benzyl alcohol and acetophenone.*[a]

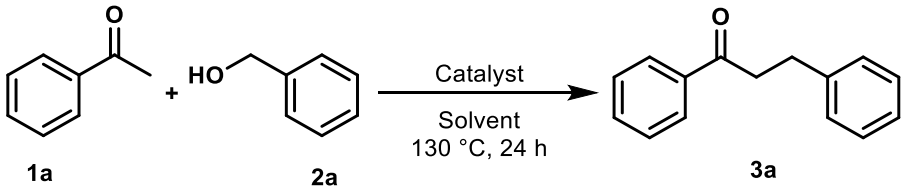

Entry	Catalyst	Solvent	Yield [%][b]
1	None	Toluene	0
2	KO^{t}Bu	Toluene	84
3	K_2CO_3	Toluene	30
4	Cs_2CO_3	Toluene	10
5	NaOH	Toluene	63
6	KOH	Toluene	49
7	KO^{t}Bu	DMF	45
8	KO^{t}Bu	1,4-dioxane	56
9	KO^{t}Bu	Acetonitrile	39
10[c]	KO^{t}Bu	Toluene	43
11[d]	rGO	Toluene	>10
12[f]	ba-rGO	Toluene	78

[a]Reaction condition: **1a** (0.5 mmol), **2a** (0.6 mmol), Base as catalyst (0.05 mmol), and toluene (2 mL) were stirred for 24 h at 130 °C. [b] The yields were calculated by ^{1}H NMR using 1,1,2,2-tetrachloroethane as an internal standard. [c] The alkylation reaction was performed at 100 °C. [d] The graphene-based materials were used 15 mg as catalyst.[f] The reaction was performed in the absence of light.

4.1.2 Surface analysis of the catalyst

The presence of the dopant elements was quantified by XPS (X-ray photoelectron spectroscopy) measurement, and also confirm if trace quantity of transition metals were involved. As shown in Figure 4.1(b), in addition to the C1s level observed at 284.2 eV, and two strong peaks appear at higher binding energy (>290) (Figure 4.1 (b), which could be assigned to K $2p_{3/2}$ and K $2p_{1/2}$, suggesting the K is successfully introduced in the graphene oxide chemistry. Furthermore, the functional groups of the graphene-based material were confirmed by FT-IR analysis (Figure 4.2). The existence of peak OH at 3441 cm^{-1}, peak at 1568 cm^{-1} correspond to C=C stretching, which suggests that the GO has been effectively reduced, characteristic peak at 1213 cm^{-1} is due to C-O-C stretching vibrations.

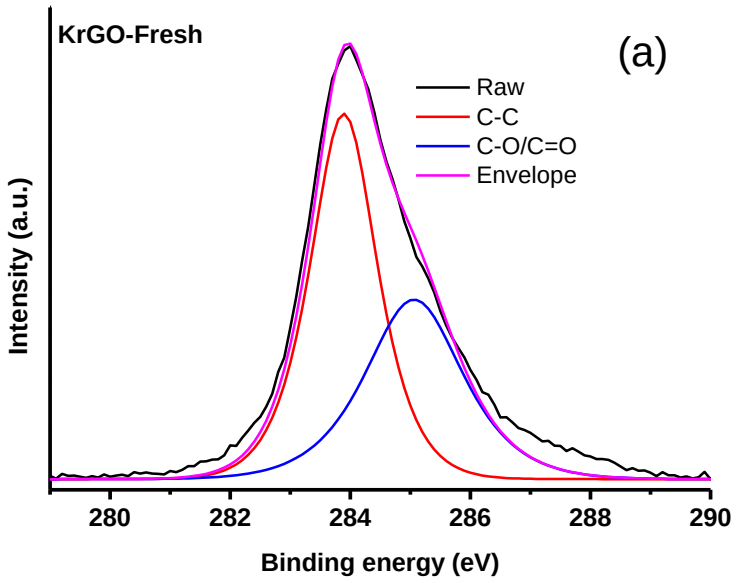

Figure 4.1a: *High-resolution XPS spectra with Gaussian fitting for C1s peaks.*

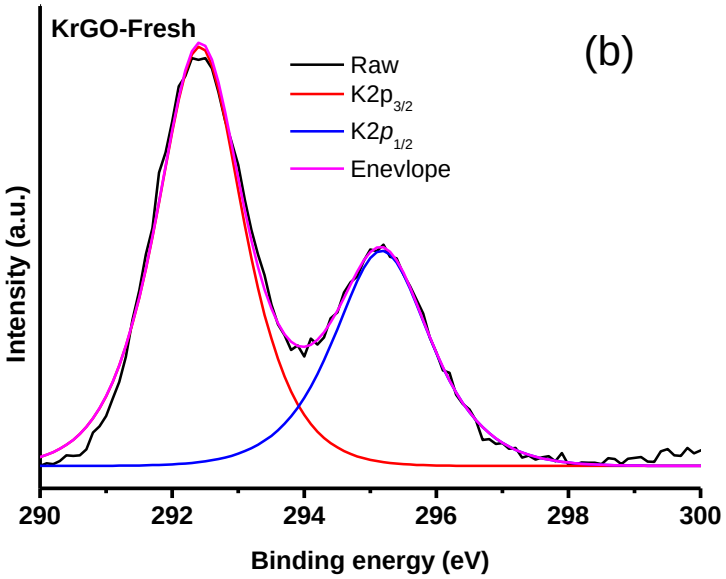

Figure 4.1b: *High-resolution XPS spectra with Gaussian fitting for K2p peaks.*

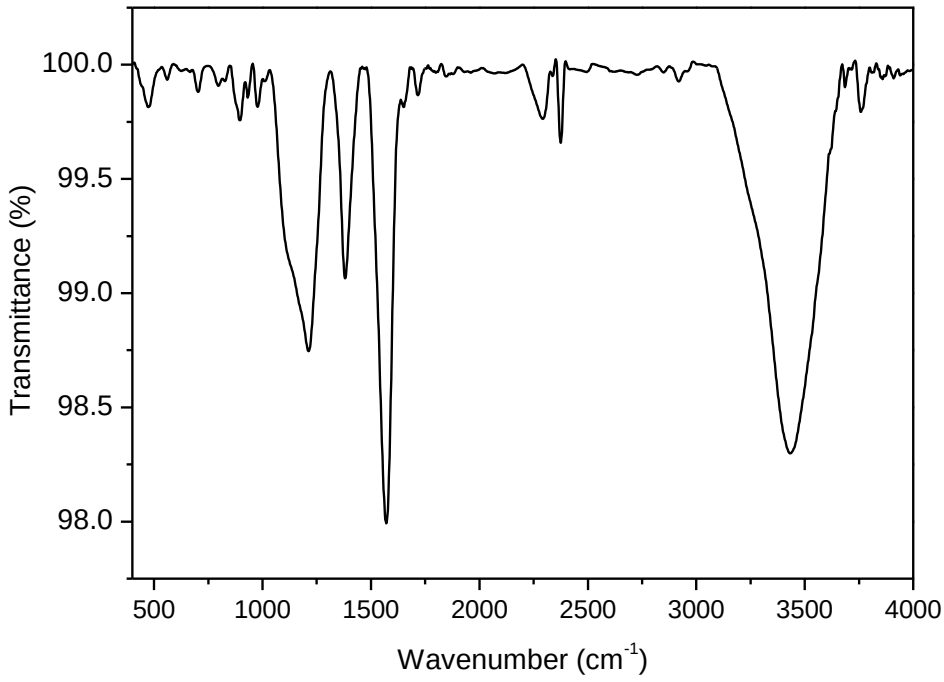

Figure 4.2: *FT-IR spectra of the ba-rGO.*

The monolayer or few-layer and/or wrinkle morphology of the graphene-based catalyst sample was suspended in the solomix solvent, and was assessed using SEM/TEM (Scanning electron microscopy/transmission electron microscopy). Figure 4.3 ((a) SEM and (b) TEM) shows the selected microscopy image of the graphene-based catalyst, which is composed of wrinkled and layered sheet morphology.

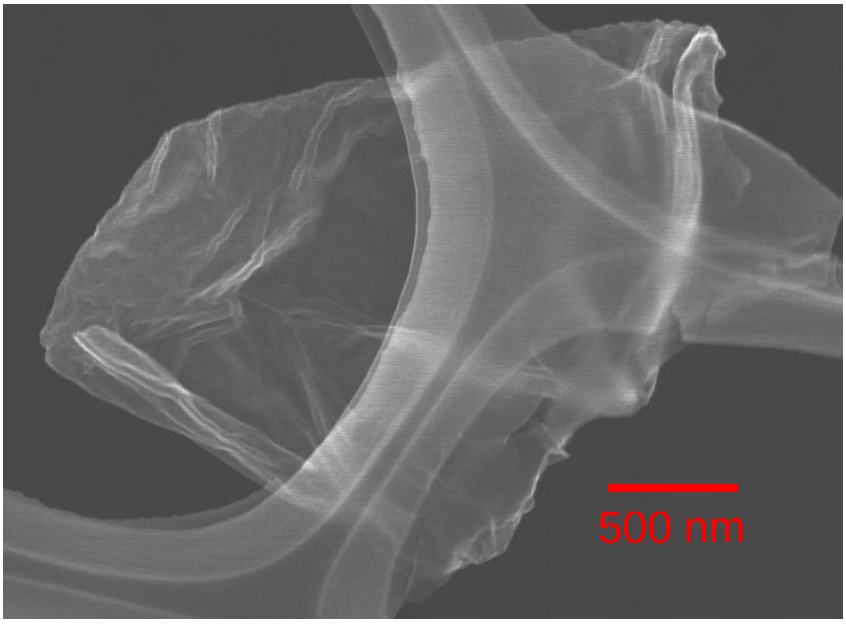

Figure 4.3(a): *The SEM images of KrGO.*

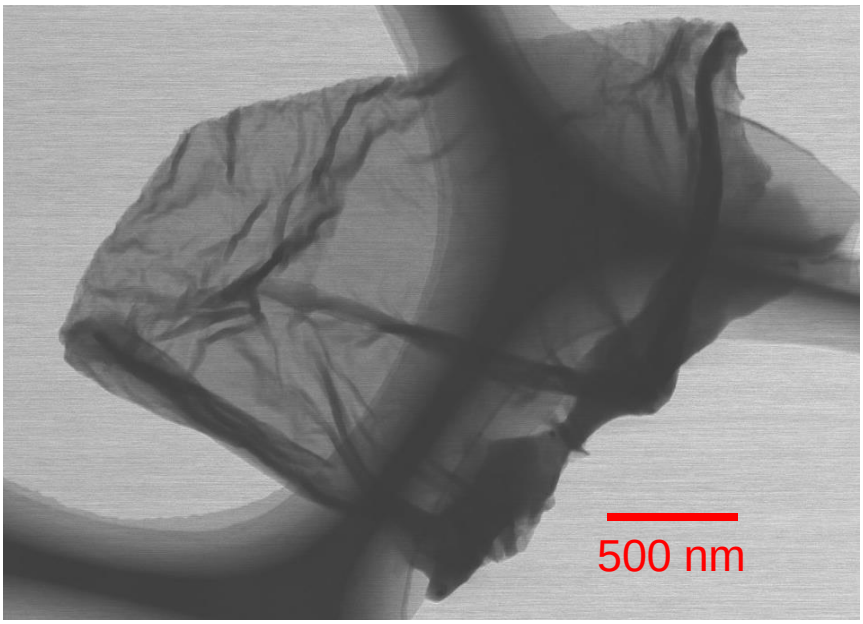

Figure 4.3(b): *The TEM images of KrGO.*

4.1.3 Reaction scope

The optimized procedure in hand was then applied to a verity of alcohol and ketones to investigate the substrate scope of the transformations, the products were isolated by flash chromatography. The catalytic reaction benzyl alcohol and acetophenone, which furnished compound **3a** in 78% yield (Table 4.2). The electron-donating groups such as methyl or methoxy of the acetophenone and benzyl alcohol were well tolerated, and all led to an excellent yield of 81-87% in table 4.2. Previously, the halogen-substituted substrates were reported poor substrates since the dehalogenation was reported.[62] While in our study, we did not observe any dehalogenation compound **3d** in 67% yield (Table 4.2). The Electron-withdrawing group with **2a** afforded the substituted 1,3-diphenylpropan-1-one derivatives, in moderate yields **3g** in 57% yield (Table 4.2). Furthermore, aliphatic benzyl alcohol yielded a trace amount of alkylated product. Similarly, we performed the reaction of aliphatic ketone such as pentan-3-one with benzyl alcohol, but we could not detect any alkylated product.

Table 4.2. *The substrate scope of synthesis of alkylated ketones.*[a]

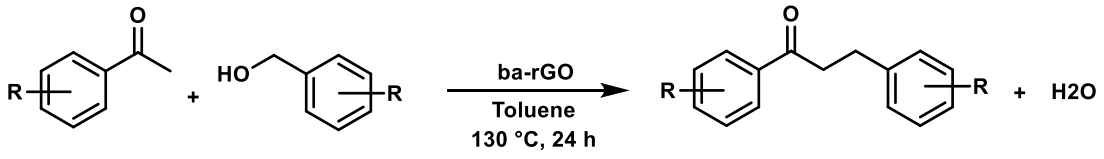

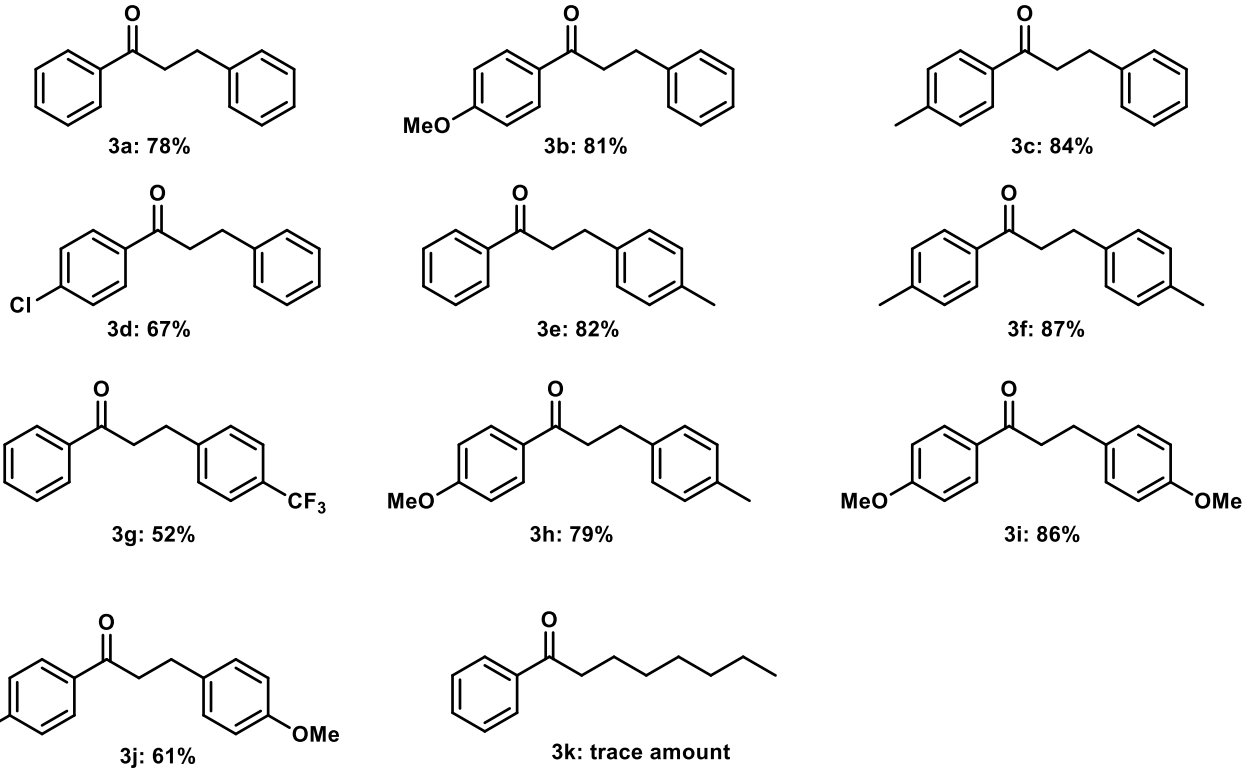

[a]Reaction condition: 1 (0.5 mmol), 2 (0.6 mmol), ba-rGO (15 mg), and toluene (2 mL) were stirred at 130 °C for 24 h. [b] The yields were calculated by 1H NMR spectroscopy using 1,1,2,2-tetrachloroethane as an internal standard.

To probe the influence of light, an experiment was carried out in toluene, in the absence of light (Table 4.1, entry 12), no change was observed in the product yield. Repeating the reaction under an atmosphere of air or oxygen resulted in the formation of chalcone Scheme 4.2, due to a base treated GO mediated aerobic alcohol oxidation reaction.[63,64]

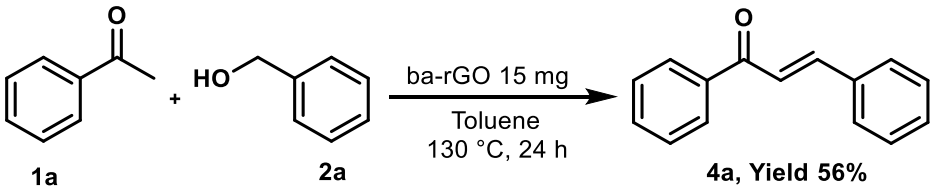

Scheme 4.2: *Alkylation in the presence of air.*

4.1.4 Mechanistic study

We then endeavored to understand the difference in mechanism of the α-alkylation reaction catalyzed by metal catalyst.[43,65] Based on this study, it's high unlikely that the coupling takes place by a MPV-O pathway, and speculations emanate whether a radical mechanism is involved in the α-alkylation reaction. Therefore, 1 Equiv. of radical scavenger (2,2,6,6-tetramethyl piperidine-1-oxyl (TEMPO)) was added to the reaction of benzyl alcohol and acetophenone along with catalyst, and the time was extended to 36 h, and led to a lower 41% yield of the alkylated product. During the radical scavenger experiment, TEMPO was mainly reduced to 2,26,6-tetramethylpiperidine, and some of 1-benzyl-2,2,6,6-tetramethylpiperidine could be detected as well by GC-MS. This result suggests that radical species mediate the reaction.

To gain further insight into the radical mechanism, several ESR experiments were then recorded under different conditions. EPR of the empty tube was recorded to determine the background, as presented in (Experimetnal section). EPR spectrum of the base (potassium tert-butoxide) was measured and found that the base is not the source of radical, can be seen (Experiemtnal section), while the ba-rGO with a singlet carbon-centered radical with *g* value of 2.004 was observed (Figure 4.4). The ESR analyses of the filtrate of the reaction mixture, but direct observation of radicals was not successful. To analyze unstable intermediate by ESR, a spin trap agent, N-tert-butyl-α-phenylnitrone (PBN), was added in the reaction mixture; as a result, ESR signals were observed (Figure 4.5). The signals are similar to ketyl radical, possibly formed from **2a** (Scheme 4.3).[66–70] Accordingly, this result suggests that benzyl alcohol is deprotonated by ba-rGO to form alkoxide (**I**).[71] It has been reported that potassium to serve as a single electron donor to form alkoxy radicals, which would rapidly remove the atom from (**I**).[57,58,72,73] Further, additional deprotonation of (**I**) to form anionic intermediates, which will convert into a radical anion (**II**) by single electron transfer to the ketone, while further proceeded via the aldol reaction

to give the chalcone intermediate (**III**), which got reduced into the final step to give the product 3 (Scheme 4.3).

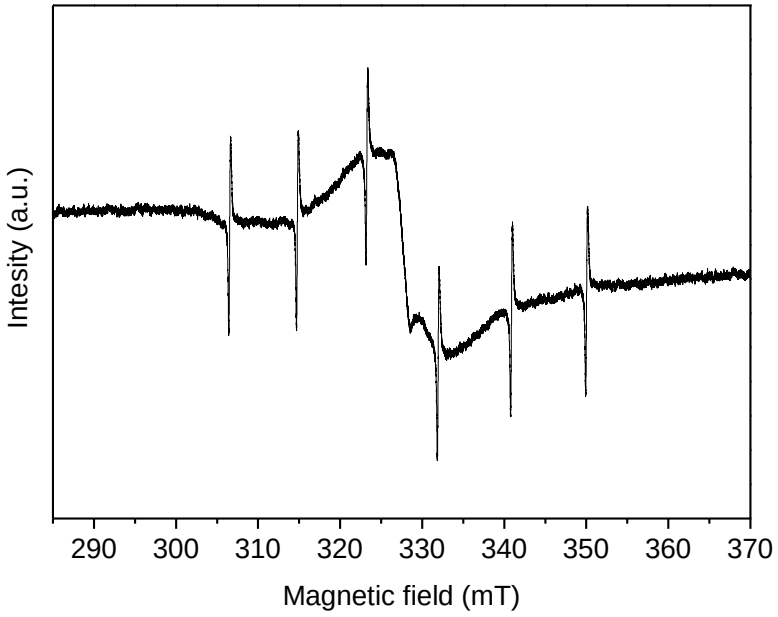

Figure 4.4: *ESR spectra for the analysis of the ba-rGO.*

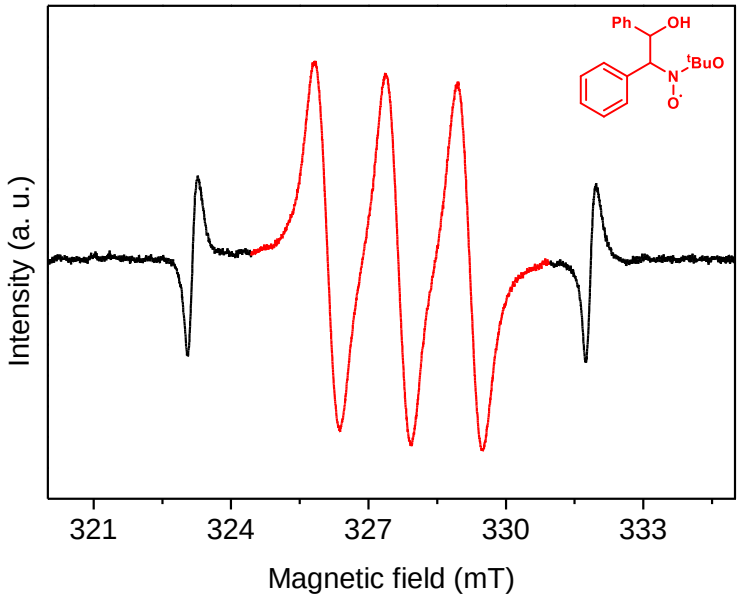

Figure 4.5: *ESR spectrum upon heating a solution of* ***1a, 2a****, ba-rGO, and spin trap agent (PBN) in toluene, and measure the filtrate.*

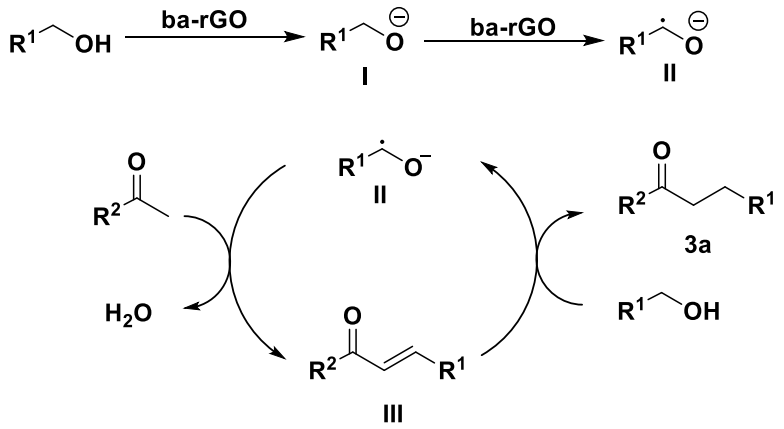

Scheme 4.3. *A plausible mechanism for the reaction of benzyl alcohol and acetophenone in the presence of ba-rGO.*

Furthermore, to confirm and support the proposed mechanism, we investigated the hydrogen transfer experiment between α,β-unsaturated ketone (**4a**) with alcohol (**2a**) as the hydrogen donor, in the presence of the ba-rGO as a result, could proceed the reaction to the corresponding product 3a in 75 % yield (Scheme 4.4).

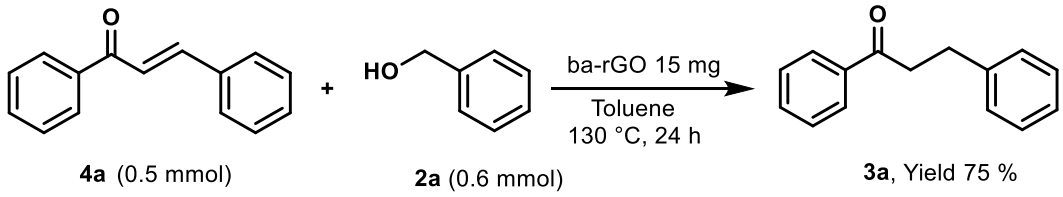

Scheme 4.4: *Hydrogenation of* ***4a*** *using* ***2a*** *as a hydrogen donor.*

In summary, we have demonstrated a new radical alkylation reaction of an alcohol with ketones to form α-alkylated ketones in the presence of potassium doped graphene as catalyst. A series of alcohol and ketones have been subjected to the transformation to generate alkylated products in good yields. Mechanistic studies revealed that the alkylation takes place by a radical pathway

where the radical anion of the benzylic alcohol is proposed as the key intermediate. Different from existing alkylation methods, this strategy permits the use of the simple potassium tert-butoxide treated graphene as a catalyst. The reaction system follows a different mechanism than metal-based reactions and or MPV-O pathways. This is especially important when ba-rGO is employed as catalyst since the basic character of the ba-rGO work as an initiator radical reaction. Overall, this system is highly efficient, green, and sustainable, and could be an alternative or complementary method to metal-based systems in the development of new radical-mediated C−C bond forming reactions with alcohols.

4.2 Experimental

4.2.1 General

Substrates alcohol, ketones, solvents (toluene, etc.), and base, all the chemicals were purchased and used without any further treatment, unless otherwise noted. The reactions were all carried out in a sealed glass schlenk tube and monitored by GC-MS or Thin-layer chromatography (TLC) and quantified by 1H NMR analysis using 1,1,2,2-tetrachloroethane as an internal standard and CDCl3 as a solvent.

The ESR analysis was performed by an electron spin resonance spectrometer (JES-X310) with 9.542 GHz microwave frequency, 100 kHz modulation frequency, 1mW power, and 2 minutes of weep time. The products were quantified by gas chromatography GC (Shimadzu GC-2014 equipped with flame ionized detector FID detector). Deuterated solvents for NMR spectroscopy were purchased from Sigma Aldrich and used as received. NMR spectra were recorded on a Varian 400-MR. Proton (1H) NMR information is given in the following format: multiplicity (s, singlet; d, doublet; t, triplet; q, quartet; m, multiplet), coupling constant(s) (J) in Hertz (Hz), the number of protons, type.

4.2.2 Catalyst preparation

Graphite powder (100 g) was dispersed into concentrated H_2SO_4 (2.5 L). After cooling the mixture in an ice bath, $KMnO_4$ (300 g) was added, and the reaction mixture was kept below 55 °C. The mixture was stirred at 35 °C for 2h to complete the oxidation process. Next, deionized water (5 L) was added slowly, and the temperature was kept below 50 °C with continuous stirring, then followed by the addition of H_2O_2 (30% aq., 250 mL) into the mixture. Finally, the brown crude graphite oxide was purified by performing ten times centrifugation, and graphene oxide (GO) is prepared. The concentration of GO was measured by drying the GO dispersion under vacuum at 50 °C. Furthermore, 1 gram of base was dissolved in 100 mL of 0.1 wt of GO. The mixture was refluxed in round bottom flask fat 90 °C for 12 h. After cooling to room temperature, the black precipitate was filtered and washed with water several times and then dried in a freeze-dried.

4.2.3 General procedure

4.2.3.1 A typical procedure for the optimization of the reaction condition

Acetophenone (0.5 mmol), benzyl alcohol (0.6 mmol), and catalyst (KO^{t}Bu, other bases as mentioned, graphene materials in table 1) (10 mol%) the mixture were dissolved in 2 mL of toluene (or other solvent shown in table 1) and placed in a glass schlenk tube. The tube was heated at 130 °C (or 100 °C) under the stirring condition for the mentioned time. The mixture was cooled, and the product was analyzed by GC-MS using dodecane as an internal standard.

4.2.3.2 Procedure for Table 4.2

0.5 mmol of ketone, 0.6 mmol of alcohol, and 15 mg of ba-rGO were added in 2 mL of toluene and placed in a glass schlenk tube. The tube was heated at 130 °C under the stirring condition for 24 h. The reaction was monitored by TLC and or GC-MS. Upon completion, the reaction mixture was cooled and diluted with ethyl acetate, quenched with 3 M aq. HCl (1.5 mL) and extracted with Ethylacetate (3x4 mL) and the combined organic layer were dried om $MgSO_4$, filter, and concentrated in vacuo. The product yield was calculated by 1HNMR using 1,1,2,2-tetrachloroethane as an internal standard. Then the residue was purified by flash chromatography on silica gel using ethyl acetate/hexane as eluent to afford the desired product.

4.2.4 ESR study

4.2.4.1 ESR spectrum measurement of the reaction mixture

- ESR spin trapping is a valuable tool in the study of transient free radicals. Spin traps react with free radicals in solution to yield stable products, spin adducts, which can be observed by ESR spectroscopy. The nitrone spin trap is widely utilized to identify oxygen or carbon-centered radicals.

- In general, the most direct and common method for characterizing and analyzing free radicals in science, especially chemistry, is detection by ESR spectroscopy. Similarly, in our study, Benzyl alcohol (0.3 mmol), acetophenone (0.25 mmol), and ba-rGO (7.5 mg) were dissolved in 1 mL toluene in a glass schlenk tube and heated at 130 °C for 10 min,

giving a dark red color mixture. The red dark-colored solution was immediately transferred to an ESR tube, sealed, and taken for measurement. A blank spectrum was also run by using the empty ESR tube.

4.2.4.2 Controlled ESR measurement

- ESR spectrum of the empty tube was recorded to determine the background, as presented in **Figure 4.6 (a)**.
- ESR spectrum of the ^{t}BuOK was recorded to determine that the base is not the source of radical, can be seen in **Figure 4.6 (b)**.
- Benzyl alcohol (0.6 mmol) and KO^{t}Bu (10 mol%) or ba-rGO (15 mg) were dissolved in 2 mL toluene in a glass schlenk tube and heated at 130 °C for 10 minutes; the resulting mixture was immediately transferred to an ESR tube and taken for measurement. As a result, no peak was detected, as shown in **Figure 4.6 (c)**.
- Acetophenone (0.5 mmol) and KO^{t}Bu (10 mol%) or ba-rGO (15 mg) were dissolved in 2 mL toluene in a glass schlenk tube and heated at 130 °C for 10 minutes; the resulting mixture was immediately transferred to an ESR tube and taken for measurement, the resulting spectrum is presented in **Figure 4.6 (d)**.
- ESR spectrum of the spin trap agents N-tert-butyl-α-phenylnitrone (PBN) and (5,5-Dimethyl-1-Pyrroline N-oxide (DMPO) was recorded, the spectra can be seen in **Figure 4.6 (e and f)**. The peak appeared due to the air.
- Another approach to study the possible involvement for alkoxide adduct generation in the reaction system, we performed the reaction in the presence of a spin trap agent (DMPO or PBN) and taken the sample for ESR measurement **(Figure 4.7)**.

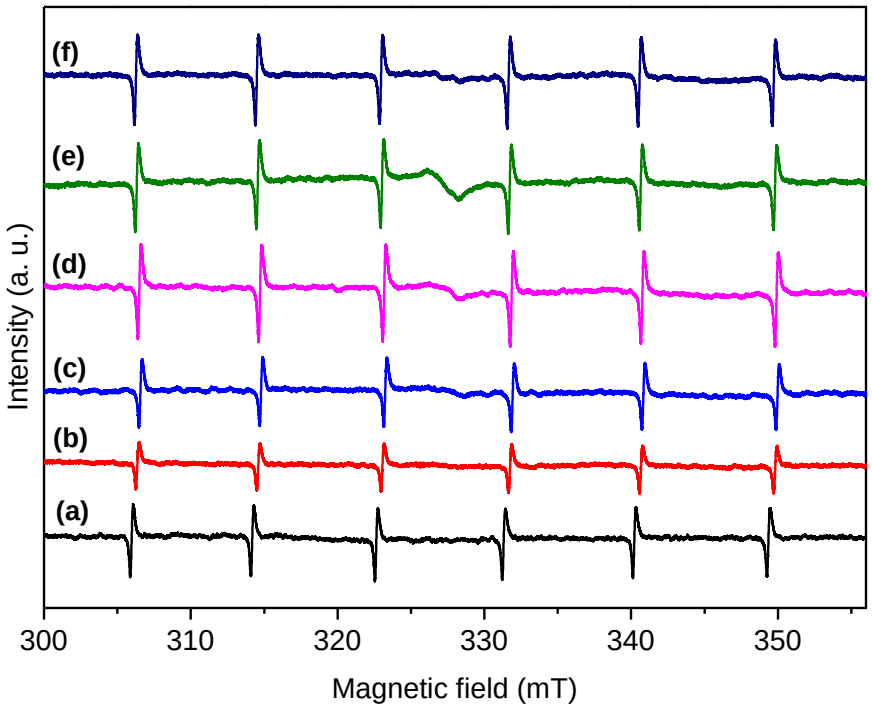

Figure 4.6: *ESR spectra for the controlled experiments.*

4.2.4.3 In-situ analysis of ESR

- The reaction mixture, benzyl alcohol (0.6 mmol), acetophenone (0.5 mmol), and catalyst (15 mg) were dissolved in 2 mL toluene, and the resulting solution was transferred to an ESR tube, sealed, and taken for measurement, the resulting data presented in **Figure 4.7**. When the reaction was repeated in the presence of spin trap agent such as DMPO (0.5mmol), and the resulting solution was transferred to an ESR tube, sealed, and taken for measurement, the data presented in **Figure 4.5.**

The successful treated GO is also reflected in the thermal gravimetric curves (**Figure 4.8**). In the analysis, the region up to 100 °C, the sample weight loss was caused by physisorbed water. Up to 200 °C, the weight loss was a result of the decomposition of labile oxygen groups (e.g., anhydride). The other region occurred between 400-550 °C and was associated with the removal of more stable oxygen groups such as carbonyl and phenol, while at high-temperature, pyrolysis of the carbon skeleton occurred

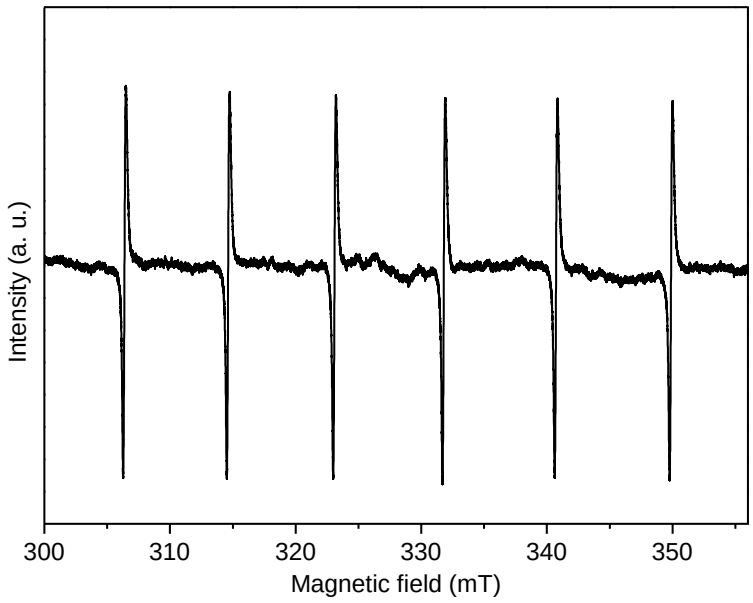

Figure 4.7. *ESR spectra for the analysis of the in-situ experiment*

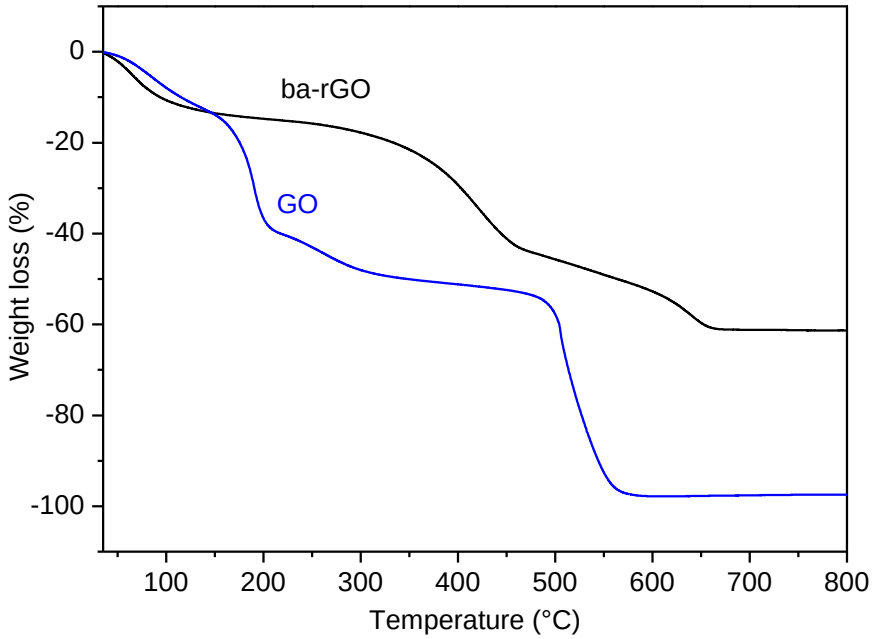

Figure 4.8. *Thermal gravimetric analysis of the ba-rGO.*

4.2.5 ^{1}H NMR data of the product

- **1,3-diphenylpropan-1-one (3a)** Following the general procedure, was obtained as a white solid, 84% yield (83.2 mg) ; ^{1}H NMR (400 MHz, $CDCl_3$) δ: 7.88 (d, J= 7.2 Hz, 2H), 7.48 (t, J= 7.2 Hz, 1H), 7.37 (t, J= 7.6 Hz, 2H), 7.22-7.17 (m, 4H), 7.05 (t, J= 7.2 Hz, 1H), 3.23 (t, J= 7.2 Hz, 2H), 2.99 (t, J= 7.2 Hz, 2H). The ^{1}H NMR spectra showed agreement with the literature data.[74]

- **1-(4-methoxyphenyl)-3-phenylpropan-1-one (3b)** Following the general procedure, was obtained as a white solid, 89% yield (97.2 mg); ^{1}H NMR (400 MHz, $CDCl_3$) δ: 7.87 (d, J=8.8 Hz, 2H), 7.24-7.11 (m, 5H), 6.84 (d, J= 8.8 Hz, 2H), 3.79 (s, 3H), 3.18 (t, J= 7.6 Hz, 2H), 2.98 (t, J= 7.6 Hz, 2H). The ^{1}H NMR spectra showed agreement with the literature data.[19]

- **3-phenyl-1-(p-tolyl)propan-1-one (3c)** Following the general procedure, was obtained as a light yellow liquid, 85% yield (93.8 mg); ^{1}H NMR (400 MHz, $CDCl_3$) δ: 8.05 (d, J= 7.2, 2H), 7.65 (t, J= 7.2 Hz, 1H), 7.54 (t, J= 7.6 Hz, 2H), 7.26-7.19 (m, 4H), 3.83 (t, J= 7.6 Hz, 2H), 3.12 (t, J= 7.6 Hz, 2H), 2.42 (s, 3H). The ^{1}H NMR spectra showed agreement with the literature data.[75]

- **1-(4-Chlorophenyl)-3-phenylpropan-1-one (3d)** Following the gernal procedure, white solid, 75% yield (75.1 mg); ^{1}H NMR (400 MHz, $CDCl_3$) δ: 7.83 (dd, J=6.4, 4.4 Hz, 2H), 7.36 (d, J=8.8 Hz, 2H), 7.23 (t, J= 7.2 Hz, 4H), 7.15 (d, J= 8.8 Hz, 1H), 3.21 (t, J= 7.6 Hz, 2H), 3.0 (t, J= 7.6 Hz, 2H). The ^{1}H NMR spectra showed agreement with the literature data.[76]

- **1-phenyl-3-(p-tolyl)propan-1-one (3e)** Following the general procedure, white solid, 86% yield (91.8 mg); ^{1}H NMR (400 MHz, $CDCl_3$) δ: 7.99 (d, J=7.2 Hz, 2H), 7.63-7.53 (m, 1H), 7.52-7.42 (m, 2H), 7.17 (q, J=8.1 Hz, 4H), 3.31 (t, J=7.2 Hz, 2H), 3.06 (t, J=7.2, 2H), 2.53 (S, 3H). The ^{1}H NMR spectra are in agreement with the literature date.[77]

- **1,3-di-p-tolylpropan-1-one (3f)** Following the general procedure, white solid, 91% yield (103.4 mg); ^{1}H NMR (400 MHz, $CDCl_3$) δ: 7.78 (d, J= 8.4 Hz, 2H), 7.17 (d, J= 8.4 Hz,

2H), 7.05 (q, J= 8.0 Hz, 4H), 3.17 (t, J= 6.8 Hz, 2H), 2.94 (t, J= 6.8 Hz, 2H), 2.33 (s, 3H), 2.24 (s, 3H). The ^{1}H NMR spectra showed agreement with the literature data.[78]

- **1-Phenyl-3-(4-(trifluoromethyl)phenyl)propan-1-one (3g)** Following the general procedure, white solid, 57% yield (72.2 mg); ^{1}H NMR (400 MHz, $CDCl_3$) δ: 7.66 (dd, J=8.8 Hz, 2H) 7.25-7.18(m, 2H), 6.94(d, J=8.8, 2H), 6.62 (d, J=8.4 Hz, 2H), 3.56 (s, 3H), 3.05-2.99(m, 2H), 2.82-2.76 (m, 2H). The ^{1}H NMR spectra are in agreement with the literature date.[79]

- **1-(4-methoxyphenyl)-3-(p-tolyl)propan-1-one (3h)** Following the general procedure, colorless oil, 93% yield (102.8 mg); ^{1}H NMR (400 MHz, $CDCl_3$) δ: 7.68 (d, J= 8.8 Hz, 2H), 7.07 (d, J= 726 Hz, 2H), 6.99 (d, J=8.8 Hz, 2H), 6.66 (d, J= 8.8 Hz, 2H), 3.61 (s, 3H), 3.06 (t, J=8.0 Hz, 2H), 2.83 (t, J= 8.0 Hz, 2H), 2.23 (s, 3H). The ^{1}H NMR spectra showed agreement with the literature data.[80]

- **1,3-bis(4-methoxyphenyl)propan-1-one (3i)** Following the gernal procedure, white solid, 93% yield (114.8 mg); ^{1}H NMR (400 MHz, $CDCl_3$) δ: 7.94 (d, J=9.2 Hz, 2H) 7.17(d, J=8.8 Hz, 2H), 6.92(d, J=8.8, 2H), 6.84 (d, J=8.4 Hz, 2H), 3.85 (s, 3H), 3.78 (s, 3H), 3.23(t, J=63.8 Hz, 2H), 2.99 (t, J= 7.2 Hz, 2H). The ^{1}H NMR spectra are in agreement with the literature date.[79]

- **1-(4-chlorophenyl)-3-(4-methoxyphenyl)propan-1-one (3j)** Following the general procedure, light yellow oil, 61% yield (83.5 mg); ^{1}H NMR (400 MHz, $CDCl_3$) δ: 7.66 (dd, J=8.8 Hz, 2H) 7.25-7.18(m, 2H), 6.94(d, J=8.8, 2H), 6.62 (d, J=8.4 Hz, 2H), 3.56 (s, 3H), 3.05-2.99(m, 2H), 2.82-2.76 (m, 2H). The ^{1}H NMR spectra are in agreement with the literature date.[81]

4.3 References

[1] A. Behr, in *Ullmanns Encycl. Ind. Chem.*, American Cancer Society, **2000**.
[2] R. Jana, T. P. Pathak, M. S. Sigman, *Chem. Rev.* **2011**, *111*, 1417–1492.
[3] X.-N. Cao, X.-M. Wan, F.-L. Yang, K. Li, X.-Q. Hao, T. Shao, X. Zhu, M.-P. Song, *J. Org. Chem.* **2018**, *83*, 3657–3668.
[4] R. Martínez, D. J. Ramón, M. Yus, *Tetrahedron* **2006**, *62*, 8988–9001.
[5] T. Kuwahara, T. Fukuyama, I. Ryu, *Org. Lett.* **2012**, *14*, 4703–4705.
[6] S.-Y. Liu, L.-Y. Xu, C.-Y. Liu, Z.-G. Ren, D. J. Young, J.-P. Lang, *Tetrahedron* **2017**, *73*, 2374–2381.
[7] J. Alós, T. Bolaño, M. A. Esteruelas, M. Oliván, E. Oñate, M. Valencia, *Inorg. Chem.* **2014**, *53*, 1195–1209.
[8] G. Onodera, Y. Nishibayashi, S. Uemura, *Angew. Chem. Int. Ed.* **2006**, *45*, 3819–3822.
[9] R. Martínez, G. J. Brand, D. J. Ramón, M. Yus, *Tetrahedron Lett.* **2005**, *46*, 3683–3686.
[10] C. Zhang, J.-P. Zhao, B. Hu, J. Shi, D. Chen, *Organometallics* **2019**, *38*, 654–664.
[11] A. R. Sahoo, G. Lalitha, V. Murugesh, C. Bruneau, G. V. M. Sharma, S. Suresh, M. Achard, *J. Org. Chem.* **2017**, *82*, 10727–10731.
[12] C. Schlepphorst, B. Maji, F. Glorius, *ACS Catal.* **2016**, *6*, 4184–4188.
[13] M. B. Chaudhari, G. S. Bisht, P. Kumari, B. Gnanaprakasam, *Org. Biomol. Chem.* **2016**, *14*, 9215–9220.
[14] D. Deng, B. Hu, M. Yang, D. Chen, *Dalton Trans.* **2019**, *48*, 13614–13621.
[15] J. Li, W. Zhang, F. Wang, M. Jiang, X. Dong, W. Zhao, *Chin. J. Chem.* **2012**, *30*, 2363–2366.
[16] C. Xu, X.-M. Dong, Z.-Q. Wang, X.-Q. Hao, Z. Li, L.-M. Duan, B.-M. Ji, M.-P. Song, *J. Organomet. Chem.* **2012**, *700*, 214–218.
[17] D. Wang, K. Zhao, P. Ma, C. Xu, Y. Ding, *Tetrahedron Lett.* **2014**, *55*, 7233–7235.
[18] P. Liu, R. Liang, L. Lu, Z. Yu, F. Li, *J. Org. Chem.* **2017**, *82*, 1943–1950.
[19] S. Genç, S. Günnaz, B. Çetinkaya, S. Gülcemal, D. Gülcemal, *J. Org. Chem.* **2018**, *83*, 2875–2881.
[20] S. Genç, B. Arslan, S. Gülcemal, S. Günnaz, B. Çetinkaya, D. Gülcemal, *J. Org. Chem.* **2019**, *84*, 6286–6297.
[21] Y. Iuchi, Y. Obora, Y. Ishii, *J. Am. Chem. Soc.* **2010**, *132*, 2536–2537.
[22] K. Fujita, C. Asai, T. Yamaguchi, F. Hanasaka, R. Yamaguchi, *Org. Lett.* **2005**, *7*, 4017–4019.
[23] X. Yu, Q. Y. Wang, Q. J. Wu, D. W. Wang, *Russ. J. Gen. Chem.* **2016**, *86*, 178–183.
[24] R. Wang, L. Huang, Z. Du, H. Feng, *J. Organomet. Chem.* **2017**, *846*, 40–43.
[25] M. L. Buil, M. A. Esteruelas, J. Herrero, S. Izquierdo, I. M. Pastor, M. Yus, *ACS Catal.* **2013**, *3*, 2072–2075.
[26] Y. Yang, A. Qin, K. Zhao, D. Wang, X. Shi, *Adv. Synth. Catal.* **2016**, *358*, 1433–1439.
[27] Y. M. A. Yamada, Y. Uozumi, *Org. Lett.* **2006**, *8*, 1375–1378.
[28] M. S. Kwon, N. Kim, S. H. Seo, I. S. Park, R. K. Cheedrala, J. Park, *Angew. Chem. Int. Ed.* **2005**, *44*, 6913–6915.
[29] C. S. Cho, *J. Mol. Catal. Chem.* **2005**, *240*, 55–60.
[30] P. Piehl, M. Peña-López, A. Frey, H. Neumann, M. Beller, *Chem. Commun.* **2017**, *53*, 3265–3268.
[31] S. Liao, K. Yu, Q. Li, H. Tian, Z. Zhang, X. Yu, Q. Xu, *Org. Biomol. Chem.* **2012**, *10*, 2973–2978.

[32] Q. Xu, J. Chen, H. Tian, X. Yuan, S. Li, C. Zhou, J. Liu, *Angew. Chem. Int. Ed.* **2014**, *53*, 225–229.
[33] Y.-F. Liang, X.-F. Zhou, S.-Y. Tang, Y.-B. Huang, Y.-S. Feng, H.-J. Xu, *RSC Adv.* **2013**, *3*, 7739–7742.
[34] D. A. Culkin, J. F. Hartwig, *Acc. Chem. Res.* **2003**, *36*, 234–245.
[35] A.-N. Alba, M. Viciano, R. Rios, *ChemCatChem* **2009**, *1*, 437–439.
[36] F. Bellina, R. Rossi, *Chem. Rev.* **2010**, *110*, 1082–1146.
[37] A. J. A. Watson, J. M. J. Williams, *Science* **2010**, *329*, 635–636.
[38] T. D. Nixon, M. K. Whittlesey, J. M. J. Williams, *Dalton Trans.* **2009**, 753–762.
[39] G. Zhang, J. Wu, H. Zeng, S. Zhang, Z. Yin, S. Zheng, *Org. Lett.* **2017**, *19*, 1080–1083.
[40] G. Xu, Q. Li, J. Feng, Q. Liu, Z. Zhang, X. Wang, X. Zhang, X. Mu, *ChemSusChem* **2014**, *7*, 105–109.
[41] A. Corma, J. Navas, M. J. Sabater, *Chem. Rev.* **2018**, *118*, 1410–1459.
[42] F. Huang, Z. Liu, Z. Yu, *Angew. Chem. Int. Ed.* **2016**, *55*, 862–875.
[43] S. Chakraborty, P. Daw, Y. Ben David, D. Milstein, *ACS Catal.* **2018**, *8*, 10300–10305.
[44] J. J. Ibrahim, C. B. Reddy, S. Zhang, Y. Yang, *Asian J. Org. Chem.* **2019**, *8*, 1858–1861.
[45] J. Ballester, A.-M. Caminade, J.-P. Majoral, M. Taillefer, A. Ouali, *Catal. Commun.* **2014**, *47*, 58–62.
[46] B. C. Roy, I. A. Ansari, S. A. Samim, S. Kundu, *Chem. – Asian J.* **2019**, *14*, 2215–2219.
[47] T. B. Boit, M. M. Mehta, N. K. Garg, *Org. Lett.* **2019**, *21*, 6447–6451.
[48] V. Polshettiwar, R. S. Varma, *Green Chem.* **2009**, *11*, 1313–1316.
[49] A. Ouali, J.-P. Majoral, A.-M. Caminade, M. Taillefer, *ChemCatChem* **2009**, *1*, 504–509.
[50] T. Ooi, H. Otsuka, T. Miura, H. Ichikawa, K. Maruoka, *Org. Lett.* **2002**, *4*, 2669–2672.
[51] G.-M. Zhao, W.-J. Sun, H.-L. Zhang, D.-L. Li, X. Yang, *J. Catal.* **2019**, *373*, 126–138.
[52] Q. Xu, J. Chen, Q. Liu, *Adv. Synth. Catal.* **2013**, *355*, 697–704.
[53] T. Suga, S. Shimazu, Y. Ukaji, *Org. Lett.* **2018**, *20*, 5389–5392.
[54] C. Bandari, K. M. Nicholas, *J. Org. Chem.* **2020**, *85*, 3320–3327.
[55] T. Suga, Y. Ukaji, *Org. Lett.* **2018**, *20*, 7846–7850.
[56] A. Kumar, T. Janes, S. Chakraborty, P. Daw, N. von Wolff, R. Carmieli, Y. Diskin-Posner, D. Milstein, *Angew. Chem. Int. Ed.* **2019**, *58*, 3373–3377.
[57] J. Cuthbertson, V. J. Gray, J. D. Wilden, *Chem. Commun.* **2014**, *50*, 2575–2578.
[58] J. P. Barham, G. Coulthard, K. J. Emery, E. Doni, F. Cumine, G. Nocera, M. P. John, L. E. A. Berlouis, T. McGuire, T. Tuttle, J. A. Murphy, *J. Am. Chem. Soc.* **2016**, *138*, 7402–7410.
[59] E. Shirakawa, K. Itoh, T. Higashino, T. Hayashi, *J. Am. Chem. Soc.* **2010**, *132*, 15537–15539.
[60] M. Sohail Ahmad, H. Suzuki, C. Wang, M. Zhao, Y. Nishina, *J. Catal.* **2018**, *365*, 344–350.
[61] M. S. Ahmad, H. He, Y. Nishina, *Org. Lett.* **2019**, *21*, 8164–8168.
[62] K. Azizi, R. Madsen, *Chem. Sci.* **2020**, *11*, 7800–7806.
[63] Y. Cui, Y. H. Lee, J. W. Yang, *Sci. Rep.* **2017**, *7*, 3146.
[64] S. Zhu, Y. Cen, M. Yang, J. Guo, C. Chen, J. Wang, W. Fan, *Appl. Catal. B Environ.* **2017**, *211*, 89–97.
[65] Y. Obora, *ACS Catal.* **2014**, *4*, 3972–3981.
[66] I. El Hassan, R. Lauricella, Béatrice. Tuccio, *Cent. Eur. J. Chem.* **2006**, *4*, 338–350.
[67] I. E. Hassan, L. Charles, R. Lauricella, B. Tuccio, *New J. Chem.* **2008**, *32*, 680–688.

[68] J. Kim, D. J. Darley, W. Buckel, A. J. Pierik, *Nature* **2008**, *452*, 239–242.
[69] L. Wang, J. M. Lear, S. M. Rafferty, S. C. Fosu, D. A. Nagib, *Science* **2018**, *362*, 225–229.
[70] C. Chatgilialoglu, D. Crich, M. Komatsu, I. Ryu, *Chem. Rev.* **1999**, *99*, 1991–2070.
[71] A. G. Davies, A. G. Neville, *J. Chem. Soc. Perkin Trans. 2* **1992**, 163–169.
[72] S. Guo, P. S. Kumar, M. Yang, *Adv. Synth. Catal.* **2017**, *359*, 2–25.
[73] B. Suchand, G. Satyanarayana, *Eur. J. Org. Chem.* **2017**, *2017*, 3886–3895.
[74] S. Chakraborty, P. Daw, Y. Ben David, D. Milstein, *ACS Catal.* **2018**, *8*, 10300–10305.
[75] B.-L. Jiang, S.-S. Ma, M.-L. Wang, D.-S. Liu, B.-H. Xu, S.-J. Zhang, *ChemCatChem* **2019**, *11*, 1701–1706.
[76] T. Song, Z. Ma, Y. Yang, *ChemCatChem* **2019**, *11*, 1313–1319.
[77] S. A. Runikhina, O. I. Afanasyev, K. Biriukov, D. S. Perekalin, M. Klussmann, D. Chusov, *Chem. – Eur. J.* **2019**, *25*, 16225–16229.
[78] X. Huang, J. Hu, M. Wu, J. Wang, Y. Peng, G. Song, *Green Chem.* **2018**, *20*, 255–260.
[79] B. Ding, Z. Zhang, Y. Liu, M. Sugiya, T. Imamoto, W. Zhang, *Org. Lett.* **2013**, *15*, 3690–3693.
[80] X. Hu, H. Zhu, X. Sang, D. Wang, **n.d.**, 44.
[81] M. K. Barman, A. Jana, B. Maji, **n.d.**, 50.

CHAPTER 4

CONCLUSIONS

4. Conclusions

Due to the very broad topic, 'functionalization of nanocarbons and application for catalyst,' it was necessary to make choices regarding both reactions that should be studied and the catalyst materials that should be investigated during the three years the project has lasted. During my Ph.D. study, I have mainly looked in to GO and made it, heterogeneous catalyst. I have attested that this carbocatalysts in the liquid phase has a bright future. It offers the unique possibility to tailor a range of functional groups, combined them into multifunctional ensembles, and control their overall reactivity. In the first project, I doped GO with nitrogen and systematically investigated the catalytic property of the C–H functionalization reaction. The doping of nitrogen in GO was confirmed by in-situ FT-IR analysis and by XPS spectroscopy. The NrGO can facilitate the C-H functionalization of unactivated arenes and obtain the biaryl product. The mechanistic study revealed that the reaction proceeds via interaction with the NH group on the catalyst and radical species contribute to the reaction, while the radicals were confirmed by ESR analysis. Moreover, the catalyst could be recycled up to 3 consecutive runs without loss of significant activity.

The results were quite encouraging as NrGO was found to be active for the coupling reaction. Further investigation was carried out to explore the role of radicals and the dopant atom for other important organic transformations. In this context, we developed a metal-free chemoselective system for the hydrogenation of substituted nitroaromatic compounds using NrGO as a catalyst and molecular hydrogen as a reducing agent. We compared the activity of other carbon materials such as GO, rGO, and carbon black, activated carbon, and NrGO, while found NrGO was active and selective. Similar catalytic performances have been reported by metal catalysts. We suggest that the selective hydrogenation reaction proceeds via a radical mechanism in which the localized radicals of NrGO activate the hydrogen. Overall, our results revealed that the abnormal activity and selectivity of NrGO has excellent potential for the selective hydrogenation reaction of multi-functionalized nitro compounds.

We have also demonstrated that the radicals on the surface of graphene materials can be localized and that localized radicals may play an important role in the organic transformations. In this context, we have demonstrated a new radical alkylation reaction of an alcohol with ketones to form α-alkylated ketones in the presence of base treated graphene as a catalyst. A series of alcohol

and ketones have been subjected to the transformation to generate α-alkylated products in good yields. Mechanistic studies revealed that the alkylation takes place by a radical pathway where the radical anion of the benzylic alcohol is proposed as the key intermediate. Different from existing alkylation methods, this strategy permits the use of the simple potassium tert-butoxide treated graphene as a catalyst. The reaction system follows a different mechanism than metal-based reactions and or MPV-O pathways. This is especially important when ba-rGO is employed as catalyst since the basic character of the ba-rGO works as an initiator radical reaction. Overall, this system is highly efficient, green, and sustainable, and could be an alternative or complementary method to metal-based systems in the development of new radical-mediated C−C bond forming reactions with alcohols.

From the above discussion, it is clear that the main advantage of the graphene materials is the possibility to generate by design active catalytic centers targeted to promote a given reaction. In order to accomplish this goal of carbocatalysts by design, it is necessary to know the architecture of the active sites.

Acknowledgments

I would like to express my sincere gratitude to my advisor Professor Yuta Nishina and co-advisor professor Seiji Suga, for providing me with the opportunity to study for this Ph.D. at Research Core Interdisciplinary Sciences, Okayama University. I thank professor Nishina for his regular guidance and patience throughout my study, and the cookies provided over many discussions. Besides, I thank you for painstakingly going through the draft of this thesis.

My expression of gratitude is recorded here to Dr. Blanchard Julliet for allowing me to work in her Lab, and I thank Dr. Bernard for supporting me in my Erasmus fellowship at Sorbonne University (France). I would also like to thank those that, although not directly involved in the project, have ensured the smooth running of the Nishina lab and equipment. These are Dr. Obata, Nakano, Matsumura, and Kumoda; they arranged chemicals, gases like argon, hydrogen, and carbon dioxide, etc., the Lab is a much safer and efficient environment because of these gentlemen, and their importance cannot be overstated. And last, but by no means least, I would like to thank Dr. Mashooq sincerely to his word of encouragement when all seems hopeless, which can be summarized by saying '*Man gets whatever he strives for*' were just important.

My colleague and friends deserve a great deal of credit as they, the one who, on a day to day basis, helped me keep my sanity, even though sadly, in some cases, that cannot be said of them. (Mr. Benoit Compeon and Ms. Asuna), they have provided a fantastic working environment in which I have thoroughly enjoyed studying, and I wish them all the very best. A word of thanks should be expressed to my lab members (Mr. Khan, Cheng, Zhao, Nakagawa, Fuji, Takeda, Iguchi, Kubo, Ms. Nusrat, Hori, and Shibahara) for their kind help, all the fun we shared and being remarkable friends.

I would also like to thank Okayama University for the financial support for me through the tuition fee award and scholarship, which were extremely helpful in carrying out my research work and for my pleasant stay in Japan.

I end this acknowledgment by thanking my family, to whom I owe everything. They have provided me with love and support whenever needed and a sense of humor, which has often been employed to take the best from a bad situation. This thesis is for you.

M. Sohail Ahmad